Studying Black Holes in Superposition Using Unruh-DeWitt Particle Detectors

by

Cemile Senem Arabaci

A thesis
presented to the University of Waterloo
in fulfillment of the
thesis requirement for the degree of
Master of Science
in
Physics

Waterloo, Ontario, Canada, 2022

Author's Declaration

This thesis consists of material all of which I authored or co-authored: see Statement of Contributions included in the thesis. This is a true copy of the thesis, including any required final revisions, as accepted by my examiners.

I understand that my thesis may be made electronically available to the public.

Statement of Contributions

Cemile Senem Arabaci was the sole author of this thesis on the collaborative research presented in Chapter 3 and Chapter 4 with Joshua Foo, Magdalena Zych, and Robert B. Mann. The forthcoming papers for publication in Chapter 3 and Chapter 4 are available for readers on arXiv respectively as:

- J. Foo, C.S. Arabaci, M. Zych, and R.B. Mann, arXiv:2208.12083 [gr-qc] (2022).
- J. Foo, C.S. Arabaci, M. Zych, and R.B. Mann, arXiv:2111.13315 [gr-qc] (2021). [Accepted to Physical Review Letters on September 16, 2022]

Abstract

In quantum gravity, we expect black holes to exist in quantum superposition. However, the measurable effects of black hole superpositions have not been studied widely. In this thesis, we study superpositions of different periodically identified Minkowski spacetimes and different Banados-Teitelboim-Zanelli (BTZ) black hole spacetimes and investigate excited state probabilities of an Unruh-DeWitt particle detector coupling to the superposition of these spacetimes.

This thesis is based on two consequent articles on the phenomenology of quantum superpositions of spacetime. The primary research focus is to superpose the mass of the Banados-Teitelboim-Zanelli (BTZ) black hole and investigate the quantum-gravitational effects produced by such a spacetime. We start by investigating a cylindrical spacetime superposition to better understand the basic framework for superposing spacetimes and the corresponding effects induced on the quantum matter. We achieve this by superposing a periodically identified Minkowski spacetime (i.e. Minkowski spacetime with a periodic boundary condition that creates a cylindrical topology), for which we develop an operational approach for constructing spacetime superpositions using the notion of nonlocal correlations and automorphic fields in curved spacetime. We then use this method to superpose a black hole of different masses for the nonrotating BTZ spacetime.

Following that, we couple quantum matter (which we model using the Unruh-DeWitt (UDW) particle detector model) to these spacetime superpositions. Firstly, we couple it to the cylindrical spacetime to demonstrate for the first time the response of a UDW detector to a scalar field in this superposed spacetime, and its dependence on the energy gap Ω, and $\gamma = l_A/l_B$, where l_A and l_B are the characteristic lengths of the periodically identified Minkowski spacetimes in superposition. The detector's response exhibits quantum-gravitational "resonances" at rational ratios of the superposed periodic length scale. Secondly, we couple a UDW particle detector to a scalar quantum field in the spacetime produced by a mass-superposition of the BTZ black hole. We show that the detector's dynamics exhibit similar resonances to the Minkowski spacetime superposition, now manifesting at rational ratios of the square root of the superposed black hole mass. Such resonances are genuinely quantum-gravitational effects arising from the black hole mass superposition that support and extend Bekenstein's original conjecture concerning the quantization of black holes in quantum gravity [1].

Acknowledgements

I would like to express my gratitude to a number of people who provided me assistance and support throughout and completion of my thesis.

First and foremost, I would like to thank my supervisor, Robert B. Mann for his constant support, patience, encouragement, and guidance during my research and my thesis writing process.

I also want to give many thanks to my collaborators Joshua Foo and Professor Magdalena for the great research discussions during our meetings. I would like to extend my sincere thanks to Joshua for helping me with my research questions and for his great dedication to giving suggestions and clarifications on my thesis.

Special thanks go to Kensuke Yoshimura Gallock for always being willing to answer my physics and Mathematica questions.

I want to thank Matthew Robbins for his mentoring me to work through extending this research topic further.

I'd like to acknowledge the assistance of the Physics Graduate Program Coordinator and Graduate Officer, Dr. Bizheva. I am also grateful to have the friendships of three brilliant graduate students, María, Aria, and Tania who gave me cheers and happy moments for celebrating each other's success, comforting and helping each other in our struggles including our academic life.

Finally, I would like to thank my family for their enduring support and encouragement during the past couple of years. They gave me strength whenever I needed it. This thesis could not have been completed without their understanding.

To the memory of my father

Table of Contents

List of Figures

Chapter 1

Introductory Remarks

1.1 Background

In the absence of a fully-fledged theory of quantum gravity, important questions about the quantum aspects of spacetime remain. One such question concerns the phenomenology of "quantum superposition states of spacetime". In this thesis, we analyze this problem using a newly developed bottom-up approach for studying quantum-gravitational effects.

Assuming that a consistent theory of quantum gravity exists, there should likewise exist solutions in which "semiclassical states of spacetime" may be placed in quantum superpositions (in analogy with "semiclassical" coherent states in quantum optics). Examples of such superpositions include a black hole or dark matter in a superposition of masses or locations [3, 4, 5], or an expanding spacetime in a superposition of expansion rates [6].

Over the past 50 years, numerous attempts have been made to formally quantize general relativity. In [7], DeWitt developed one such framework by considering wavefunctions, clocks, and superpositions of these wavefunctions [7]. This led to the derivation of the Wheeler-DeWitt (WDW) equation which is a field equation based on wave functions over geometries, or in other words a wavefunction of any described gravitational field. The WDW equation allowed for the possibility of quantum superpositions of different spacetimes [7, 8, 9]. In the late 20^{th} century, loop quantum gravity was formulated by pioneers like Rovelli and Thiemann [10], a framework that attempts to treat spacetime distance and volume as fundamentally discrete observables with associated eigenspectra [11]. It arose out of the formal quantization of

canonical general relativity, out of which came the above-mentioned quantization of geometry and the so-called "spin network" description of quantum geometry [12]. These ideas were consonant with previous work by Bekenstein and others, who treated (for example) the metric variables (e.g. the mass and angular momentum) describing objects like black holes as fundamentally quantum in nature. Applying his ideas to black holes, Bekenstein showed that when treating a black hole as possessing a quantized horizon area (and hence mass) in units of the Planck area its Hawking radiation likewise possesses a discrete emission spectrum. This quantization of black holes is called Bekenstein's conjecture and has potential verification by gravitational wave astronomy. There are potential imprints of black hole quantization in gravitational wave signals of merging black holes, with black hole rotation improving its observability as a quantum effect [13, 14]. Tentative observational evidence of these echoes were reported for the first time by Abedi et al. [15]. In the light of gravitational wave echoes, a new promising study on the spectrum of quantum black holes provides insight into their inner structure, unlike their classical counterparts [16]. Hence, LQG, a top-down approach for quantizing black holes gave rise to the active research area investigating quantum black holes (QBH). Further to these "top-down" approaches to quantizing spacetime, others in the LQG community have sought to develop formal frameworks for constructing superpositions of spacetime, see for example the review by Gambini et. al. [17, 18]. Other approaches by Arrasmith et. al. and Demers et. al. study intrinsic decoherence effects of black hole spatial superpositions via employing toy models [19, 20, 21].

While such "top-down" approaches have yielded numerous advances, recently there has been increasing interest in attacking the problem from the "bottom-up". By bottom-up, we mean approaches to studying quantum gravity problems that do not seek to formally quantize the gravitational field. Recently, such superpositions have been applied and considered in studies of indefinite causal order [22], quantum reference frames and the equivalence principle [23, 24, 25], quantum conformal transformations [26], analog gravity [27] (in which an analog model possibly may build states corresponding to the putative superposition of spacetime) and implementation of table-top experiments designed to test the quantumness of gravity [28, 29, 30]. The study of indefinite causal order investigates the quantum effects that arise when classical assumptions about the background causal structure are relaxed. It is a particularly relevant area of study for quantum gravity, where it is expected that the dynamical background of GR and the indeterminacy

of QM leads to such causal indefiniteness [22]. Recent work in the field of quantum reference frames has associated a "spacetime quantum reference frame" to a quantum particle in spacetime with the purpose of discerning observable quantum gravitational effects in this frame [23]. Reference frames are also associated with quantum systems in superposition to test quantum versions of the equivalence principle [25]. In a different work, a unitary transformation of such reference frames is constructed [24]. A very recent article has attempted to construct, using symmetry principles, a conformal transformation between a scenario involving a Klein-Gordon field on a background in a quantum superposition, with that of a field with a superposition of mass parameters on a classical spacetime [26].

All of these studies seek to develop bottom-up frameworks for the physics of spacetime superpositions, and how general relativity and quantum mechanics may govern such superpositions. The question remains as to the in-principle measurable, quantitative effects produced by spacetime superpositions, for example, those produced by black holes in quantum superpositions of masses, locations, or angular momentum. These questions perhaps require us to develop a newly profound formal approach. Lacking such an approach at present we can however investigate operationally how quantum matter and superpositions of spacetime can interact with each other. Using the tools we know – quantum information and quantum field theory in curved spacetime (QFT-CS) – we can check if superpositions of spacetime exhibit any quantum gravitational effects that can be considered as quantum gravity behavior.

In this thesis, we use an Unruh-DeWitt (UDW) particle detector to access the local and nonlocal field correlation functions that arise when the underlying spacetime is in quantum superposition. Such an approach builds off recent work by Foo et. al., who originally studied quantum-controlled detectors in quantum superpositions of trajectories on a single spacetime background [6, 31, 32, 33]. By using this model, we can compute observables like the detector transition probability in such spacetimes, to ascertain the novel, possibly quantum-gravitational effects that emerge. We explore these transition probabilities for a range of lengths for the quantized circumference length of cylindrically quotient Minkowski spacetime, and masses in the spacetime produced by a mass-superposed BTZ black hole. This allows us to identify the observable characteristics of the quantum superposition when applied to the background spacetime itself. It should be noted that our operational approach does not allow us to quantize spacetime itself (ala LQG).

Instead, it treats spacetime "semiclassically" (in analogy with "semiclassical coherent states in quantum optics"), upon which correlations functions for the field on different "spacetime amplitudes" may be computed, which themselves are used to computing detector observables as mentioned above.

1.2 Thesis Outline

This thesis is organized as follows. In Chapter 2.1, we introduce the background spacetimes of interest, followed by the recent model for quantum-controlled UDW detectors in Chapter 2.2. In the following chapters, we explicitly present our operational approach of quantum superposition of spacetime, including the calculation of detector observables. We apply our formalism to (3+1)-dimensional Minkowski spacetime in a superposition of periodic identifications in Chapter 3 and for the nonrotating BTZ black hole in Chapter 4. Finally, we summarize our work and results with final thoughts and prospects for future research in Chapter 5.

Chapter 2

Background

2.1 Spacetime Geometries

In this Section, we introduce the relevant geometric details for the spacetimes of interest for this thesis. In Chapters 3 and 4, we specifically study the operational effects produced by quantum superpositions of these spacetimes.

We first consider (3+1)-dimensional "cylindrical" Minkowski spacetime, which is constructed by quotienting Minkowski spacetime with an isometry group that generates periodic identifications in one spatial dimension. The purpose of considering this simple example is to understand the correct approach to operationally construct spacetime superpositions via field correlation functions, from which more interesting scenarios (e.g. superpositions of black hole spacetimes) may be studied. Constructing a quantum field theory on such a background requires the theory of automorphic fields, which we discuss in Sec. 3.1. Automorphic field theory is also used to study quantum fields on the Banados-Teitelboim-Zanelli (BTZ) black hole, which is formed by periodically identifying anti-de Sitter-Rindler (AdS-Rindler) spacetime [34].

2.1.1 The Cylindrical Quotient Space of Minkowski Spacetime

The periodically identified quotient space M_0 is constructed by imposing periodic boundary conditions along the z-axis on the (3+1)-dimensional

Minkowski spacetime coordinates (t, x, y, z) with line element

$$\mathrm{d}s^2 = -\mathrm{d}t^2 + \mathrm{d}x^2 + \mathrm{d}y^2 + \mathrm{d}z^2. \tag{2.1}$$

Note that we have assumed the metric signature $(-,+,+,+)$. The flat spacetime $\mathcal{M}_0 = \mathcal{M}/J_0$ is built as a quotient of $\mathcal{M}$ under the isometry group $Z \simeq J_0^n$, where the action of J_0 is given by

$$J_0 : (t, x, y, z) \mapsto (t, x, y, z + l) \tag{2.2}$$

and l is a characteristic length that we associate with the circumference of the cylindrical spacetime [35, 36]. In other words, it is a topological periodic identification of length l along the z-axis in Minkowski spacetime. Henceforth we refer to $\mathcal{M}_0$ as a cylindrical spacetime. J_0 preserves space and time orientation and acts freely and properly, ensuring that $\mathcal{M}$ is a space and time orientable Lorentzian manifold. $\mathcal{M}_0$ is a flat spacetime since J_0 does not affect the Minkowski line element.

2.1.2 AdS-Rindler and the BTZ Black Hole in (2+1) Dimensions

Anti-de Sitter (AdS) spacetime is a maximally symmetric Lorentzian manifold with constant negative scalar curvature. In AdS spacetime, empty space itself has negative energy density but positive pressure. In a way similar to Rindler coordinates in Minkowski spacetime (see Figure 2.1), AdS-Rindler coordinates in AdS space define "Rindler wedges" of the full manifold that uniformly accelerated observers are restricted to. The main difference between the two cases is that in the latter, there exists a threshold value of the acceleration achievable by such observers, inversely proportional to the length scale l of the spacetime. As in Minkowski spacetime in Figure 2.1, AdS-Rindler observers perceive an acceleration horizon beyond which spacetime events remain inaccessible.

The three metrics of interest are as follows.

$\mathbf{AdS}_3$ The AdS_3 line element is given by

$$\mathrm{d}s^2 = -\left(\frac{r^2}{l^2} + 1\right)\mathrm{d}t^2 + \left(\frac{r^2}{l^2} + 1\right)^{-1}\mathrm{d}r^2 + r^2\mathrm{d}\theta^2 \tag{2.3}$$

where $\theta \in [0, 2\pi)$ is the angular coordinate, r is the radial coordinate, t is the time component of spacetime coordinates and l is the curvature of the spacetime.

AdS_3-Rindler The AdS_3-Rindler line element is given by [37]

$$\mathrm{d}s^2 = -\left(\frac{\lambda^2}{l^2} - 1\right)\mathrm{d}\eta^2 + \left(\frac{\lambda^2}{l^2} - 1\right)^{-1}\mathrm{d}\lambda^2 + \lambda^2 \mathrm{d}Y^2 \tag{2.4}$$

The AdS-Rindler spacetime is not compact in the Y coordinate: $Y \in [-\infty, \infty]$. λ is the transformed radial coordinate from r at the AdS_3.

Banados-Teitelboim-Zanelli (BTZ) Black Hole The BTZ black hole has line element given by

$$\mathrm{d}s^2 = -\left(\frac{R^2}{l^2} - M\right)\mathrm{d}T^2 + \left(\frac{R^2}{l^2} - M\right)^{-1}\mathrm{d}R^2 + R^2\mathrm{d}\phi^2 \tag{2.5}$$

where $-\infty < T < \infty$ and $\phi \in [0, 2\pi)$. Here, M parametrizes the mass of the black hole, while R is a radial coordinate. This metric can be obtained from the identification $Y \to Y + 2\pi\sqrt{M}$ in the AdS-Rindler metric, and setting $\eta = \sqrt{M}T$, and $\lambda = R/\sqrt{M}$, $Y = \sqrt{M}\phi$.

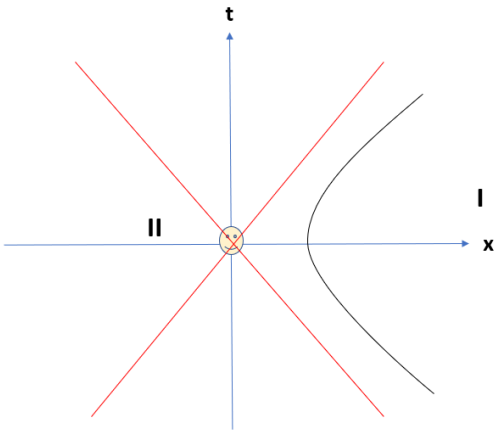

Figure 2.1: Minkowski-Rindler accelerated observer light cone coordinate in (1+1)-dimensions. The accelerated observer is a particle detector on a trajectory of the black line. The stationary observer is at the origin illustrated as a smiley face with a light cone that does not intercept the motion of the particle detector [2].

To understand the relationship between AdS spacetime, AdS-Rindler spacetime, and the BTZ black hole, let us consider the explicit coordinate transformation between these respective geometries. Three-dimensional anti-de Sitter space (AdS_3) can be obtained from flat $R^{2,2}$, with coordinates (X_1, X_2, T_1, T_2) and metric

$$\mathrm{d}s^2 = \mathrm{d}X_1^2 + \mathrm{d}X_2^2 - \mathrm{d}T_1^2 - \mathrm{d}T_2^2, \tag{2.6}$$

by restricting the submanifold on a 3-dimensional hyperboloid

$$-l^2 = X_1^2 - T_1^2 + X_2^2 - T_2^2 \tag{2.7}$$

This metric solves the $(2+1)$-dimensional Einstein equations with negative cosmological constant $\Lambda = -1/l^2$.

The embedding coordinates for the AdS_3-Rindler spacetime are given by

$$\begin{aligned} T_1 &= l\sqrt{\frac{r^2}{l^2}}\cosh\phi, \qquad & X_1 &= l\sqrt{\frac{r^2}{l^2}}\sinh\phi, \\ T_2 &= l\sqrt{\frac{r^2}{l^2}-1}\sinh\frac{t}{l}, \qquad & X_2 &= l\sqrt{\frac{r^2}{l^2}-1}\cosh\frac{t}{l}, \end{aligned} \tag{2.8}$$

from which one obtains the AdS-Rindler metric, Eqn. 2.4:

$$\mathrm{d}s^2 = -\left(\frac{r^2}{l^2} - 1\right)\mathrm{d}t^2 + \left(\frac{r^2}{l^2} - 1\right)\mathrm{d}r^2 + r^2\mathrm{d}\phi^2 \tag{2.9}$$

where $\eta = t$, $\lambda = r$, $Y = \phi$, which corresponds to a wedge of AdS_3 for a uniformly accelerated observer. To obtain the BTZ metric from Eq. (2.9), one defines $r = \tilde{r}/\sqrt{M}$, $t = \tilde{t}\sqrt{M}$ and $\phi = \tilde{\phi}\sqrt{M}$, which yields

$$\mathrm{d}s^2 = -\left(\frac{\tilde{r}^2}{l^2} - M\right)\mathrm{d}\tilde{t}^2 + \left(\frac{\tilde{r}^2}{l^2} - M\right)^{-1}\mathrm{d}\tilde{r}^2 + \tilde{r}^2\mathrm{d}\tilde{\phi}^2 \tag{2.10}$$

where $\tilde{\phi}$ is identified with period 2π. Alternatively, one can begin directly from Eq. (2.6) and utilize the parametrization

$$\begin{aligned} T_1 &= l\sqrt{\frac{r^2}{Ml^2}}\cosh(\sqrt{M}\phi), \qquad X_1 = l\sqrt{\frac{r^2}{Ml^2}}\sinh(\sqrt{M}\phi), \\ T_2 &= l\sqrt{\frac{r^2}{Ml^2} - 1}\sinh\frac{\sqrt{M}t}{l}, \qquad X_2 = l\sqrt{\frac{r^2}{Ml^2} - 1}\cosh\frac{\sqrt{M}t}{l}, \end{aligned} \tag{2.11}$$

which yields the same metric [37], provided ϕ in (2.11) is identified with the period 2π.

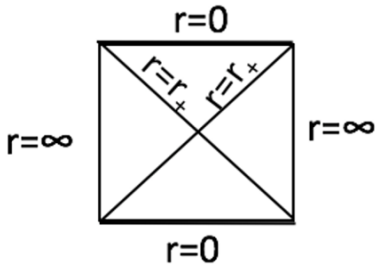

Figure 2.2: The Penrose diagrams for the static black hole

A Penrose diagram for the BTZ spacetime is shown in Figure 2.2. For the UDW detector detection, we consider scalar fields on BTZ black hole spacetime and therefore scalar quantum field theory on curved spacetime. Scalar fields allow us to evaluate the detector-field interaction with greater ease than vector fields. Hence, we use this simpler version than the more realistic interaction with vector fields. There are three proper boundary conditions

for a scalar field in spatial infinity: Dirichlet, Neumann, and "transparent" boundary conditions. Here, we consider the "transparent" boundary condition due to its feasibility in the calculations which we discuss further in 4. In Figure 2.2, the Penrose diagram is for the static BTZ black hole with the $0 = r_- < r_+$ and we consider the "transparent" boundary condition here as well and r for the detector distance from black hole origin is considered as $r_+ < r < \infty$.

In Chapters 3 and 4, we will see how to detect a superposition state (shown in Figure 2.3) that consists of the two periodical identifications of AdS-Rindler spacetime. In other words, we will see how to superpose two BTZ black holes of different mass states where mass is one of the parameters the black hole spacetime metric depends on.

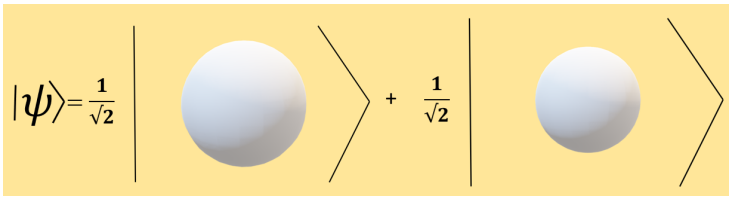

Figure 2.3: Superposition state of 2 BTZ black hole masses system

2.2 Unruh-Dewitt Detector Superposition Models

2.2.1 "Standard" UDW Detector

QFT−CS investigates the nature of quantum fields on a background of a classical gravitational field formed by solving the Einstein equations of general relativity. It studies the interaction between the quantum field and the classical gravitational background, neglecting any quantum properties of the gravitational field itself. It is common to make the simplification to scalar fields since this captures the essential physics while being mathematically simpler than the full vector-valued field associated with quantum electrodynamics.

A widely used tool in QFT−CS is the Unruh-DeWitt (UDW) detector, which is a simple model of an atom interacting (coupling) with a field on a

curved spacetime [38, 39, 40, 41, 42, 43, 44, 45]. UDW detectors are two-level quantum systems (qubits), with the ground and excited states $|g\rangle$ and $|e\rangle$, separated by an energy gap Ω. For the detector Hilbert space, $\mathcal{H}_{D,0}$ the orthonormal basis formed by these states is associated with internal degrees of freedom of the atom (detector) and it is the detector Hamiltonian expression without any interaction, which can also be interpreted as the atom's internal energy. Its free evolution is governed by a Hamiltonian which has Ω energy gap between its ground and excited states. For example, as a general description, it can be shown as excited and ground states possessing $\frac{\Omega}{2}$ or excited having Ω, while the ground state has no energy as in the expressions

$$H_{\mathrm{D},0} = \frac{\Omega}{2}(|e\rangle\langle e| - |g\rangle\langle g|), \qquad H_{\mathrm{D},0} = \Omega|e\rangle\langle e|. \tag{2.12}$$

The UDW detector is commonly considered as coupling linearly to the scalar field which has its field Hamiltonian in the total Hamiltonian as

$$H_{\mathrm{tot}} = H_{\mathrm{F},0} + H_{\mathrm{D},0} + H_{\mathrm{int.}} \tag{2.13}$$

As mentioned previously scalar fields are only approximations to more realistic models of electromagnetic fields, which are vector fields and in general, more computationally difficult. Fortunately, the UDW model interacting with a scalar field is a good approximation of the light-matter interaction [46] under the neglect of angular momentum, which allows us to simplify the usual dipole coupling to a monopole particle detector interacting with a scalar field. The simplest form of the UDW interaction Hamiltonian is

$$\hat{H}_{\mathrm{int.}} = \lambda\eta(\tau)(\hat{\sigma}^{+}(\tau) + \hat{\sigma}^{-}(\tau)) \otimes \hat{\phi}(\mathsf{x}_D(\tau)) \tag{2.14}$$

where λ is a weak coupling constant, $\eta(\tau)$ a switching function, $\sigma^{\pm}(\tau)$ ladder operators between the energy eigenstates $|g\rangle$, $|e\rangle$ of the detector with gap Ω, and $\hat{\phi}(\mathsf{x}_D(\tau))$ the scalar field pulled back to the worldline $\mathsf{x}_D(\tau)$. During the measurement process, the duration of the interaction between the detector and the field, the time evolution of the system is described by the unitary operator formed with the interaction Hamiltonian in Eqn. 2.14.

$$\hat{U} := \mathcal{T}\exp\left(-i\int d\tau \hat{H}_{\mathrm{int.}}(\tau)\right)$$

where $\mathcal{T}$ denotes time-ordering. We can expand the unitary operator out to some arbitrary order using the Dyson series perturbative expansion. In

general, the effects we are interested in will manifest in second order in the coupling constant λ, so

$$\hat{U} := \mathbb{I} + (-i)\int d\tau \hat{H}_{\text{int.}} + \frac{(-i)^2}{2}\int d\tau d\tau' \mathcal{T}\hat{H}_{int.}(\tau)\hat{H}_{\text{int.}}(\tau') + \mathcal{O}(\lambda^3) \quad (2.15)$$

where the terms are defined as

$$\hat{U}^{(0)} := \mathbb{I} \quad (2.16)$$

$$\hat{U}^{(1)} := (-i)\int d\tau \hat{H}_{int.} \quad (2.17)$$

$$\hat{U}^{(2)} := \frac{(-i)^2}{2}\int d\tau d\tau' \mathcal{T}\hat{H}_{int.}(\tau)\hat{H}_{int.}(\tau') \quad (2.18)$$

and the integration interval is $\tau \in (-\infty, \infty)$. The effect of the time-ordering operator $\mathcal{T}$ is given by $\mathcal{T}A(t)B(t') := \theta(t-t')A(t)B(t') + \theta(t'-t)B(t')A(t)$. Typically, before the measurement ($\tau \to -\infty$), the detector is prepared at the ground state and the field is in the vacuum state $|0\rangle$. Let us take this unitary operator to the interaction picture. We should evolve the initial state operator to a final state operator via

$$\hat{\rho}_f = \hat{U}\hat{\rho}_i\hat{U}^\dagger \quad (2.19)$$

where the initial state of the detector field system is

$$\hat{\rho}_i = |g\rangle\langle g| \otimes |0\rangle\langle 0| \quad (2.20)$$

Then the final state of the detector, $\rho_D \in S(\mathcal{H}_D)$ after tracing out the field degrees of freedom in final state of the detector field system,

$$\hat{\rho}_D := \text{Tr}_\phi[\hat{U}(|g\rangle\langle g| \otimes |0\rangle\langle 0|)\hat{U}^\dagger] = \begin{pmatrix} 1-P_D & 0 \\ 0 & P_D \end{pmatrix} + \mathcal{O}(\lambda^4) \quad (2.21)$$

where the detector density matrix is in the basis $\{|0\rangle_D, |1\rangle_D\}$. P_D is the transition probability for the detector transitioning its excited state given below

$$P_D = \int \mathrm{d}\tau \int \mathrm{d}\tau' \chi(\tau)\overline{\chi}(\tau')W\big(\mathsf{x}(\tau), \mathsf{x}(\tau')\big) \quad (2.22)$$

where $\chi(\tau) = \eta(\tau)e^{-i\Omega\tau}$, while vacuum Wightman function, the scalar field correlation functions, evaluated with respect to the trajectories $\mathsf{x}(\tau), \mathsf{x}(\tau')$ is

$$W\big(\mathsf{x}(\tau), \mathsf{x}(\tau')\big) := \langle 0|\hat{\phi}(\mathsf{x}(\tau))\hat{\phi}(\mathsf{x}(\tau'))|0\rangle \quad (2.23)$$

2.2.2 "Quantum-Controlled" UDW Detector

Having introduced the standard UDW detector model, we are now in a position to extend this to include superpositions of the detector's trajectory. This was first achieved in [31, 32, 33, 47] by introducing a control degree of freedom for the detector's semiclassical trajectory. In the original case of UDW detector with quantum control, the detector interacts with the quantum field on a classical spacetime background in a superposition of two trajectory states. The control system is prepared in the superposition state $|\chi\rangle = (|1\rangle_{\rm C} + |2\rangle_{\rm C})/\sqrt{2}$, where the orthogonal states $|1\rangle_{\rm C}$ and $|2\rangle_{\rm C}$ designate the two paths that the detector traverses in superposition. Such a system can be described in the tensor product of the Hilbert space $\mathcal{H} = \mathcal{H}_{\rm T}\otimes\mathcal{H}_{\rm UDW}\otimes\mathcal{H}_{\mathcal{F}}$, where these Hilbert spaces respectively are associated with the trajectory, detector and field degrees of freedom. In the next Chapter, we reinterpret the control governing the quantum-controlled spacetime degrees of freedom. Upon including the control state $|\chi\rangle$, the initial of the combined system becomes

$$|\Psi\rangle_{\rm CFD} = |\chi\rangle \otimes |g\rangle_D \otimes |0\rangle_F. \tag{2.24}$$

The interaction Hamiltonian, with the inclusion of the quantum control, is now given by [31]

$$\hat{H}_{\rm int.}(\tau) = \sum_{i=1}^{N} \hat{\mathcal{H}}_i(\tau) \otimes |i\rangle\langle i|_{\rm C} \tag{2.25}$$

for $N = 2$, where

$$\hat{\mathcal{H}}_i(\tau) = \lambda\hat{\sigma}(\tau)\eta_i(\tau)\hat{\phi}\big(\mathsf{x}_i(\tau)\big) \tag{2.26}$$

governs the interaction along the worldline $\mathsf{x}_i(\tau)$ of the ith branch of the superposition.

The time-evolution of the control-field-detector system now occurs in a superposition of the N paths:

$$\hat{U} = \sum_{i=1}^{N} \hat{U}_i \otimes |i\rangle\langle i|_{\rm C} \tag{2.27}$$

where, to leading order in perturbation theory

$$\hat{U}_i = 1 - i\lambda \int {\rm d}\tau\, \hat{\mathcal{H}}_i(\tau) + \mathcal{O}(\lambda^2). \tag{2.28}$$

Using Eq. (2.27), after time-evolving the initial state we obtain

$$\hat{U}|\Psi\rangle_{\rm CFD} = \frac{1}{\sqrt{N}}\sum_{i=1}^{N}\hat{U}_i|i\rangle_{\rm C}|0\rangle|g\rangle. \tag{2.29}$$

Following [6, 31, 32, 33, 47, 48], the conditional state of the detector given the control, is measured in some fixed state, which we arbitrarily take to be its initial state, $|\chi\rangle$. This yields the final detector field state

$$\langle\chi|\hat{U}|\Psi\rangle_{\rm CFD} \equiv |\Psi'\rangle_{\rm FD} = \frac{1}{N}\sum_{i=1}^{N}\hat{U}_i|0\rangle|g\rangle. \tag{2.30}$$

From this, one can obtain the density matrix of the system in the usual way, by tracing out the field degrees of freedom:

$$\hat{\rho}_D = \begin{pmatrix} 1-P_D & 0 \\ 0 & P_D \end{pmatrix} + \mathcal{O}(\lambda^4) \tag{2.31}$$

where

$$P_D = \frac{\lambda^2}{N^2}\sum_{i,j=1}^{N}P_{ij,D} = \frac{\lambda^2}{N^2}\left\{\sum_{i=j}^{N}P_{ij,D} + \sum_{i\neq j}P_{ij,D}\right\} \tag{2.32}$$

is the transition probability of the detector (or fraction of excited detectors within an identically prepared ensemble) conditioned on the measurement of the control system in the asymptotic future [31, 32, 33]. The individual contributions take the form

$$P_{ij,D} = \int {\rm d}\tau \int {\rm d}\tau' \chi_i(\tau)\overline{\chi}_j(\tau')W_{ji}\big(\mathsf{x}_i(\tau),\mathsf{x}_j(\tau')\big) \tag{2.33}$$

where $\chi(\tau) = \eta(\tau)e^{-i\Omega\tau}$, while

$$W_{ji}\big(\mathsf{x}_i(\tau),\mathsf{x}_j(\tau')\big) := \langle 0|\hat{\phi}(\mathsf{x}_i(\tau))\hat{\phi}(\mathsf{x}_j(\tau'))|0\rangle \tag{2.34}$$

are the field correlation (Wightman) functions evaluated with respect to the trajectories $\mathsf{x}_i(\tau), \mathsf{x}_j(\tau')$ [49], associated with the i-jth amplitude of the superposition.

Unlike a detector traveling along a single, classical trajectory, P_D now features "nonlocal" correlation functions between each respective pair of amplitudes in the superposition, $i \neq j$. These nonlocal terms are equivalent

to the off-diagonal terms L_{AB} in the bipartite reduced density matrix for a system of two detectors interacting locally with the field on classical trajectories, which motivates our choice of nomenclature for these terms in later chapters.

As usual, we can choose for simplicity a Gaussian switching function, $\eta(\tau) = \exp(-\tau^2/2\sigma^2)$, where σ is a characteristic timescale of the interaction. For stationary trajectories, the Wightman functions only depend on $s = \tau - \tau'$ and the outer integral of Eq. (2.33) can be evaluated, yielding the simplified expression

$$P_D = \frac{\lambda^2\sqrt{\pi}\sigma}{N^2}\sum_{i,j=1}^{N}\int \mathrm{d}s\, e^{-s^2/4\sigma^2}e^{-i\Omega s}W_{ji}(s). \tag{2.35}$$

In these time-independent scenarios, it is sometimes useful to work with the normalised transition probability

$$\mathcal{F}(\Omega) = \frac{P_D}{\lambda^2\sqrt{\pi}\sigma}, \tag{2.36}$$

which we refer to as the response function. In the infinite-interaction time limit, $\sigma \to \infty$, the response function becomes

$$\mathcal{F}(\Omega) = \frac{1}{N^2}\sum_{i,j=1}^{N}\int_{-\infty}^{\infty} \mathrm{d}s\, e^{-i\Omega s}W_{ji}(s). \tag{2.37}$$

2.2.3 UDW Detector on a "Quantum-Controlled" Spacetime Superposition

In the previous Section, we considered an additional control degree of freedom that we assigned to the quantized "trajectory states" of the detector, traveling on a single, classical spacetime background. This detector superposition model can be shown to be physically equivalent to that of a detector traversing a single classical trajectory where the spacetime is in a superposition of spatial translations [6, 50]. The latter system can be described in the tensor product Hilbert space $\mathcal{H} = \mathcal{H}_{\mathrm{S}} \otimes \mathcal{H}_{\mathrm{UDW}} \otimes \mathcal{H}_{\mathrm{F}}$, where each Hilbert space is respectively associated with the spacetime, detector and field degrees of freedom. In other words, the quantum trajectory degrees of freedom are replaced with quantum spacetime degrees of freedom. To show the physical

equivalence of the two cases, let us consider a detector in a superposition of two trajectories, and express the trajectory states in terms of some worldline $\xi \equiv \xi(\tau)$:

$$|1\rangle_C \to |\xi\rangle \tag{2.38}$$

$$|2\rangle_C \to |\xi + \mathcal{L}\rangle \tag{2.39}$$

as the trajectory states, where $\mathcal{L} \equiv \mathcal{L}(\tau)$ is some possibly time-dependent function that relates the coordinates of the two worldlines. For simplicity, let us assume a fixed $\mathcal{L}$, which yields a constant spatial translation. The global coordinate transformation $\mathcal{L}$ can be expressed as some unitary operator $\hat{\mathcal{T}}(\mathcal{L})$, since it is a symmetry of the dynamics. Importantly $\hat{\mathcal{T}}(\mathcal{L})$ acts on both the trajectory state and the coordinates of the field operator (since this depends on the spacetime coordinates), as follows:

$$\begin{aligned} |\xi + \mathcal{L}\rangle \otimes |0\rangle_F &= \hat{\mathcal{T}}(\mathcal{L})|\xi\rangle \otimes |0\rangle_F \\ &= \hat{\mathcal{T}}_\xi(\mathcal{L})|\xi\rangle \otimes \hat{\mathcal{T}}_\phi(\mathcal{L})|0\rangle_F. \end{aligned} \tag{2.40}$$

Note also the action of the translation operator on the field as enacting a coordinate transformation, expressed in the Heisenberg picture as:

$$\hat{\Phi}(\xi + \mathcal{L}) = \hat{\mathcal{T}}_\phi(\mathcal{L})^\dagger \hat{\Phi}(\xi) \hat{\mathcal{T}}_\phi(\mathcal{L}). \tag{2.41}$$

Until now, we should understand that $|\xi\rangle$, $|\xi + \mathcal{L}\rangle$ are two trajectories states in a single spacetime. Using the representation Eq. (2.40) however, the combined system describing the trajectory, field, and detector can now be expressed in terms of a single detector trajectory with modified dynamics:

$$\begin{aligned} |\Psi\rangle_{\text{TFD}} &= \frac{1}{\sqrt{2}}(|\xi\rangle + |\xi + \mathcal{L}\rangle)|0\rangle_F|g\rangle \\ &= \frac{1}{\sqrt{2}}(\mathbb{I} + \hat{\mathcal{T}}(\mathcal{L}))|\xi\rangle|0\rangle_F|g\rangle \end{aligned} \tag{2.42}$$

The time evolution of the state with this "superposition of unitaries" is given by

$$\hat{U}|\Psi\rangle_{\text{TFD}} = \frac{1}{\sqrt{2}}(\hat{U} + \hat{U}\hat{\mathcal{T}}(\mathcal{L}))|\xi\rangle|0\rangle_F|g\rangle. \tag{2.43}$$

Let us now consider a "measurement" of the control (i.e. the trajectory state) in the modified basis $|\chi\rangle = (\mathbb{I}+\hat{\mathcal{T}}(\mathcal{L}))|\xi\rangle/\sqrt{2}$, giving the conditional detector-field state,

$$|\Psi\rangle_{FD} = \frac{1}{2}\Big(\langle\xi|\hat{U}|\xi\rangle + \langle\xi|\hat{U}\hat{\mathcal{T}}(\mathcal{L})|\xi\rangle + \langle\xi|\hat{\mathcal{T}}(\mathcal{L})^\dagger\hat{U}|\xi\rangle + \langle\xi|\hat{\mathcal{T}}(\mathcal{L})^\dagger\hat{U}\hat{\mathcal{T}}(\mathcal{L})|\xi\rangle\Big) \otimes |0\rangle_F \otimes |g\rangle \tag{2.44}$$

Now, recall that the time evolution operator, Eq. (2.27), can be expressed as a sum over the paths of the superposition:

$$\hat{U} = \sum_{\xi=\text{paths}} \hat{U}(\xi) \otimes |\xi\rangle\langle\xi| \tag{2.45}$$

But now there is one trajectory state $|\xi\rangle$

$$\hat{U} = \hat{U}(\xi) \otimes |\xi\rangle\langle\xi| \tag{2.46}$$

and from Eq. (2.46) we have

$$\langle\xi|\hat{U}|\xi\rangle = \hat{U}(\xi), \tag{2.47}$$

$$\langle\xi|\hat{\mathcal{T}}(\mathcal{L})^\dagger\hat{U}\hat{\mathcal{T}}(\mathcal{L})|\xi\rangle) = \hat{\mathcal{T}}_\phi(\mathcal{L})^\dagger\hat{U}(\xi)\hat{\mathcal{T}}_\phi(\mathcal{L}) \tag{2.48}$$

yielding

$$|\Psi\rangle_{\text{FD}} = \frac{1}{2}(\hat{U}(\xi) + \hat{U}(\xi+\mathcal{L}))|0\rangle_F|g\rangle \tag{2.49}$$

where the second and third terms in Eq. (2.44) vanish, and the time evolution operators are functions of the field operators whose coordinates are associated with the two spatial translations of the original superposition of trajectories. The physical scenario is that of a detector on a single worldline ξ, interacting with a field whose coordinates are in a superposition of spatial translations (i.e. a field quantized on a quantum-controlled spacetime in a superposition of spatial translations). What Joshua at. al. [6] have demonstrated is that this is physically equivalent to the scenario in which the detector traverses a superposition of trajectories on a single classical background.

For completeness, let us show how detector observables are also invariant between the two perspectives. In general, we have

$$\hat{U}(\xi) = 1 - i\int \mathrm{d}\tau\, \hat{\mathcal{H}}_{int}(\xi) + \mathcal{O}(\lambda^2), \tag{2.50}$$

$$\hat{U}(\xi+\mathcal{L}) = 1 - i\int \mathrm{d}\tau\, \hat{\mathcal{H}}_{int}(\xi+\mathcal{L}) + \mathcal{O}(\lambda^2), \tag{2.51}$$

which are the time-evolution operators associated with a field in a superposition of coordinate transformations ξ and $\xi+\mathcal{L}$.

After computing the reduced density matrix of the detector, Eq. (2.49), the total transition probability can be shown to be a sum of the same field $i \neq j$ correlations at initial and final times and cross-correlations between $\hat{\Phi}(\xi)$ and $\hat{\Phi}(\xi+\mathcal{L})$, giving

$$P_D = \frac{\lambda^2}{4}\left\{\sum_{i=j} P_{ij,D} + \sum_{i\neq j} P_{ij,D}\right\}, \tag{2.52}$$

which is identical to Eq. (2.32), where now the transition probabilities consist of transition amplitudes that are transformed under $\hat{\mathcal{T}}_\phi$ at the level of the Wightman functions,

$$P_{ij,D} = \int \mathrm{d}\tau \int \mathrm{d}\tau' \chi(\tau)\overline{\chi}(\tau')\langle 0|\hat{\Phi}(\mathsf{x}(i))\hat{\Phi}(\mathsf{x}(j'))|0\rangle_F \tag{2.53}$$

where $i = \xi, \xi+\mathcal{L}$ at some time τ and $j' = \xi', \xi'+\mathcal{L}$ at some later time τ'. A schematic diagram of how the correlation functions are computed is shown in Fig. 2.4.

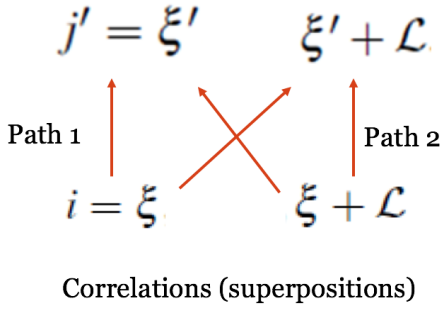

Figure 2.4: Schematic diagram of how the field correlations between the two amplitudes of the superposition, at the times τ, τ', are calculated.

In summary, the scenario in which a UDW detector travels in a superposition of trajectories related by a global coordinate transformation (i.e.

diffeomorphism) is identical to that in which the detector travels on a single worldline but interacts with the field in a superposition of equivalent coordinate transformations. The latter can be interpreted as the spacetime itself being in a superposition of coordinate transformations (the simplest case being a constant spatial translation), on which the field is quantized. All observables, like detector transition probabilities, are invariant between both perspectives. Applying this argument to a simple conceptual example, then it demonstrates that a black hole centred at $x = 0$, with a detector in a superposition of positions $x = 1, 2$, is physically equivalent to the same black hole being in a superposition of "positions" $x = -1, 0$ with the detector at a fixed trajectory at $x = 1$. What this of course emphasizes is that coordinates do not possess absolute meaning and that only relative distances have physical significance.

In [6], the authors apply these ideas to superpositions of de Sitter spacetime. As above, they show that superposition states of the spacetime, where the constituent states are related by a diffeomorphism (in particular, rotations in the higher-dimensional embedding space), are physically equivalent to the scenario in which there is one spacetime and the detector is in a superposition of angular positions. On the other hand, they also studied the case where the de Sitter length, proportional to the constant positive cosmological constant of the spacetime, was in a quantum superposition of two values. Such superpositions of curvature do not have a straightforward equivalence with a superposition of detector trajectories on a classical spacetime (one unique solution to Einstein's equation). This is because the two "universes" represent unique solutions to Einstein's equations; they are not related by a mere coordinate transformation.

This latter case is one motivation for the main goal of this thesis, which is to construct an unambiguously "quantum-gravitational" spacetime constructed from individual "spacetime states" not related by a coordinate transformation. Let us give an illustration to compare two different superpositions in a model where two different spacetime masses of a black hole are superposed. A schematic diagram of the field correlations between the two spacetime amplitudes in superposition is illustrated in Fig. 2.5.

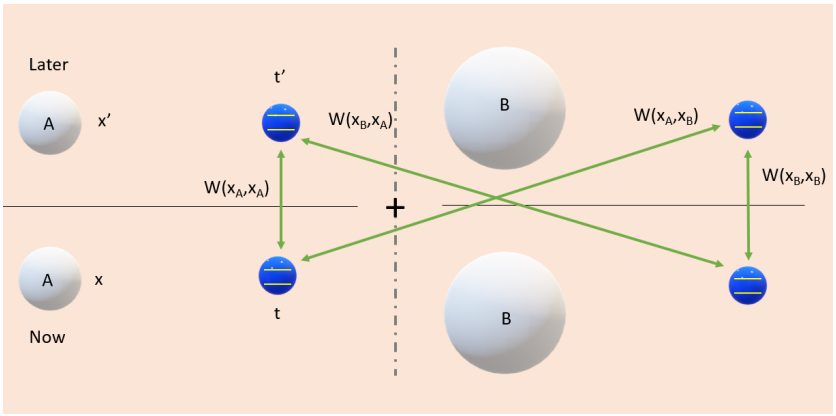

Figure 2.5: Schematic diagram of the field correlations accessed by the detector (modeled as the blue circles) as it couples to the black hole mass superposition. The black hole is in a superposition of masses denoted by "A" and "B". The Wightman functions are computed between the different amplitudes of the superposition, at the times t, t', yielding four Wightman functions.

In Fig. 2.6, we have illustrated the black hole mass superposition with the detector situated at a fixed radial distance from the origin of the coordinates. The detector essentially couples to the field which is in a superposition of amplitudes corresponding to different masses of the black hole. We are interested in any novel effects induced by the superposition to which the detector is sensitive to.

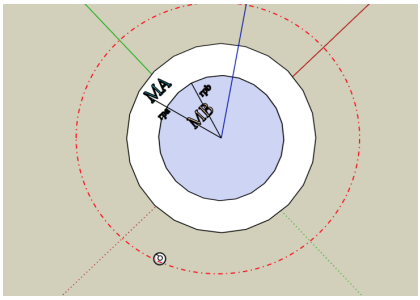

Figure 2.6: Schematic diagram of the black hole mass superposition, with a UDW detector situated at a fixed radial position and fixed angle outside.

Chapter 3

Quantum Superpositions of Minkowski Spacetime

Before moving to the mass-superposed BTZ black hole, and developing our approach for studying the operational effects of spacetime superpositions, we first consider the problem of superposing different nontrivial topological deformations of (3+1)-dimensional Minkowski spacetime. Studying quantum superpositions of Minkowski spacetime is perhaps the simplest situation in which nontrivial effects of spacetime superpositions emerge, offering considerable insight into this phenomenon. More specifically, we consider (3+1)-dimensional Minkowski spacetime with a periodic boundary condition imposed along one spatial dimension, introduced in Chapter 2.1.1. We then consider the scenario where the characteristic length scale of this periodicity is in a quantum-controlled superposition of different values.

3.1 Automorphic Field Theory in Topologically Identified Minkowski Spacetime

It is instructive to derive the flat spacetime Wightman function from the first principles. Let us consider a massless scalar field $\hat{\phi}$, which is a solution to the Klein-Gordon equation $\Box\hat{\phi}(\mathsf{x}) = 0$ (where $\Box$ is the usual d'Alembertian operator) and may be expanded in the plane wave basis

$$\hat{\phi}(\mathsf{x}) = \int \frac{\mathrm{d}^3k}{(2\pi)^{3/2}} \frac{1}{\sqrt{2|\mathbf{k}|}} \left(e^{-i|\mathbf{k}|t + i\mathbf{k}\cdot\mathbf{x}} \hat{a}_{\mathbf{k}} + e^{i|\mathbf{k}|t - i\mathbf{k}\cdot\mathbf{x}} \hat{a}^{\dagger}_{\mathbf{k}} \right) \tag{3.1}$$

where $\mathbf{k} = (k_x, k_y, k_z)$, $\mathbf{x} = (x, y, z)$ are the momentum and position three-vectors respectively, and $\hat{a}_{\mathbf{k}}$ ($\hat{a}^\dagger_{\mathbf{k}}$) are annihilation (creation) operators of a single-frequency mode. Letting $|0\rangle$ denote the Minkowski vacuum state annihilated by $\hat{a}_{\mathbf{k}}$, it can be shown that the Wightman function pulled back to the worldlines x, x' is given by [51]

$$W_{\mathcal{M}}(\mathsf{x}, \mathsf{x}') = \frac{1}{4\pi i}\mathrm{sgn}(t - t')\delta(\sigma(\mathsf{x}, \mathsf{x}')) - \frac{1}{4\pi^2\sigma(\mathsf{x}, \mathsf{x}')} \tag{3.2}$$

where $W(\mathsf{x}, \mathsf{x}') := \langle 0|\hat{\phi}(\mathsf{x})\hat{\phi}(\mathsf{x}')|0\rangle$, $\mathrm{sgn}(t - t') = \pm 1$ depending on the sign of $t - t'$, and the geodesic distance $\sigma(\mathsf{x}, \mathsf{x}')$ in a given spacetime is

$$\sigma(\mathsf{x}, \mathsf{x}') = (t - t')^2 - (x - x')^2 - (y - y')^2 - (z - z')^2. \tag{3.3}$$

As discussed previously, the Wightman function quantifies correlations in the quantum field at one spacetime event x with the same field at a different spacetime event x'. The UDW detector is therefore used to probe these correlations by interacting with the field along its trajectory parametrized by the coordinates x, x'.

In Chapter 2.1.1, we introduced the quotient space $\mathcal{M}/J_0$ (which we refer to as a cylindrical spacetime) obtained via a nontrivial topological identification of one of the spatial dimensions. To construct a quantum field theory on such a spacetime, we define the automorphic field $\hat{\psi}(\mathsf{x})$ constructed from the ordinary (massless scalar) field $\hat{\phi}(\mathsf{x})$ as the sum [52]

$$\hat{\psi}(\mathsf{x}) = \frac{1}{\sqrt{\mathcal{N}}}\sum_n \eta^n \hat{\phi}(J_0^n \mathsf{x}) \tag{3.4}$$

where $\mathcal{N} = \sum_n \eta^{2n}$ is a normalisation factor chosen to ensure that

$$\left[\hat{\psi}(\mathsf{x}), \hat{\dot{\psi}}(\mathsf{x}')\right] = \delta(\mathsf{x} - \mathsf{x}') + \text{image terms}, \tag{3.5}$$

and $\eta = \pm 1$ denotes an untwisted (twisted) field. For simplicity, we consider untwisted fields in the following. Although the normalization factor $\mathcal{N}$ is formally divergent, when computing Wightman functions with an infinite number of terms, the whole expressions are convergent. To perform numerical computations, we will in general truncate these sums at sufficiently high number of terms to achieve convergence.

To obtain the Wightman functions for a single Minkowski spacetime, we utilize Eq. (3.4) to define the two-point correlator,

$$W_{J_0}^{(D)}(\mathsf{x},\mathsf{x}') = \langle 0_M|\hat{\psi}(\mathsf{x})\hat{\psi}(\mathsf{x}')|0_M\rangle, \tag{3.6}$$

$$= \frac{1}{\mathcal{N}}\sum_{n,m}\eta^n\eta^m W_{\mathcal{M}}(J_{0_D}^n\mathsf{x}, J_{0_D}^m\mathsf{x}'), \tag{3.7}$$

where the superscript $D = A, B$ denotes the individual amplitudes of the superposition with lengths l_A, l_B. Specifically, $J_{0_A}^n$ and $J_{0_B}^m$ denote the respective isometries

$$J_{0_A} : (t,x,y,z) \mapsto (t,x,y,z+l_A), \tag{3.8}$$

$$J_{0_B} : (t,x,y,z) \mapsto (t,x,y,z+l_B). \tag{3.9}$$

Eq. 3.6 can be simplified as follows:

$$\begin{aligned} W_{J_0}^{(D)}(\mathsf{x},\mathsf{x}') &= \frac{1}{\mathcal{N}}\sum_{n,m}\eta^n(\eta^n\eta^m)W_{\mathcal{M}}(J_{0_D}^n\mathsf{x}, J_{0_D}^nJ_{0_D}^m\mathsf{x}'),\\ &= \frac{1}{\mathcal{N}}\sum_{n,m}\eta^{2n}\eta^m W_{\mathcal{M}}(\mathsf{x}, J_{0_D}^m\mathsf{x}'),\\ &= \sum_m \eta^m W_{\mathcal{M}}(\mathsf{x}, J_{0_D}^m\mathsf{x}'). \end{aligned} \tag{3.10}$$

To arrive at Eq. (3.10), we have utilized the fact that $J_{0_D}^n$, $J_{0_D}^m$ belong to the same group, allowing for the association $J_{0_D}^n \mapsto J_{0_D}^nJ_{0_D}^m$. While it is common to use the simplified form of $W_{J_0}^{(D)}$ shown in Eq. (3.10), such treatment is insufficient when considering superpositions of spacetimes. That is, for superpositions of the characteristic length of the quotient space $\mathcal{M}/J_0$, one must construct correlation functions that are essentially superpositions of the topological identification J_0, which generates two *different* discrete isometries on the fields in superposition.

Let us return to Eq. (3.6). It is important to note that the evaluation of this amplitude occurs with respect to the Minkowski vacuum state. The identification of the spacetime enforcing periodicity in the z-direction can be understood as the action of the operator J_{0_D} on the coordinates of the field. For superpositions of two cylindrical spacetimes, the Wightman function is given by

$$W_{J_0}^{(AB)}(\mathsf{x},\mathsf{x}') = \frac{1}{\mathcal{N}}\sum_{n,m}\eta^n\eta^m W_{\mathcal{M}}(J_{0_A}^n\mathsf{x}, J_{0_B}^m\mathsf{x}') \tag{3.11}$$

where

$$W_{\mathcal{M}}(J^n_{0_A}\mathsf{x}, J^m_{0_B}\mathsf{x}') = \langle 0|\hat{\phi}(J^n_{0_A}\mathsf{x})\hat{\phi}(J^m_{0_B}\mathsf{x}')|0\rangle \tag{3.12}$$

is a quantum-mechanical amplitude evaluated with respect to a single vacuum state, $|0\rangle$. While one could conceive of a scenario in quantum gravity where the vacuum state itself is quantum-controlled, this simple case does not require such an assumption. The construction of superposed quantum amplitudes of the spacetime superposition occurs through the action of two different discrete isometries $J^n_{0_A}$, $J^m_{0_B}$.

We construct the Wightman functions for the field operators quantized on the respective amplitudes of the spacetime superposition by effectively "superposing" the action of two different discrete isometries $J^n_{0_A}$, $J^m_{0_B}$ acting on the coordinates. Below, we utilize these Wightman functions to compute the transition probability of a detector situated on a background Minkowski spacetime in a superposition of these different periodic identifications.

Returning to the Wightman functions, we have explicitly for both single and superposed spacetime states

$$\begin{aligned} W^{(D)}_{J_0}(\mathsf{x},\mathsf{x}') = \frac{1}{\mathcal{N}}\sum_{n,m}\eta^n\eta^m\Bigg[&\frac{\mathrm{sgn}(t-t')\delta(\sigma(J^n_{0_D}\mathsf{x}, J^m_{0_D}\mathsf{x}'))}{4\pi i} \\ &- \frac{1}{4\pi^2\sigma(J^n_{0_D}\mathsf{x}, J^m_{0_D}\mathsf{x}')}\Bigg] \end{aligned} \tag{3.13}$$

$$\begin{aligned} W^{(AB)}_{J_0}(\mathsf{x},\mathsf{x}') = \frac{1}{\mathcal{N}}\sum_{n,m}\eta^n\eta^m\Bigg[&\frac{\mathrm{sgn}(t-t')\delta(\sigma(J^n_{0_A}\mathsf{x}, J^m_{0_B}\mathsf{x}'))}{4\pi i} \\ &- \frac{1}{4\pi^2\sigma(J^n_{0_A}\mathsf{x}, J^m_{0_B}\mathsf{x}')}\Bigg] \end{aligned} \tag{3.14}$$

where we take the superposition of two different lengths l_A, l_B for the respective discrete isometries. The UDW detector is in the same position (the origin) of the coordinate system in each spacetime. Therefore the geodesic distances for a single spacetime and for the superposition of spacetimes are respectively

$$\sigma(J^n_{0_D}x, J^m_{0_D}x') = (t-t')^2 - l_D^2(n-m)^2 \tag{3.15}$$

$$\sigma(J^n_{0_A}x, J^m_{0_B}x') = (t-t')^2 - (l_An - l_Bm)^2 \tag{3.16}$$

where $D = A, B$ in Eq. 3.15, for the isometries $(t, x, y, z) \mapsto (t, x, y, z + l_A)$ and $(t, x, y, z) \mapsto (t, x, y, z + l_B)$.

For a single cylindrical universe (taking $\eta = 1$ for simplicity), we further simplify the Wightman function into seperate image sums as $n \neq m$ and $n = m$ as shown below

$$\begin{aligned}
W_{J_0}(\mathsf{x}, \mathsf{x}') &= \frac{1}{\mathcal{N}} \sum_{n,m} \left[\frac{\mathrm{sgn}(\tau - \tau')\delta((\tau - \tau')^2 - l^2(n-m)^2)}{4\pi i} \right. \\
&\left. - \frac{1}{4\pi^2((\tau - \tau'^2 - l^2(n-m)^2)} \right] \\
&= \frac{1}{\mathcal{N}} \sum_{n,m} \left[\frac{\mathrm{sgn}(s)\delta(s^2 - l^2(n-m)^2)}{4\pi i} - \frac{1}{4\pi^2(s^2 - l^2(n-m)^2)} \right] \\
&= \frac{1}{\mathcal{N}} \sum_{n=m} \left[\frac{\mathrm{sgn}(s)\delta(s^2)}{4\pi i} - \frac{1}{4\pi^2 s^2} \right] + \frac{1}{\mathcal{N}} \sum_{n \neq m} \left[\frac{\mathrm{sgn}(s)\delta(s^2 - l^2(n-m)^2)}{4\pi i} \right. \\
&\left. - \frac{1}{4\pi^2(s^2 - l^2(n-m)^2)} \right] \\
&= W_{\mathcal{M}}(s) + \frac{1}{\mathcal{N}} \sum_{n \neq m} \left[\frac{\mathrm{sgn}(s)\delta(s^2 - l^2(n-m)^2)}{4\pi i} \right. \\
&\left. - \frac{1}{4\pi^2(s^2 - l^2(n-m)^2)} \right] \qquad (3.17)
\end{aligned}$$

where we have defined $s = \tau - \tau'$.

From the form of (3.17), we find that the Wightman function for the cylindrical spacetime comprises a contribution from standard Minkowski space ($W_{\mathcal{M}}(s)$) and another term containing contributions from the topological identification of the z-coordinate.

For the superposition case (taking $\eta = 1$ for simplicity), we group the image sums in a similar way, splitting up the sum into contributions from $l_A n \neq l_B m$ and $l_A n = l_B m$, obtaining

$$\begin{aligned}
W_{J_0}^{AB} &= \frac{1}{\sum_n \eta^{2n}} \sum_{n=-\infty}^{\infty} \sum_{m=-\infty}^{\infty} \left[\frac{1}{4\pi i} \mathrm{sgn}(t - t')\delta((t - t')^2 - (l_A n - l_B m)^2) \right. \\
&\left. - \frac{1}{4\pi^2(t - t')^2 - (l_A n - l_B m)^2} \right],
\end{aligned}$$

$$
\begin{aligned}
&= \frac{1}{\sum_n \eta^{2n}} \sum_{l_A n = l_B m} \left[\frac{1}{4\pi i} \mathrm{sgn}(t-t') \delta((t-t')^2) - \frac{1}{4\pi^2 (t-t')^2} \right] \\
&+ \frac{1}{\sum_n \eta^{2n}} \sum_{l_A n \neq l_B m} \left[\frac{1}{4\pi i} \mathrm{sgn}(t-t') \delta((t-t')^2 - (l_A n - l_B m)^2) \right. \\
&\left. - \frac{1}{4\pi^2 (t-t')^2 - (l_A n - l_B m)^2} \right] \\
&= \frac{1}{\sum_n \eta^{2n}} \left[\sum_{l_A n = l_B m} W_{\mathcal{M}} + \sum_{l_A n \neq l_B m} \left[\frac{1}{4\pi i} \mathrm{sgn}(t-t') \delta((t-t')^2 \right. \right. \\
&\left. \left. - (l_A n - l_B m)^2) - \frac{1}{4\pi^2 (t-t')^2 - (l_A n - l_B m)^2} \right] \right] \qquad (3.18)
\end{aligned}
$$

3.2 Unruh-DeWitt Detector in Superposed Minkowski Spacetime

We aim to study the effects induced by the superposed Minkowski spacetime via a relativistic quantum matter which is coupled to the spacetime through its interaction with a (massless scalar) quantum field. As usual, we can describe this system in the Hilbert space $\mathcal{H} = \mathcal{H}_{\mathrm{S}} \otimes \mathcal{H}_{\mathrm{F}} \otimes \mathcal{H}_{\mathrm{M}}$ which is a tensor product of the spacetime, quantum field, and matter degrees of freedom respectively. We shall employ the formalism from Chapter 2.2 for UDW detectors in superposed spacetime.

As discussed in the previous subsection, we consider the topologically identified M_0 spacetime in a superposition of two characteristic identification lengths l_A and l_B, and the field in the Minkowski vacuum state. The state of the combined spacetime-field-detector system is given by,

$$
|\psi(t_i)\rangle = \frac{1}{\sqrt{2}} (|l_A\rangle + |l_B\rangle) |0\rangle |g\rangle \qquad (3.19)
$$

where $|0\rangle$ is the vacuum field state and $(|l_A\rangle + |l_B\rangle)/\sqrt{2}$ is the superposition state of the spacetime with two different characteristic lengths l_A and l_B.

The coupling between the spacetime superposition, field, and detector is described by the following interaction Hamiltonian:

$$
\hat{H}_{\mathrm{int.}} = \lambda \eta(\tau) \hat{\sigma}(\tau) \sum_{i=A,B} \hat{\psi}(\mathsf{x}_i(\tau)) \otimes |l_i\rangle\langle l_i|. \qquad (3.20)
$$

The projector $|l_i\rangle\langle l_i|$ acts as a quantum control for the spacetime. The quantum control could be some ancillary system that is entangled with spacetime and can be ideally time-evolved and measured in a Mach-Zehnder-type interferometer. For simplicity, we need not posit such an ancilla, since we already know the cylindrical identifications of Minkowski spacetime put it in a superposition of circumference lengths, and assume, as recent work has, that a "measurement" can be performed that allows one to witness interference effects between the spacetime amplitudes in superposition [53].

Formally, the basis states $|l_i\rangle$ are energy eigenstates of the free Hamiltonian where $\hat{H}_{0,S}|l_i\rangle = E_i|l_i\rangle$ where E_i are the (Casimir) energies associated with the periodic length l_i. This will generally introduce a time-dependent phase into the evolution of the superposition. For simplicity, it is instructive to consider a rotating frame transformation [54] for which the evolution of the superposition state is "frozen" to the initial phase relationship. Such an assumption greatly simplifies the calculations without losing a significant amount of insight into the problem.

As usual, we evolve the initial state in time with the unitary

$$\hat{U} = \sum_{i=A,B} \hat{U}_i|l_i\rangle\langle l_i|, \tag{3.21}$$

yielding

$$\hat{U}|\psi(t_i)\rangle = \frac{1}{\sqrt{2}}(\hat{U}_A|l_A\rangle + \hat{U}_B|l_B\rangle)|0\rangle|g\rangle \tag{3.22}$$

before measuring the control state in the superposition basis $|\pm\rangle = (|l_A\rangle \pm |l_B\rangle)/\sqrt{2}$ and tracing out the final field states. This leaves the following result for the joint transition probability of the detector,

$$\hat{\rho}_D = \begin{pmatrix} 1 - P_G^{(\pm)} & 0 \\ 0 & P_E^{(\pm)} \end{pmatrix}, \tag{3.23}$$

where the $\pm$ signs indicate a measurement in the $|\pm\rangle$ basis. Note that the state Eq. (3.23) is not normalized, since we are considering final *conditional* states of the detector. The excited state transition probability of the detector is more specifically given by

$$P_E^{(\pm)} = \frac{\lambda^2}{4}\Big(P_A + P_B \pm 2L_{AB}\Big) \tag{3.24}$$

where

$$P_D = \int_{-\infty}^{\infty} \mathrm{d}\tau \int_{-\infty}^{\infty} \mathrm{d}\tau' \chi(\tau)\overline{\chi}(\tau') W_{J_0}^{D}(\mathsf{x},\mathsf{x}') \tag{3.25}$$

is the transition probability of a single detector in a cylindrical spacetime with characteristic identification length l_D ($D = A, B$), and

$$L_{AB} = \int_{-\infty}^{\infty} \mathrm{d}\tau \int_{-\infty}^{\infty} \mathrm{d}\tau' \chi(\tau)\overline{\chi}(\tau') W_{J_0}^{AB}(\mathsf{x},\mathsf{x}') \tag{3.26}$$

is a cross-correlation term between the field on the background spacetime in a superposition of two characteristic identification lengths, l_A and l_B. We have also defined

$$\chi(\tau) = \exp\left(-\frac{\tau^2}{2\sigma^2}\right) e^{-i\Omega\tau} \tag{3.27}$$

as a Gaussian switching function with characteristic width σ. The introduction of a time-dependent switching function is necessary for a particle detector in flat Minkowski spacetime to detect any field quanta. A detector eternally interacting with the field will remain in its ground state. The result is interpreted as a manifestation of the energy-time uncertainty principle, in which rapidly switched interactions may promote virtual vacuum fluctuations into the detection of real field quanta (thus exciting the detector).

If one traces out the control qubit rather than measuring it in a superposition basis, the detector transition probability becomes a classical mixture of the individual contributions from spacetime amplitudes A and B:

$$P_E^{(\mathrm{Tr})} = \frac{\lambda^2}{2}\Big(P_A + P_B\Big), \tag{3.28}$$

as expected.

Returning to the conditional transition probability (conditioned on measuring the control/spacetime in the state $|\pm\rangle$), we can insert the Wightman functions, (3.13) and (3.14), into (3.25) and (3.26), to obtain the "local" contribution to the transition probability. We have for the "local contributions" to the transition probability, P_D where $D = A, B$, given by

$$P_D = \frac{1}{\sum_n \eta^{2n}} \sum_{n,m} \int_{-\infty}^{\infty} \mathrm{d}\tau \int_{-\infty}^{\infty} \mathrm{d}\tau' e^{-\frac{\tau^2}{2\sigma^2}} e^{-\frac{\tau'^2}{2\sigma^2}} e^{-i\Omega(\tau-\tau')}$$

$$\left[\frac{\mathrm{sgn}(\tau-\tau')\delta((\tau-\tau')^2-l^2(n-m)^2)}{4\pi i}-\frac{1}{4\pi^2((\tau-\tau')^2-l^2(n-m)^2)}\right]$$
$$=\frac{1}{\sum_n \eta^{2n}}\sum_{n=m}\int_{-\infty}^{\infty}\mathrm{d}\tau\int_{-\infty}^{\infty}\mathrm{d}\tau' e^{-\frac{\tau^2}{2\sigma^2}}e^{-\frac{\tau'^2}{2\sigma^2}}e^{-i\Omega(\tau-\tau')}\left[\frac{\mathrm{sgn}(\tau-\tau')\delta((\tau-\tau')^2}{4\pi i}\right.$$
$$\left.-\frac{1}{4\pi^2(\tau-\tau')^2}\right]$$
$$+\frac{1}{\sum_n \eta^{2n}}\sum_{n\neq m}\int_{-\infty}^{\infty}\mathrm{d}\tau\int_{-\infty}^{\infty}\mathrm{d}\tau' e^{-\frac{\tau^2}{2\sigma^2}}e^{-\frac{\tau'^2}{2\sigma^2}}e^{-i\Omega(\tau-\tau')}$$
$$\left[\frac{\mathrm{sgn}(\tau-\tau')\delta((\tau-\tau')^2-l^2(n-m)^2)}{4\pi i}-\frac{1}{4\pi^2((\tau-\tau')^2-l^2(n-m)^2)}\right]$$
$$=P_{\mathcal{M}}-\frac{\sigma}{4\sqrt{\pi}l_D\sum_n \eta^{2n}}\Big[S_1-S_2\Big] \tag{3.29}$$

where

$$P_{\mathcal{M}}=\frac{1}{4\pi}\left[e^{-\sigma^2\Omega^2}-\sqrt{\pi}\sigma\Omega\mathrm{erfc}(\sigma\Omega)\right] \tag{3.30}$$

is the transition probability of a single detector in flat Minkowski spacetime with no identifications, and

$$S_1=2\sum_{n-m>0}\frac{e^{-\frac{l_D^2(n-m)^2}{4\sigma^2}}}{n-m}\sin(\Omega l_D(n-m)), \tag{3.31}$$

$$S_2=\sum_{n\neq m}\frac{e^{-\frac{l_D^2(n-m)^2}{4\sigma^2}}}{(n-m)}\mathrm{Im}\left[e^{il_D(n-m)\Omega}\mathrm{erf}\left(\frac{il_D(n-m)}{2\sigma}+\sigma\Omega\right)\right], \tag{3.32}$$

which we have derived in the Appendix. Equation (3.29) is formally equivalent to the expression studied in [51] for the single-detector transition probability in the M_0 spacetime. We see that there is both a Minkowski contribution and an image sum contribution that accounts for the possible identifications in the M/J_0 space.

Meanwhile, the cross-correlation term L_{AB} has the same form as P_D in (3.29) but with $l_An = l_Bm$ and $l_An \neq l_Bm$ image sum conditions. This cross-correlation term simplifies to the expression below, as shown in Appendix A. We find

$$L_{AB}=\frac{K_\gamma}{\sum_n \eta^{2n}}P_{\mathcal{M}}+\frac{\sigma}{4\sqrt{\pi}\sum_n \eta^{2n}}\Big[J_1-J_2\Big] \tag{3.33}$$

where

$$J_1 = \sum_{l_A n \neq l_B m} \frac{e^{-\frac{l_{nm}^2}{4\sigma^2}}}{l_{nm}} \mathrm{Im}\left[e^{i l_{nm}\Omega} \mathrm{erf}\left[\frac{i l_{nm}}{2\sigma} + \sigma\Omega \right] \right] \tag{3.34}$$

$$J_2 = 2 \sum_{l_{nm}>0} \frac{e^{-\frac{l_{nm}^2}{4\sigma^2}}}{l_{nm}} \sin(\Omega l_{nm}) \tag{3.35}$$

and $l_{nm} = l_A n - l_B m$. Likewise, we have defined

$$K_\gamma = \mathsf{coeff}\left(\sum_{n,m} f\left(n - \gamma m\right), f(0) \right) \tag{3.36}$$

where $\gamma = l_B/l_A$ is the ratio of the cylindrical spaces in superposition, and $\mathsf{coeff}(x(y), y)$ is the coefficient of y in the function $x(y)$. The appearance of this function results from the evaluation of the image sum contributions to L_{AB}. Notice in particular that the Wightman function for the cross-term, Eq. (3.14), contains multiple singular points whenever $n - \gamma m = 0$ (see for example the denominator of Eq. (3.34) and (3.35)). These poles are treated differently in comparison to the single pole, which is presented in the Minkowski Wightman function given at the beginning of Chapter 3.1. Thus, when summing over the identification variables (n, m), one "pulls out" a Minkowski contribution to the total expression for L_{AB}, whenever $n - \gamma m = 0$. The appearance of these "resonances" whenever $n = \gamma m$ for rational n and m numbers is something that we shall also encounter when we consider the BTZ spacetime. In that scenario, we shall see that the mass ratios for which a "resonance" appeared agree with those predicted by Bekenstein in his famous quantum black hole conjecture, wherein the black hole mass is treated as a quantum number.

3.3 Results

We are now able to plot the response of the detector to the field, situated in this universe that is in a superposition of topologies.

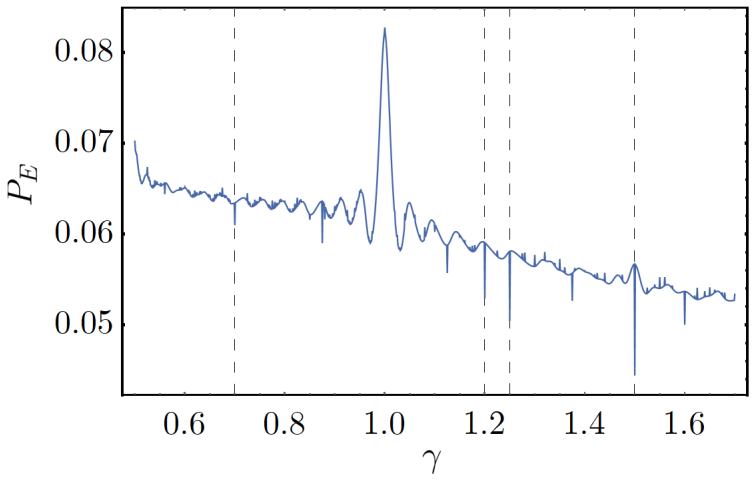

Figure 3.1: The transition probability of the detector after the control is measured in the $|+\rangle$ state, as a function of γ. We have marked out a few values at which resonances in the transition probability are visible. We have set $\Omega\sigma = 1/100$ and $l_A = 1$.

In Fig. 3.1, we have plotted the transition probability of the detector as a function of γ, the ratio of the characteristic lengths of the superposed spacetimes. There are several physical features of the transition probability worth noting. Most interestingly, we observe discontinuous resonant peaks in the transition probability at rational values of γ – some of these values are marked with vertical dashed lines. In reality, we expect a countably infinite number of these discrete peaks at every rational value of γ, just by inspecting the discontinuous form of the interference term in Eq. (A.12). Of course, the magnitude of these peaks may not necessarily be visible; moreover, we are limited by the finite computational step size of MATHEMATICA. Nevertheless, this effect, as measured by an Unruh-DeWitt-type detector, seems to be the first of its kind as a prescription for the detection of a quantum-gravitational effect.

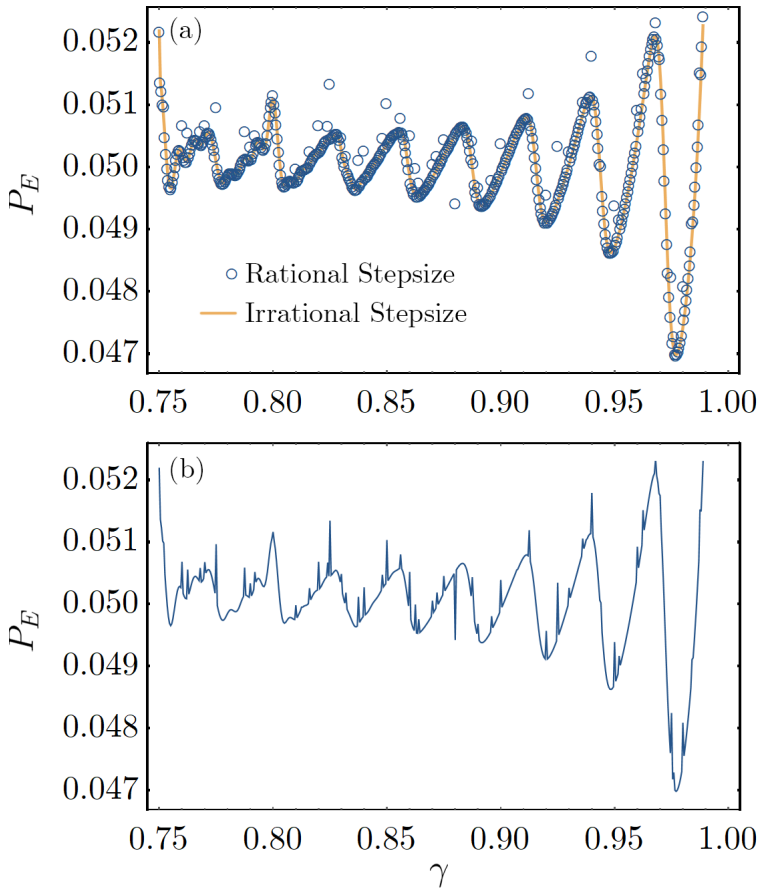

Figure 3.2: (a) Illustration of the discontinuous behavior of the transition probability as a function of γ. The continuous yellow line was plotted with irrational step size, and hence the resonant peaks at values of γ do not appear. (b) The same dataset is shown with the open circles in (a), but with the data points connected. We have used the settings $\Omega\sigma = 1/100$ and $l_A = 2$.

To illustrate this further, we have plotted the transition probability of the detector as a function of γ using rational and irrational step sizes in Fig. 3.2. When the step size used to plot P_E is irrational, the transition probability appears to be smooth and continuous. This is in strong contrast with the discontinuous nature of P_E when utilizing rational step sizes in MATHEMATICA, and thus confirms the source of the resonant effect shown in Fig. 3.1.

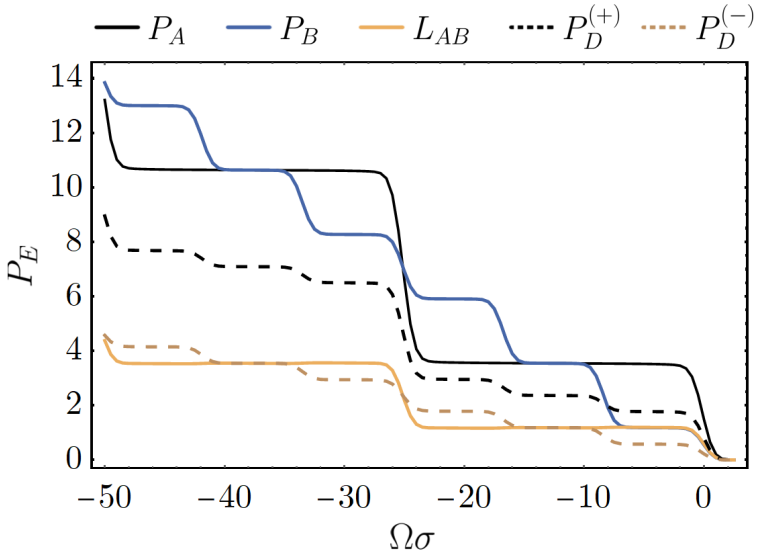

Figure 3.3: Transition probability of the detector as a function of the energy gap. The black dashed line represents the transition probability when the control is measured in $|+\rangle$, while the brown dashed line represents the transition probability when the control is measured in $|-\rangle$. We have chosen $l_A/\sigma = 0.25$, $l_B/\sigma = 0.75$.

In Fig. 3.3, we have plotted the transition probability as a function of the energy gap of the detector, for a superposition of two lengths l_A, l_B. The individual contributions to the transition probability are shown in different colors, giving the total result displayed with the dashed lines (the different colors representing two different measurement bases for the control).

Overall we found our results exhibit the induced resonance for the ratios of particle's transition probabilities at the topology superposition of background spacetimes. Thus, this result legitimizes the use of vacuum state when studying quantum effects of spacetime superpositions and led us to continue on superposing spacetimes that can reveal more explicit quantum gravitational effects as in Chapter 4.

Chapter 4

Mass Superpositions of the BTZ Black Hole

In light of the results from the previous research, in which we derived a novel resonance effect of the Minkowski spacetime superposition, the purpose of this Chapter is to study the operational effects produced by a mass-superposed black hole, as detected by a static UDW detector situated outside it.

As in the Minkowski case, to construct a QFT on the BTZ black hole background, we need the theory of automorphic fields. Instead of periodic identifications of Minkowski spacetime, the BTZ black hole is now constructed from periodic identifications of AdS-Rindler spacetime. The method of constructing the black hole superposition is similar to that applied to Minkowski spacetime in the previous Chapter.

We consider the field quantized on a background arising from superposing BTZ spacetimes with different black hole masses. This can be achieved by superposing two different identifications Γ_A and Γ_B of the Y coordinate in Eq. 2.4. As usual, the black hole–quantum field system can be described in the tensor product Hilbert space $\mathcal{H} = \mathcal{H}_{\rm BH} \otimes \mathcal{H}_{\rm F}$, where we consider the black hole to be (without loss of generality) in a symmetric superposition[1] of two mass states $|M_A\rangle$, $|M_B\rangle$ while the field is in the AdS vacuum $|0\rangle$. Again, we consider an automorphic field $\hat{\psi}(\mathsf{x})$ that is constructed from an ordinary (conformally coupled massless scalar) field $\hat{\phi}$ in (2+1)-dimensional

[1] Conceptually, a black hole mass-superposition may be generated by sending a photon prepared in a wavepacket distribution of frequencies into the black hole. This would in general create a black hole in a superposition of energy (i.e. mass-energy) eigenstates.

AdS spacetime (AdS_3) via the periodic identification Γ, which enacts the identification $Y \to Y + 2\pi n\sqrt{M}$ coordinate (Henceforth, we use the nomenclature ϕ in the place of Y, denoting an angular coordinate in the black hole spacetime) in AdS-Rindler spacetime, yielding [55]

$$\hat{\psi}(\mathsf{x}) := \frac{1}{\sqrt{\mathcal{N}}} \sum_n \eta^n \hat{\phi}(\Gamma^n \mathsf{x}) \tag{4.1}$$

where $\mathsf{x} = (t, r, \phi)$ are spatial coordinates of the black hole spacetime. The image sum is a result of the periodic identification of AdS-Rindler space as in Eq. (2.5). As we have done previously, we consider untwisted fields corresponding to $\eta = +1$, and $\mathcal{N} = \sum_n \eta^{2n}$ is a normalization constant.

As usual, we require Wightman functions evaluated "locally" (on the individual amplitudes of the spacetime superposition) and "nonlocally" (between the spacetime amplitudes in superposition). The local terms (the Wightman function for a single spacetime) are constructed from the AdS_3 Wightman function,

$$\begin{aligned} W^{(D)}_{\mathrm{BTZ}}(\mathsf{x}, \mathsf{x}') &= \frac{1}{\mathcal{N}} \sum_{n,m} \eta^n \eta^m \langle 0 | \hat{\phi}(\Gamma^n_D \mathsf{x}) \hat{\phi}(\Gamma^m_D \mathsf{x}') | 0 \rangle \\ &= \frac{1}{\sum_n \eta^{2n}} \sum_n \sum_m \eta^n \eta^m W_{\mathrm{AdS}}(\Gamma^n_D \mathsf{x}, \Gamma^m_D \mathsf{x}') \end{aligned} \tag{4.2}$$

where $\Gamma_D \mathsf{x}$ denotes the action of the identification $\phi \to \phi + 2\pi n\sqrt{M_D}$ on the spacetime point x. As demonstrated previously, this form of the Wightman function is equivalent to the more commonly used (and simplified) form in the literature [56]

$$W^{(D)}_{\mathrm{BTZ}}(\mathsf{x}, \mathsf{x}') = \sum_m \eta^m W_{\mathrm{AdS}}(\mathsf{x}, \Gamma^m_D \mathsf{x}'). \tag{4.3}$$

When computing the cross-correlation Wightman functions between black holes of different masses, we need the more general form Eq. (4.2). Note that we have assumed that the field state on the right-hand side of Eq. (4.2) is the AdS Rindler vacuum state $|0\rangle$, analogous to our choice of the Minkowski vacuum state as the ground state in the cylindrical universe superposition. In the standard BTZ spacetime (no superposition), the vacuum thermal properties of the black hole arise from the topological identifications acting on the

field state $|0\rangle$ (see [57] for details of constructing the BTZ Wightman function as an image sum of the vacuum AdS Wightman function and demonstrating its thermal properties via periodicity in imaginary time).

To derive the relevant BTZ Wightman functions, we begin with the Wightman function for a massless, conformally coupled scalar field in the AdS_3 vacuum, given by [57, 58]

$$W_{\rm AdS}(\mathsf{x},\mathsf{x}') = \frac{1}{4\pi l\sqrt{2}}\left[\frac{1}{\sqrt{\sigma(\mathsf{x},\mathsf{x}')}} - \frac{\zeta}{\sqrt{\sigma(\mathsf{x},\mathsf{x}')+2}}\right] \tag{4.4}$$

where

$$\sigma(\mathsf{x},\mathsf{x}') = \frac{1}{2l^2}\left[(X_1-X_1')^2 - (T_1-T_1')^2 + (X_2-X_2')^2 - (T_2-T_2')^2\right] \tag{4.5}$$

is the squared geodesic between x and x' in the embedding space $\mathbb{R}^{(2,2)}$ and (X_1,T_1,X_2,T_2) are given by Eq. (2.11). The parameter $\zeta\in[-1,1]$ encodes the boundary condition at infinity for AdS spacetime, while the special values $\zeta=\{-1,0,1\}$ correspond to Neumann, transparent, and Dirichlet boundary conditions respectively. For simplicity, we consider only transparent boundary conditions ($\zeta=0$), however, the results are easily extended to generic boundary conditions.

Returning to our Wightman function Eq. (4.2), we need to calculate $\sigma(\Gamma_D^n\mathsf{x},\Gamma_D^m x')$. Inserting the BTZ-scaled AdS_3 coordinates (2.8) into Eq. (4.5) along with the periodic identification of the ϕ coordinate $\phi\to\phi+2\pi n\sqrt{M_D}$, we obtain

$$\begin{aligned}\sigma(\Gamma^n\mathsf{x},\Gamma^m\mathsf{x}') &= \frac{R_D^2}{l^2}\cosh\left[2\pi(m-n)\sqrt{M_D}\right] - 1 - \left[\frac{R_D^2}{l^2}-1\right]\cosh\frac{t-t'}{l}\\ &= \tilde\gamma_D^2\left[\frac{\tilde R_D^2}{M_D\tilde\gamma_D^2 l^2}\cosh\left[2\pi(m-n)\sqrt{M_D}\right] - \frac{1}{\tilde\gamma_D^2} - \cosh\frac{t-t'}{l}\right],\end{aligned} \tag{4.6}$$

where $\tilde\gamma_D=\sqrt{\tilde R_D^2/l^2-1}$ and the tildes denote that we have identified the AdS R_D with the scaled BTZ coordinate. Since the time coordinate will be integrated over when computing the transition probability, we have not rescaled the time coordinate. The BTZ Wightman function can thus be

written as

$$W^{(D)}_{\mathrm{BTZ}}(\mathsf{x},\mathsf{x}') = \frac{1}{\sum_n \eta^{2n}} \frac{1}{\tilde{\gamma}_D} \frac{1}{4\pi l\sqrt{2}} \sum_n \sum_m \frac{1}{\sqrt{\frac{\tilde{R}_D^2}{M_D \tilde{\gamma}_D^2 l^2} \cosh(2\pi(m-n)\sqrt{M_D}) - \frac{1}{\tilde{\gamma}_D^2} - \cosh(s/l)}} \tag{4.7}$$

where $s = t - t'$. For the cross term, the geodesic distance is

$$\begin{aligned}
\sigma(\Gamma_A^n \mathsf{x}, \Gamma_B^m \mathsf{x}') &= \sqrt{\frac{R_A^2}{l^2}}\sqrt{\frac{R_B^2}{l^2}} \cosh\left[2\pi(m\sqrt{M_A} - n\sqrt{M_B})\right] \\
&\quad - 1 - \sqrt{\frac{R_A^2}{l^2} - 1}\sqrt{\frac{R_B^2}{l^2} - 1} \cosh\frac{t-t'}{l} \qquad (4.8) \\
&= \tilde{\gamma}_A \tilde{\gamma}_B \left[\sqrt{\frac{\tilde{R}_A^2}{M_A \tilde{\gamma}_A^2 l^2}}\sqrt{\frac{\tilde{R}_B^2}{M_B \tilde{\gamma}_B^2 l^2}} \cosh\left[2\pi(m\sqrt{M_B} - n\sqrt{M_B})\right]\right. \\
&\quad \left. - \frac{1}{\tilde{\gamma}_A \tilde{\gamma}_B} - \cosh\frac{t-t'}{l}\right. \qquad (4.9) \\
&= \tilde{\gamma}_A \tilde{\gamma}_B \left[\frac{\tilde{R}_D^2}{\tilde{\gamma}_A \tilde{\gamma}_B \sqrt{M_A M_B} l^2} \cosh\left[2\pi(m\sqrt{M_A} - n\sqrt{M_B})\right]\right. \\
&\quad \left. - \frac{1}{\tilde{\gamma}_A \tilde{\gamma}_B} - \cosh\frac{t-t'}{l}\right. \qquad (4.10)
\end{aligned}$$

In the last line, we have assumed that detector is at a single radial coordinate $R_A = R_B = R_D$. The Wightman function is straightforwardly obtained by substituting Eq. (4.10) into Eq. (4.2). We finally note that $W^{(AB)}_{\mathrm{BTZ}}(\mathsf{x},\mathsf{x}')$ straightforwardly reduces to $W^{(D)}_{\mathrm{BTZ}}(\mathsf{x},\mathsf{x}')$ when $M_A \to M_B = M_D$.

4.1 Unruh DeWitt Detector Coupling to Superposed BTZ Black Hole Spacetime

Having derived the Wightman functions relevant to the problem (two "local" amplitudes and two "nonlocal" ones that a UDW will naturally access via its interaction with the field), we now wish to compute the transition probability of a detector residing in the mass-superposed BTZ spacetime.

First, let us recall that in the interaction picture, states evolve as

$$|\psi(t_f)\rangle = e^{-i\hat{H}_{0,S}t_f}\hat{U}e^{i\hat{H}_{0,S}t_i}|\psi(t_i)\rangle \tag{4.11}$$

where $\hat{H} = \hat{H}_0 + \hat{H}_{\text{int.}}$ is the full Hamiltonian, comprised of a free Hamiltonian and an interaction Hamiltonian. t_i and t_f are the initial and final times of the evolution. The detector couples to the field and black hole via the interaction Hamiltonian,

$$\hat{H}_{\text{int.}} = \lambda\eta(\tau)\hat{\sigma}(\tau)\sum_{D=A,B}\hat{\psi}(\mathsf{x}_D)\otimes|M_D\rangle\langle M_D| \tag{4.12}$$

where $|M_D\rangle\langle M_D|$ is a projector on the black hole mass, and $\hat{\psi}(x_D)$ is the field operator for the spacetime associated with amplitude D of the black hole mass superposition. This interaction means that for each BTZ black hole mass M_D, the field is identified accordingly, i.e. $(t, r, \phi) \to (t, r, \phi + 2\pi n\sqrt{M_D})$.

$\hat{U}_I(t_f, t_i)$ is our usual interaction picture time-evolution operator expanded (for ease of communication) to second order in the coupling constant λ:

$$\hat{U}_I(t_f, t_i) = I - i\lambda\int_{t_i}^{t_f}\mathrm{d}\tau\,\hat{H}_{\text{int.}}(\tau) - \lambda^2\int_{t_i}^{t_f}\int_{t_i}^{\tau}\mathrm{d}\tau\mathrm{d}\tau'\hat{H}_{\text{int.}}(\tau)\hat{H}_{\text{int.}}(\tau') \tag{4.13}$$

In the previous Chapter, we took the integral bounds to be $(-\infty, \infty)$ instead of from t_i to t_f. This was due to our neglect of the free evolution of the control state associated with the spacetime amplitudes. Here, we wish to incorporate these free dynamics into our analysis, for which finite time integral limits are necessary (this is a common technique in atomic physics when considering superpositions of mass-energy eigenstates). We note also that we are assuming that the times t_i, t_f are determined with respect to a faraway observer at sufficiently large r, whose "clock state" is factorizable from the rest of the system. Such a choice is justified since for sufficiently large radial coordinate r, the fractional difference in proper times of the clock between two spacetimes with mass M_A and M_B respectively is $(M_B - M_A)l^2/r^2$. We note that another choice for the "clock state" is one that is entangled with the black hole's mass. It is expected for a theory of quantum gravity description of spacetime superpositions to permit both of these kinds of states [59], though for simplicity we have assumed the former. Now, let us take

our initial state of the black hole to be a superposition of mass (energy) eigenstates:

$$|\psi_S(t_i)\rangle = \frac{1}{\sqrt{2}}\left(|M_1\rangle + |M_2\rangle\right)|0\rangle|g\rangle \tag{4.14}$$

Thus, the full evolution is

$$\begin{aligned}|\psi(t_f)\rangle = e^{-i\hat{H}_{0,S}t_f}e^{i\hat{H}_{0,S}t_i}\frac{1}{\sqrt{2}}(|M_A\rangle + |M_B\rangle)|0\rangle|g\rangle \\ - e^{-i\hat{H}_{0,S}t_f}(i\lambda)\int \mathrm{d}\tau\ \hat{H}_{\text{int.}}(\tau)e^{i\hat{H}_{0,S}t_i}\frac{1}{\sqrt{2}}(|M_A\rangle + |M_B\rangle)|0\rangle|g\rangle \\ - e^{-i\hat{H}_{0,S}t_f}(\lambda^2)\iint_{\mathcal{T}}\mathrm{d}\tau\mathrm{d}\tau'\hat{H}_{\text{int.}}(\tau)\hat{H}_{\text{int.}}(\tau')e^{i\hat{H}_{0,S}t_i}\frac{1}{\sqrt{2}}(|M_A\rangle + |M_B\rangle)|0\rangle|g\rangle\end{aligned} \tag{4.15}$$

After factorization, a relative phase is introduced between the states of the black hole, yielding the following terms in the final state:

$$|\psi(t_f)\rangle^{(0)} = \frac{1}{\sqrt{2}}(|M_A\rangle + e^{-i\Delta E\Delta t}|M_B\rangle)|0\rangle|g\rangle \tag{4.16}$$

$$|\psi(t_f)\rangle^{(1)} = -\frac{i\lambda}{\sqrt{2}}\int_{t_i}^{t_f}\mathrm{d}\tau\ \eta(\tau)e^{i\Omega\tau}\Big[\hat{\psi}(\mathsf{x}_A)|M_A\rangle + \hat{\psi}(\mathsf{x}_B)e^{-i\Delta E\Delta t}|M_B\rangle\Big]|0\rangle|e\rangle \tag{4.17}$$

$$\begin{aligned}|\psi(t_f)\rangle^{(2)} = -\frac{\lambda^2}{\sqrt{2}}\int_{t_i}^{t_f}\int_{t_i}^{t_f}\mathrm{d}\tau\mathrm{d}\tau'\eta(\tau)\eta(\tau')e^{-i\Omega(\tau-\tau')}\Big[\hat{\psi}(\mathsf{x}_A)\hat{\psi}(\mathsf{x}'_A)|M_A\rangle \\ + \hat{\psi}(\mathsf{x}_B)\hat{\psi}(\mathsf{x}'_B)e^{-i\Delta E\Delta t}|M_B\rangle\Big]|0\rangle|g\rangle\end{aligned} \tag{4.18}$$

where $\Delta E = E_B - E_A$ is the energy gap between the eigenstates and $\Delta t = t_f - t_i$. Below, we consider the final conditional detector-field state for various measurements of the black hole. A detailed evaluation of the final state is shown in Appendix B.

4.1.1 Measurement in the $|\pm\rangle = (|M_A\rangle \pm |M_B\rangle)/\sqrt{2}$ Basis

Let us first consider a conditional measurement in the $|\pm\rangle = (|M_A\rangle \pm |M_B\rangle)/\sqrt{2}$. The terms at zeroth, first, and second order in the coupling

are given by:

$$\langle \pm|\psi(t_f)\rangle^{(0)} = \frac{(\langle M_1| \pm \langle M_2|)}{2}\left(|M_1\rangle + e^{-i\Delta E\Delta t}|M_2\rangle\right)|0\rangle|g\rangle \tag{4.19}$$

$$\langle \pm|\psi(t_f)\rangle^{(1)} = -\frac{i\lambda}{2}\int \mathrm{d}\tau\, \eta(\tau)e^{i\Omega\tau}\Big[\hat{\psi}(\mathsf{x}_A) \pm \hat{\psi}(\mathsf{x}_B)e^{-i\Delta E\Delta t}\Big]|0\rangle|e\rangle \tag{4.20}$$

$$\begin{aligned}\langle \pm|\psi(t_f)\rangle^{(2)} = -\frac{\lambda^2}{2}\iint_{\mathcal{T}} \mathrm{d}\tau\mathrm{d}\tau'\eta(\tau)\eta(\tau')e^{-i\Omega(\tau-\tau')}\Big[\hat{\psi}(\mathsf{x}_A)\hat{\psi}(\mathsf{x}'_A) \\ \pm \hat{\psi}(\mathsf{x}_B)\hat{\psi}(\mathsf{x}'_B)e^{-i\Delta E\Delta t}\Big]|0\rangle|g\rangle\end{aligned} \tag{4.21}$$

When computing the reduced density matrix (after tracing out the field) we are left with the following expressions:

$$\mathrm{Tr}_\psi\left[\hat{U}^{(0)}\hat{\rho}_{\mathrm{FD}}\hat{U}^{(0)\dagger}\right] = \frac{1}{4}\Big[2 \pm 2\cos\Delta E\Delta t\Big]|g\rangle\langle g| \tag{4.22}$$

$$\begin{aligned}\mathrm{Tr}_\psi\left[\hat{U}^{(0)}\hat{\rho}_{\mathrm{FD}}\hat{U}^{(2)\dagger}\right] = -\frac{\lambda^2|g\rangle\langle g|}{4}\iint_{\mathcal{T}} \mathrm{d}\tau\mathrm{d}\tau'\eta(\tau)\eta(\tau')e^{i\Omega(\tau-\tau')} \\ \Big[W(\mathsf{x}_A,\mathsf{x}'_A)\Big(1 \pm e^{-i\Delta E\Delta t}\Big) + W(\mathsf{x}_B,\mathsf{x}'_B)\Big(1 \pm e^{i\Delta E\Delta t}\Big)\Big]\end{aligned} \tag{4.23}$$

$$\begin{aligned}\mathrm{Tr}_\psi\left[\hat{U}^{(2)}\hat{\rho}_{\mathrm{FD}}\hat{U}^{(0)\dagger}\right] = -\frac{\lambda^2|g\rangle\langle g|}{4}\iint_{\mathcal{T}} \mathrm{d}\tau\mathrm{d}\tau'\eta(\tau)\eta(\tau')e^{-i\Omega(\tau-\tau')} \\ \Big[W(\mathsf{x}_A,\mathsf{x}'_A)\Big(1 \pm e^{i\Delta E\Delta t}\Big) + W(\mathsf{x}_B,\mathsf{x}'_B)\Big(1 \pm e^{-i\Delta E\Delta t}\Big)\Big]\end{aligned} \tag{4.24}$$

$$\begin{aligned}\mathrm{Tr}_\psi\left[\hat{U}^{(1)}\hat{\rho}_{\mathrm{FD}}\hat{U}^{(1)\dagger}\right] = \frac{\lambda^2|e\rangle\langle e|}{4}\iint \mathrm{d}\tau\mathrm{d}\tau'\eta(\tau)\eta(\tau')e^{-i\Omega(\tau-\tau')} \\ \Big[W(\mathsf{x}_A,\mathsf{x}'_A) + W(\mathsf{x}_B,\mathsf{x}'_B) \pm W(\mathsf{x}_A,\mathsf{x}'_B)\Big(2\cos\Delta E\Delta t\Big)\Big]\end{aligned} \tag{4.25}$$

Here, the density matrix amplitudes of the states are the excitation and ground state probabilities of the detector at the positive and negative superposition state as a result of coupling to the field:

$$P_G^{(\pm)} = \mathrm{Tr}_\psi\left[\hat{U}^{(0)}\hat{\rho}_{\mathrm{FD}}\hat{U}^{(0)\dagger} + \hat{U}^{(0)}\hat{\rho}_{\mathrm{FD}}\hat{U}^{(2)\dagger} + \hat{U}^{(2)}\hat{\rho}_{\mathrm{FD}}\hat{U}^{(0)\dagger}\right]$$

$$= \frac{1}{2}\Big(1 \pm \cos\Delta E\Delta t\Big)\Big[1 - \frac{\lambda^2}{2}\int_{t_i}^{t_f} \mathrm{d}\tau \int_{t_i}^{t_f} \mathrm{d}\tau' \eta(\tau)\eta(\tau') e^{-i\Omega(\tau-\tau')} \Big(W(\mathsf{x}_A, \mathsf{x}'_A) + W(\mathsf{x}_B, \mathsf{x}'_B)\Big)\Big] \tag{4.26}$$

$$P_E^{(\pm)} = \mathrm{Tr}_\psi\Big[\hat{U}^{(1)}\hat{\rho}_{\mathrm{FD}}\hat{U}^{(1)\dagger}\Big]$$
$$= \frac{\lambda^2}{4}\int_{t_i}^{t_f} \mathrm{d}\tau \int_{t_i}^{t_f} \mathrm{d}\tau' \eta(\tau)\eta(\tau') e^{-i\Omega(\tau-\tau')}\Big[W(\mathsf{x}_A, \mathsf{x}'_A) + W(\mathsf{x}_B, \mathsf{x}'_B) \pm W(\mathsf{x}_A, \mathsf{x}'_B)\Big(2\cos\Delta E\Delta t\Big)\Big] \tag{4.27}$$

We can write the transition probabilities as

$$P_G^{(\pm)} = \frac{1}{2}\Big(1 \pm \cos(\Delta E\Delta t)\Big)\Big[1 - \frac{\lambda^2}{2}\Big(P_A + P_B\Big)\Big] \tag{4.28}$$

$$P_E^{(\pm)} = \frac{\lambda^2}{4}\Big(P_A + P_B \pm 2\cos(\Delta E\Delta t)L_{AB}\Big) \tag{4.29}$$

Since we consider the conditional state, we normalise the final detector state (detector transition probabilities) to satisfy $\frac{P_G}{P_G+P_E} + \frac{P_E}{P_G+P_E} = 1$ at Appendix B.0.1.

To summarize, we measured the transition probability in four different conditions. One is when the detector is at ground state and the black hole is at positive phase. We also measure when the detector is at excited state and the black hole is at positive phase. Another case is the negative phase black hole measurement with the detector at the ground and excited states. A black hole's complete state is the sum of the positive and negative phases. Hence, the total transition probability is

$$P_G^{+} = \frac{1}{2}\Big(1 + \cos\Delta E\Delta t\Big)\Big[1 - \frac{\lambda^2}{2}\Big(P_A + P_B\Big)\Big] \tag{4.30}$$

$$P_G^{-} = \frac{1}{2}\Big(1 - \cos\Delta E\Delta t\Big)\Big[1 - \frac{\lambda^2}{2}(P_A + P_B)\Big] \tag{4.31}$$

$$P_E^{+} = \frac{\lambda^2}{4}\Big(P_A + P_B + 2\cos\Delta E\Delta t L_{AB}\Big) \tag{4.32}$$

$$P_E^{-} = \frac{\lambda^2}{4}\Big(P_A + P_B - 2\cos\Delta E\Delta t L_{AB}\Big) \tag{4.33}$$

where the conditional transition probabilities are unnormalized. Note that

$P_G^+ + P_G^- + P_E^+ + P_E^- = 1$. That is,

$$\sum_{i=g,e}\sum_{j=+,-}\left|\langle i|\langle j|\hat{U}|\psi(t_i)\rangle\right|^2 = 1 \tag{4.34}$$

4.1.2 Measurement in the $|\pm i\rangle = (|M_A\rangle \pm i|M_B\rangle)/\sqrt{2}$ basis

Let us condition the black hole state on the $|\pm i\rangle = (|M_A\rangle \pm i|M_B\rangle)/\sqrt{2}$ superposition basis, giving

$$\langle \pm i|\psi(t_f)\rangle^{(0)} = \frac{1}{\sqrt{2}}(1 \pm ie^{-i\Delta E\Delta t})|0\rangle|g\rangle \tag{4.35}$$

$$\langle \pm i|\psi(t_f)\rangle^{(1)} = -\frac{i\lambda}{\sqrt{2}}\int_{t_i}^{t_f} \mathrm{d}\tau\, \eta(\tau)e^{i\Omega\tau}\Big[\hat{\psi}(\mathsf{x}_A) \pm i\hat{\psi}(\mathsf{x}_B)e^{-i\Delta E\Delta t}\Big]|0\rangle|e\rangle \tag{4.36}$$

$$\begin{aligned}\langle \pm i|\psi(t_f)\rangle^{(2)} = -\frac{\lambda^2}{\sqrt{2}}\int_{t_i}^{t_f} \mathrm{d}\tau \int_{t_i}^{t_f} \mathrm{d}\tau' \eta(\tau)\eta(\tau')e^{-i\Omega(\tau-\tau')} \\ \times \Big[\hat{\psi}(\mathsf{x}_A)\hat{\psi}(\mathsf{x}'_A) \pm i\hat{\psi}(\mathsf{x}_B)\hat{\psi}(\mathsf{x}'_B)e^{-i\Delta E\Delta t}\Big]|0\rangle|g\rangle\end{aligned} \tag{4.37}$$

The contributions to the reduced density matrix are given by

$$\mathrm{Tr}_\psi\left[\hat{U}^{(0)}\hat{\rho}_{\mathrm{FD}}\hat{U}^{(0)\dagger}\right] = \frac{1}{4}\Big[2 \pm 2\sin\Delta E\Delta t\Big]|g\rangle\langle g| \tag{4.38}$$

$$\begin{aligned}\mathrm{Tr}_\psi\left[\hat{U}^{(0)}\hat{\rho}_{\mathrm{FD}}\hat{U}^{(2)\dagger}\right] = -\frac{\lambda^2|g\rangle\langle g|}{4}\iint_{\mathcal{T}} \mathrm{d}\tau\mathrm{d}\tau' \eta(\tau)\eta(\tau')e^{i\Omega(\tau-\tau')} \\ \Big[W(\mathsf{x}_A,\mathsf{x}'_A)\Big(1 \pm ie^{-i\Delta E\Delta t}\Big) + W(\mathsf{x}_B,\mathsf{x}'_B)\Big(1 \mp e^{i\Delta E\Delta t}\Big)\Big]\end{aligned} \tag{4.39}$$

$$\begin{aligned}\mathrm{Tr}_\psi\left[\hat{U}^{(2)}\hat{\rho}_{\mathrm{FD}}\hat{U}^{(0)\dagger}\right] = -\frac{\lambda^2|g\rangle\langle g|}{4}\iint_{\mathcal{T}} \mathrm{d}\tau\mathrm{d}\tau' \eta(\tau)\eta(\tau')e^{-i\Omega(\tau-\tau')} \\ \Big[W(\mathsf{x}_A,\mathsf{x}'_A)\Big(1 \mp e^{i\Delta E\Delta t}\Big) + W(\mathsf{x}_B,\mathsf{x}'_B)\Big(1 \pm e^{-i\Delta E\Delta t}\Big)\Big]\end{aligned} \tag{4.40}$$

$$\begin{aligned}\mathrm{Tr}_\psi\left[\hat{U}^{(1)}\hat{\rho}_{\mathrm{FD}}\hat{U}^{(1)\dagger}\right] = \frac{\lambda^2|e\rangle\langle e|}{4}\iint \mathrm{d}\tau\mathrm{d}\tau' \eta(\tau)\eta(\tau')e^{-i\Omega(\tau-\tau')} \\ \Big[W(\mathsf{x}_A,\mathsf{x}'_A) + W(\mathsf{x}_B,\mathsf{x}'_B) \pm W(\mathsf{x}_A,\mathsf{x}'_B)\Big(2\sin\Delta E\Delta t\Big)\Big]\end{aligned} \tag{4.41}$$

The out of phase conditional ground and excited transitional probabilities become

$$P_G = \frac{1}{2}\Big(1 \pm \sin\Delta E\Delta t\Big)\Big[1 - \frac{\lambda^2}{2}\int_{t_i}^{t_f} \mathrm{d}\tau \int_{t_i}^{t_f} \mathrm{d}\tau' \eta(\tau)\eta(\tau') e^{-i\Omega(\tau-\tau')}\Big(W(\mathsf{x}_A, \mathsf{x}'_A) + W(\mathsf{x}_B, \mathsf{x}'_B)\Big)\Big] \tag{4.42}$$

$$P_E = \frac{\lambda^2}{4}\int_{t_i}^{t_f} \mathrm{d}\tau \int_{t_i}^{t_f} \mathrm{d}\tau' \eta(\tau)\eta(\tau') e^{-i\Omega(\tau-\tau')}\Big[W(\mathsf{x}_A, \mathsf{x}'_A) + W(\mathsf{x}_B, \mathsf{x}'_B) \pm W(\mathsf{x}_A, \mathsf{x}'_B)\Big(2\sin\Delta E\Delta t\Big)\Big] \tag{4.43}$$

in terms of transition probability definitions, the out of phase transition probability can be written as

$$P_G = \frac{1}{2}\Big(1 \pm \sin\Delta E\Delta t\Big)\Big[1 - \frac{\lambda^2}{2}\Big(P_A + P_B\Big)\Big] \tag{4.44}$$

$$P_E = \frac{\lambda^2}{4}\Big(P_A + P_B \pm 2\sin\Delta E\Delta t L_{AB}\Big) \tag{4.45}$$

Adding all of the possible outcomes yields a total transition probability of 1.

4.1.3 Transition Probability for Finite Time interactions

In the previous Section, we computed the general form of the detector conditional transition probabilities for measurements of the control in different superposition states. Now we need to evaluate the transition probability integrals for P_A, P_B, and L_{AB} explicitly using the BTZ Wightman functions.

Following our approach in obtaining the BTZ Wightman functions from the AdS-Rindler coordinates, the quantities R_D, γ_D, γ_A and γ_B should henceforth be understood as $\tilde{R}_D$, $\tilde{\gamma}_D$, $\tilde{\gamma}_A$ and $\tilde{\gamma}_B$ for simplicity. The contribution to the total transition probability coming from the individual amplitudes of the black hole superposition (which is identical to the transition probability of a detector in a classical spacetime given by one of the masses) is

$$P_D = \int_{-t_f}^{t_f} \mathrm{d}\tau \int_{-t_f}^{t_f} \mathrm{d}\tau' \eta(\tau)\eta(\tau') e^{-i\Omega(\tau-\tau')} W^{(D)}_{\mathrm{BTZ}}(\mathsf{x}_D(\tau_D), \mathsf{x}'_D(\tau'_D)) \tag{4.46}$$

where $D = A, B$ denotes the associated amplitude, and where we have considered the symmetric integral bounds $t_i = -t_f$ for simplicity. Including the redshifts on the proper time, we obtain

$$P_D = \gamma_D^2 \int_{-t_f}^{t_f} \mathrm{d}t \int_{-t_f}^{t_f} \mathrm{d}t' \eta(\gamma_D t)\eta(\gamma_D t') e^{-i\Omega\gamma_D(t-t')} W_{\mathrm{BTZ}}^{(D)}(\mathsf{x}_D(\tau_D), \mathsf{x}'_D(\tau'_D)). \tag{4.47}$$

Making the substitution $u = t$ and $s = t - t'$ yields

$$P_D = \gamma_D^2 \int_{-t_f}^{t_f} \mathrm{d}u \int_{u-t_f}^{u+t_f} \mathrm{d}s\, \eta(\gamma_D u)\eta(\gamma_D(u-s)) e^{-i\Omega\gamma_D s} W_{\mathrm{BTZ}}^{(D)}(s). \tag{4.48}$$

At this point, we can specialize to a particular profile for the switching function of the detector. In both cases, we choose the switching functions with characteristic width σ such that $\sigma \ll t_f$ i.e. the detector switching is much narrower than the interaction time of the entire system. In such a regime, the following condition is satisfied

$$\int_{-t_f}^{t_f} \mathrm{d}u \int_{u-t_f}^{u+t_f} \mathrm{d}s\, \eta(\gamma_D u)\eta(\gamma_D(u-s)) \simeq \int_{-t_f}^{t_f} \mathrm{d}u \int_{-t_f}^{t_f} \mathrm{d}s\, \eta(\gamma_D u)\eta(\gamma_D(u-s)) \tag{4.49}$$

for switching functions strongly localized around $u = 0$, $u - s = 0$ (given that $\sigma \ll t_f > 0$). This approximation is demonstrated numerically for Gaussian switching functions evaluated in the integral (4.49) as ΔI in Fig. 4.1. We have also shown that for compact switching, we could implement cosine for our switching function [60]. For simplicity, we focus on Gaussian switching throughout our calculations.

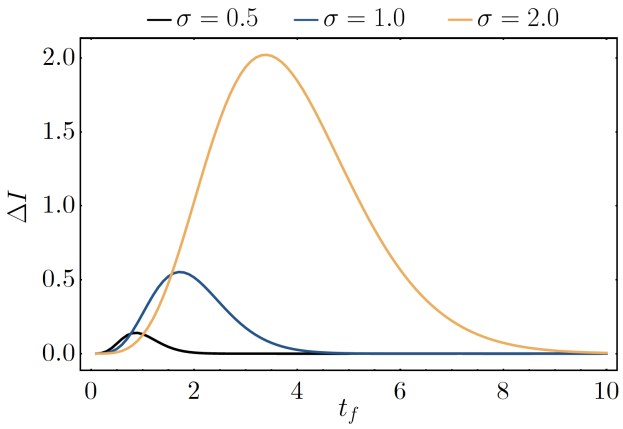

Figure 4.1: The difference, ΔI between the exact and approximated evaluation of the integrals in Eq. (4.49), corresponding to the left- and right-hand sides respectively. We have plotted ΔI as a function of t_f for three fixed values of σ. As $t_f \gg \sigma$, the difference between the exact and approximated integrals vanishes.

This approximation allows us to simplify the integration limits and variables. Hence, our transition probability takes the following form

$$P_D \simeq \lambda^2 \gamma_D^2 \int_{-t_f}^{t_f} \mathrm{d}u \int_{-t_f}^{t_f} \mathrm{d}s \, \eta(\gamma_D u)\eta(\gamma_D(u-s))e^{-i\Omega\gamma_D s} W_{\mathrm{BTZ}}^{(D)}(s). \tag{4.50}$$

Such a simplification is justified because the narrow bandwidth Gaussians in u and $u-s$ only have strong support in the regions $u \in [-t_f, t_f]$ and $s \in [-t_f, t_f]$. For the cross term, we have

$$L_{AB} = \int_{-t_f}^{t_f} \mathrm{d}\tau \int_{-t_f}^{t_f} \mathrm{d}\tau' \eta(\tau)\eta(\tau')e^{-i\Omega(\tau-\tau')} W_{\mathrm{BTZ}}^{(AB)}(\mathsf{x}_A(\tau_A), \mathsf{x}'_B(\tau'_B)) \tag{4.51}$$

Including the redshifts and performing the usual change of variables, one obtains the expression

$$L_{AB} = \gamma_A\gamma_B \int_{-t_f}^{t_f} \mathrm{d}u \int_{-t_f}^{t_f} \mathrm{d}s \, \eta(\gamma_A u)\eta(\gamma_B(u-s))e^{-i\Omega(\gamma_A u - \gamma_B(u-s))} W_{\mathrm{BTZ}}^{(AB)}(s) \tag{4.52}$$

Let us consider first a Gaussian switching function of the form $\eta(\tau) = \exp(\tau^2/2\sigma^2)$. The transition probability becomes

$$P_D = \gamma_D^2 \int_{-t_f}^{t_f} \mathrm{d}u \int_{-t_f}^{t_f} \mathrm{d}s\, e^{-\frac{\gamma_D^2 u^2}{2\sigma^2}} e^{-\frac{\gamma_D^2 (u-s)^2}{2\sigma^2}} e^{-i\Omega\gamma_D s} W_{\mathrm{BTZ}}^{(D)}(s) \tag{4.53}$$

$$= \frac{\sqrt{\pi}\gamma_D \sigma}{2} \int_{-t_f}^{t_f} \mathrm{d}s\, e^{-\frac{\gamma_D^2 s^2}{4\sigma^2}} e^{-i\Omega\gamma_D s} H_0(s) W(s) \tag{4.54}$$

where $H_0(s) = \mathrm{erf}\left[\frac{\gamma_D(s+2t_f)}{2\sigma}\right] - \mathrm{erf}\left[\frac{\gamma_D(s-2t_f)}{2\sigma}\right]$. For the cross term,

$$L_{AB} = \gamma_A \gamma_B \int_{-t_f}^{t_f} \mathrm{d}u \int_{-t_f}^{t_f} \mathrm{d}s\, e^{-\frac{\gamma_A^2 u^2}{2\sigma^2}} e^{-\frac{\gamma_B^2 (u-s)^2}{2\sigma^2}} e^{-i\Omega(\gamma_A u - \gamma_B(u-s))} W_{\mathrm{BTZ}}^{(AB)}(s) \tag{4.55}$$

and then performing the integration over u,

$$L_{AB} = \frac{\gamma_A \gamma_B \sigma \sqrt{\pi}}{\sqrt{2}\sqrt{\gamma_A^2 + \gamma_B^2}} e^{-\frac{(\gamma_A - \gamma_B)^2 \sigma^2 \Omega^2}{2(\gamma_A^2 + \gamma_B^2)}} \int_{-t_f}^{t_f} \mathrm{d}s\, e^{-\frac{\gamma_A^2 \gamma_B^2 s^2}{2(\gamma_A^2 + \gamma_B^2)\sigma^2}} e^{-\frac{i\Omega s \gamma_A \gamma_B (\gamma_A + \gamma_B)}{\gamma_A^2 + \gamma_B^2}} Q_0(s) W_{\mathrm{BTZ}}^{(AB)}(s) \tag{4.56}$$

where

$$Q_0(s) = \mathrm{erf}\left[\frac{(\gamma_A^2 + \gamma_B^2)t_f + i(\gamma_A - \gamma_B)\Omega\sigma^2 - \gamma_B^2 s}{\sqrt{2}\sigma\sqrt{\gamma_A^2 + \gamma_B^2}}\right] + \mathrm{erf}\left[\frac{(\gamma_A^2 + \gamma_B^2)t_f - i(\gamma_A - \gamma_B)\Omega\sigma^2 + \gamma_B^2 s}{\sqrt{2}\sigma\sqrt{\gamma_A^2 + \gamma_B^2}}\right] \tag{4.57}$$

4.1.4 Integral expressions for P_D and L_{AB} with Gaussian switching

Finally, we calculate the transition probability after substituting the Wightman function for static detector D.

$$\frac{P_D}{\sigma} = \frac{\sqrt{\pi} H_0(0)}{8} - \frac{i}{8\sqrt{\pi}} \mathrm{PV} \int_{-t_f/2l}^{t_f/2l} \frac{\mathrm{d}z\, X_0(2lz) H_0(2lz)}{\sinh(z)} + \frac{1}{4\sqrt{2\pi}\sum_n \eta^{2n}} \sum_{n \neq m} \mathrm{Re} \int_0^{t_f/l} \frac{\mathrm{d}z\, X_0(lz) H_0(lz)}{\sqrt{\beta_{nm} - \cosh(z)}} \tag{4.58}$$

where $X_0(z)$, $H_0(z)$ are functions of the detector and spacetime parameters derived in the Appendix. Likewise, cross-correlation term quantifying the correlations between the different fields on the spacetime superposition is given by

$$\frac{L_{AB}}{\sigma} = \frac{Y_0}{\sum_n \eta^{2n}} \sum_{n,m} \int_0^{t_f/l} \frac{\mathrm{d}z\, Z_0(lz) Q_0(lz)}{\sqrt{\alpha_{nm} - \cosh(z)}}. \tag{4.59}$$

Y_0 and $Z_0(z)$ are likewise derived in the Appendix B.0.3. The constants beneath the roots (also appearing in the compact switching case) take the form

$$\beta_{nm} = \frac{1}{\gamma_D^2} \left[\frac{R_D^2 \cosh(2\pi(n-m)\sqrt{M_D})}{M_D l^2} - 1 \right], \tag{4.60}$$

$$\alpha_{nm} = \frac{1}{\gamma_A \gamma_B} \left[\frac{R_D^2 \cosh(2\pi(m\sqrt{M_A} - n\sqrt{M_B}))}{\sqrt{M_A M_B} l^2} - 1 \right]. \tag{4.61}$$

4.2 Metric for spacetime superpositions

Before presenting our results for the response of the detector in the mass-superposed spacetime, we pause to remark about a "conditional metric" that may be obtained for the spacetime. It is so-called due to our "conditioning" of the spacetime on a certain measurement basis, yielding a combination of Wightman functions parametrizing the correlations in the field between the spacetime amplitudes of interest. This builds off the recent arguments given by Saravani et. al. and Kempf [61, 62, 63]. Recall that in general relativity, spacetime is described by a differentiable manifold (M) and Synge world function (or as we have been calling it, the geodesic distance σ) between two spacetime events (x, x'). The separation of these two distances is sufficient to express the metric in terms of this distance [61, 62]

$$g_{\mu\nu}(x) = -\lim_{x \to x'} \frac{\partial}{\partial x^\mu} \frac{\partial}{\partial x'^\nu} \sigma(x, x'). \tag{4.62}$$

where the metric is subject to changes from the correlations that decay as the separation increases. The authors of [61, 62] consider Feynman propagators in deriving the metric (for a classical background) via correlations in the field. However, other correlation functions such as the Wightman function are also

applicable. After applying the Wightman function, the metric (again, for a classical background) takes the form

$$g_{\mu\nu} = \Upsilon(d) \lim_{x\to x'} \frac{\partial}{\partial x^{\mu}} \frac{\partial}{\partial x'^{\nu}} W(\mathsf{x},\mathsf{x}')^{\frac{2}{d-2}} \tag{4.63}$$

where $\Upsilon(d) = -(1/2)(\Gamma(d/2-1)/(4\pi^{d/2}))^{\frac{2}{d-2}}$ and $d > 2$ is the spacetime dimension[2]. In this context, building a spacetime in superposition occurs at the level of the field operator. By taking $\hat{\psi}(x) \to \hat{\psi}(\mathbf{x}) = \sum_D f_D \hat{\psi}(x_D)$ (where $\mathbf{x} = \{x_D\}$, $\sum_D |f_D|^2 = 1$ and the relative phases between f_D are determined by the state in which the black hole is measured), the Wightman function becomes a sum over all two-point correlators between the fields $\hat{\psi}(x_D)$, $\hat{\psi}(x'_{D'})$, defined with respect to the coordinates of the spacetime states in superposition. Equation (4.63) is then modified as follows, yielding a conditional metric (i.e. conditioned on a particular measurement of the control) describing a superposition of spacetimes:

$$g_{\mu\nu} = \Lambda(d) \lim_{x\to x'} \frac{\partial}{\partial x^{\mu}} \frac{\partial}{\partial x'^{\nu}} \sum_{D,D'} f_D f^{\star}_{D'} W(x_D, x'_{D'})^{\frac{2}{d-2}}. \tag{4.64}$$

Equation (4.64) involves correlations between the field operators parametrized with coordinates covering black hole spacetimes associated with different masses; it represents a "conditional metric" effectively seen by a detector in the quantum superposition of spacetimes.

4.3 Results

We can analyze the response of the detector outside the mass-superposed black hole. In Fig. 4.2, we have plotted the response of the detector as a function of the mass ratio of the black hole superposition, $\sqrt{M_B/M_A}$.

[2] A unique expression exists for $d = 2$

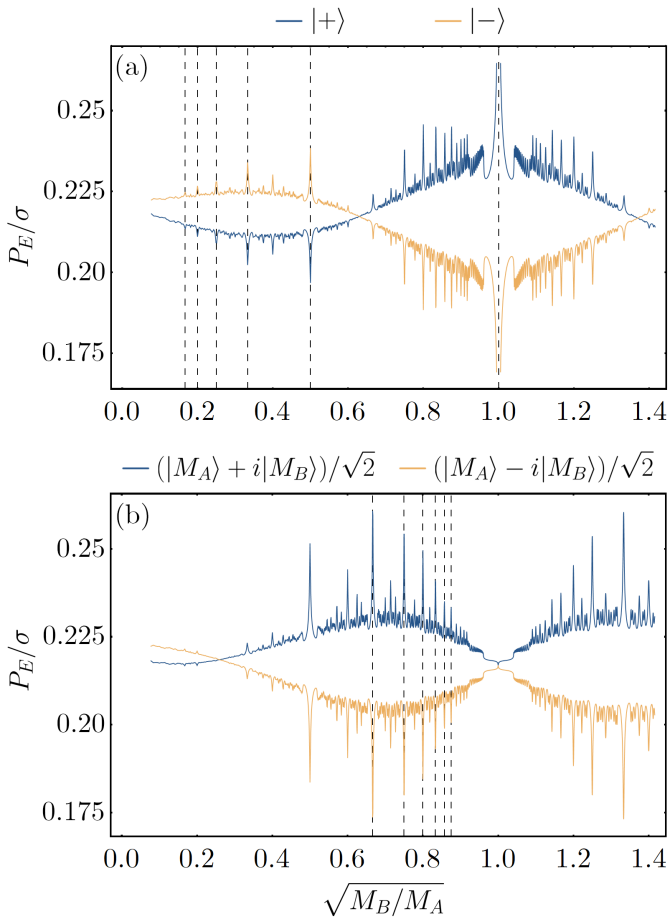

Figure 4.2: Transition probability of the detector as a function of $\sqrt{M_B/M_A}$. The measurement basis corresponding to the relevant plot is indicated by the legend. In (a), the dashed lines correspond to $\sqrt{M_B/M_A} = 1/n$ where $n = \{1, \dots 6\}$. In (b), the dashed lines correspond to $\sqrt{M_B/M_A} = (n-1)/n$ where $n = \{3, \dots 8\}$. Moreover, the oscillating cross term in (b) is $\pi/2$ out-of-phase with that for the black hole measured in the (anti)symmetric basis. In all plots we have also used $l/\sigma = 5$, $R/\sigma = 25$, $t_f = 5\sigma$ and $M_A l^2 = 2$.

Fig. 4.2(a) shows the conditional transition probabilities for measurements in the symmetric and antisymmetric superposition basis, while Fig. 4.2(b) considers measurements in the $|i\pm\rangle = (|M_A\rangle \pm i|M_B\rangle)/\sqrt{2}$ basis. There are recurring behaviors of the transition probabilities with respect to the ratios of the superpositions associated with different masses. These features,

that translate into resonant peaks, occur at rational values of the square root ratio of the superposed masses. In Fig. 4.2(a), we have denoted some of these ratios with dashed lines. The transition probability occurs continuously for both $M_B < M_A$ and $M_B > M_A$. There are many values of the square root mass ratio for the effect to occur. We ascribe this behavior to a constructive interference between the field modes associated with topologically closed AdS spacetimes, yielding resonances in the detector response at integer values of $\sqrt{M_B/M_A}$.

In Fig. 4.2(a) and (b) respectively, we have highlighted the ratios at the sharp spikes as $\sqrt{M_B/M_A}$ as $1/n$ for $n = \{1, \ldots 6\}$ and $(n-1)/n$ for $n \in \{3, \ldots 8\}$. The analytical explanation to this is, in our cross term transition probability 4.59, the variable Eq. (4.61) at the integrand denominator, the $cosh(x)$ vanishes when $m\sqrt{M_A} = n\sqrt{M_B}$. As we sum over the image terms n and m, these "coincidences" occur only when $\sqrt{M_A/M_B}$ is a rational number. Furthermore, this relation between black hole masses studied by Bekenstein's quantum black hole conjecture supports our ratio calculation to be rational numbers. Specifically, the allowed mass values of the BTZ black hole, assuming the Bohr-Sommerfeld quantization scheme for the horizon radius, are given by [64]:

$$r_H = \sqrt{M}l = n, \qquad n = 1, 2, \ldots \tag{4.65}$$

We consider all ranges of rational and irrational values for our calculations, however, the resonances that are significant come from Eq. (4.61). Hence, the response of the detector to the superposition of black hole masses is unique for the mass ratios predicted by Bekenstein's conjecture. While our construction does not require that the superposed masses are quantized in integer values, the form of Eq. (4.61) explains the origin of the signatory resonances. The detector responds uniquely to black hole mass superpositions with mass ratios corresponding to the masses predicted by Bekenstein's conjecture. This result is a one of its kind prescription for the detection of a quantum gravitational effect of a quantum black hole. And it constitutes a new method for investigating effects implied by Bekenstein's conjecture about the quantization of black hole masses.

Chapter 5

Summary

The objective of this thesis was to use a UDW detector to develop a "superposition of spacetime detection protocol" and explore unique properties produced by such superpositions. In particular, the kinds of superpositions we considered were periodic identifications of Minkowski spacetime (yielding a cylindrical spacetime in a superposition of characteristic lengths) and AdS_3 (yielding a mass superposition of the BTZ black hole).

In Chapter 3 (the first containing new research), we utilized the theory of automorphic fields to calculate the Wightman functions accessible to a detector on a background Minkowski spacetime in a superposition of periodic identifications. The detector, interacting with a scalar field on this background, had a response function that exhibited discontinuous resonant peaks at rational values of the superposed characteristic lengths, $\gamma = l_B/l_A$. In studying this simple case, we were able to clarify the appropriate choice of the vacuum state of the field (which we chose to be the Minkowski vacuum, the ground state of the "embedding space" of the cylindrically identified spacetimes). This motivated our choice of the AdS_3 vacuum in the following Chapter.

In Chapter 4, we extended our investigation by considering the spacetime superposition produced by a BTZ black hole in a superposition of masses (constructed from a superposition of identifications of AdS_3). We found signatures of genuine quantum-gravitational phenomena via the same UDW detector coupling. The response of a UDW detector to these fields in this spacetime identifies two types of terms as "local" corresponding to individual mass-energy eigenstates and "cross-correlation" of fields of the mass-energy eigenstates in superposition originated from BTZ spacetimes with mass iden-

tifications. We reported that the rational mass ratios of the superpositions are not only more sensible to the detector but also there are signatory peaks in rational square root of mass ratios. Finally, the BTZ superposition study suggested that our operational approach can be used for the detection of quantum gravitational effects for the first time during the hypothetical superpositions of spacetime and it acts as a new method for investigating effects implied by Bekenstein's conjecture. Additionally, for our superposition of spacetimes, we presented a spacetime metric derived from the correlations of the fields (as a measure of distance) a notion first proposed by Saravani et. al. and Kempf [61, 62].

The results of this thesis pave the way for a deeper understanding of quantum gravity ideas such as quantum black holes and quantum superpositions of spacetime. Although superpositions of spacetimes have been considered in the literature, our new approach has the advantage of being based on operationalism (i.e. giving quantitative predictions based on in-principle measurements). By tying our work to the spacetime metric, we have opened the possibility of further research on the dynamics of spacetime superpositions and what effects that may induce on, for example, low-energy particles geodesics in quantum gravity. A natural extension to the results of Chapter 4 includes studying black holes in a superposition of angular momenta. From the perspective of quantum thermodynamics and information, our work motivates questions about operationally defining phenomena such as superpositions of Hawking radiation and temperature. This work may also be considered for entanglement between detectors in various black hole spacetime superpositions. Finally, it would be interesting to ask "Are there any superselection rules for spacetime superpositions that we can study via the UDW detector model?"

Though observational evidence of Hawking radiation is limited, there are possibilities of experimentally simulating the effects derived in this thesis. Regarding the topology superposition of Chapter 3, experiments have realized superfluid Helium condensates on toroidal cavities. The fundamental mode providing the "analog metric" for phonons in the condensate therein can interact with incident photons, thus suggesting an opportunity to study "light-controlled" effective quantum-superposed backgrounds [65, 66]. Likewise, experimental techniques in atomic Bose-Einstein condensates and fluid surface waves have realized analog black holes in the lab. Such experiments commonly treat "sonic" or "fluid" black holes in (1+1)- or (2+1)-dimensions. Our results may have significant observational consequences for superposed

UDW detectors in a "sonic" or "fluid" black hole [67] or perhaps even for a single UDW detector in a mass- superposition of such a black hole.

Bibliography

[1] Jacob D Bekenstein. The quantum mass spectrum of the kerr black hole. In *JACOB BEKENSTEIN: The Conservative Revolutionary*, pages 331–334. World Scientific, 2020.

[2] Joshua Foo and Timothy. C. Ralph. Continuous-variable quantum teleportation with vacuum-entangled rindler modes. *Phys. Rev. D*, 101:085006, Apr 2020.

[3] Andrew Arrasmith, Andreas Albrecht, and Wojciech H. Zurek. Decoherence of black hole superpositions by hawking radiation. *Nature Communications*, 10(1), Mar 2019.

[4] Jean-Guy Demers and Claus Kiefer. Decoherence of black holes by hawking radiation. *Physical Review D*, 53(12):7050–7061, Jun 1996.

[5] Itamar J. Allali and Mark P. Hertzberg. General relativistic decoherence with applications to dark matter detection. *Phys. Rev. Lett.*, 127:031301, Jul 2021.

[6] Joshua Foo, Robert B Mann, and Magdalena Zych. Schrödinger's cat for de sitter spacetime. *Classical and Quantum Gravity*, 38(11):115010, 2021.

[7] Bryce S. DeWitt. Quantum theory of gravity. i. the canonical theory. *Phys. Rev.*, 160:1113–1148, Aug 1967.

[8] John Archibald Wheeler. Superspace and the nature of quantum geometrodynamics. 1968.

[9] Carlo Rovelli. The strange equation of quantum gravity. *Classical and Quantum Gravity*, 32(12):124005, jun 2015.

[10] Carlo Rovelli and Francesca Vidotto. *Covariant loop quantum gravity: an elementary introduction to quantum gravity and spinfoam theory*. Cambridge University Press, 2015.

[11] Carlo Rovelli. Loop quantum gravity. *Living reviews in relativity*, 11(1):1–69, 2008.

[12] Abhay Ashtekar and Eugenio Bianchi. A short review of loop quantum gravity. *Reports on Progress in Physics*, 84(4):042001, mar 2021.

[13] Ivan Agullo, Vitor Cardoso, Adrián del Rio, Michele Maggiore, and Jorge Pullin. Potential gravitational wave signatures of quantum gravity. *Phys. Rev. Lett.*, 126:041302, Jan 2021.

[14] Vitor Cardoso, Valentino F. Foit, and Matthew Kleban. Gravitational wave echoes from black hole area quantization. *Journal of Cosmology and Astroparticle Physics*, 2019(08):006–006, aug 2019.

[15] Jahed Abedi, Hannah Dykaar, and Niayesh Afshordi. Echoes from the abyss: Tentative evidence for planck-scale structure at black hole horizons. *Phys. Rev. D*, 96:082004, Oct 2017.

[16] Naritaka Oshita, Daichi Tsuna, and Niayesh Afshordi. Quantum black hole seismology. i. echoes, ergospheres, and spectra. *Phys. Rev. D*, 102:024045, Jul 2020.

[17] Rodolfo Gambini, Javier Olmedo, and Jorge Pullin. Quantum black holes in loop quantum gravity. *Classical and Quantum Gravity*, 31(9):095009, apr 2014.

[18] Rodolfo Gambini and Jorge Pullin. Loop quantization of the schwarzschild black hole. *Phys. Rev. Lett.*, 110:211301, May 2013.

[19] Andrew Arrasmith, Andreas Albrecht, and Wojciech H Zurek. Decoherence of black hole superpositions by hawking radiation. *Nature communications*, 10(1):1024, March 2019.

[20] Jean-Guy Demers and Claus Kiefer. Decoherence of black holes by hawking radiation. *Phys. Rev. D*, 53:7050–7061, Jun 1996.

[21] Claus Kiefer. Conceptual Problems in Quantum Gravity and Quantum Cosmology. *ISRN Math. Phys.*, 2013:509316, 2013.

[22] Magdalena Zych, Fabio Costa, Igor Pikovski, and Časlav Brukner. Bell's theorem for temporal order. *Nature Communications*, 10, 08 2019.

[23] Flaminia Giacomini. Spacetime Quantum Reference Frames and superpositions of proper times. *Quantum*, 5:508, July 2021.

[24] Flaminia Giacomini and Časlav Brukner. Einstein's equivalence principle for superpositions of gravitational fields and quantum reference frames, 2020.

[25] Flaminia Giacomini and Časlav Brukner. Quantum superposition of spacetimes obeys einstein's equivalence principle. *AVS Quantum Science*, 4(1), 2022.

[26] Viktoria Kabel, Anne-Catherine de la Hamette, Esteban Castro-Ruiz, and Časlav Brukner. Quantum conformal symmetries for spacetimes in superposition, 2022.

[27] Carlos Barceló, Luis J. Garay, and Gerardo García-Moreno. Superposing spacetimes: lessons from analogue gravity, 2021.

[28] Marios Christodoulou and Carlo Rovelli. On the possibility of laboratory evidence for quantum superposition of geometries. *Physics Letters B*, 792:64–68, May 2019.

[29] C. Marletto and V. Vedral. Gravitationally induced entanglement between two massive particles is sufficient evidence of quantum effects in gravity. *Phys. Rev. Lett.*, 119:240402, Dec 2017.

[30] Sougato Bose, Anupam Mazumdar, Gavin W. Morley, Hendrik Ulbricht, Marko Toroš, Mauro Paternostro, Andrew A. Geraci, Peter F. Barker, M. S. Kim, and Gerard Milburn. Spin entanglement witness for quantum gravity. *Phys. Rev. Lett.*, 119:240401, Dec 2017.

[31] Joshua Foo, Sho Onoe, and Magdalena Zych. Unruh-dewitt detectors in quantum superpositions of trajectories. *Phys. Rev. D*, 102:085013, Oct 2020.

[32] Joshua Foo, Sho Onoe, Robert B. Mann, and Magdalena Zych. Thermality, causality, and the quantum-controlled unruh–dewitt detector. *Phys. Rev. Research*, 3:043056, Oct 2021.

[33] Joshua Foo, Robert B. Mann, and Magdalena Zych. Entanglement amplification between superposed detectors in flat and curved spacetimes. *Phys. Rev. D*, 103:065013, Mar 2021.

[34] Lee Hodgkinson and Jorma Louko. Static, stationary, and inertial unruh-dewitt detectors on the btz black hole. *Phys. Rev. D*, 86:064031, Sep 2012.

[35] R. Banach and J. S. Dowker. The Vacuum Stress Tensor for Automorphic Fields on Some Flat Space-times. *J. Phys. A*, 12:2545, 1979.

[36] R Banach. The quantum theory of free automorphic fields. *Journal of Physics A: Mathematical and General*, 13(6):2179–2203, jun 1980.

[37] Laura J. Henderson, Robie A. Hennigar, Robert B. Mann, Alexander R.H. Smith, and Jialin Zhang. Anti-hawking phenomena. *Physics Letters B*, 809:135732, 2020.

[38] Everett Patterson and Robert B. Mann. Fisher information of a black hole spacetime, 2022.

[39] Cendikiawan Suryaatmadja, Wan Cong, and Robert . B. Mann. Entanglement harvesting of inertially moving unruh-dewitt detectors in minkowski spacetime, 2022.

[40] Erickson Tjoa and Robert B. Mann. Unruh-DeWitt detector in dimensionally-reduced static spherically symmetric spacetimes. *JHEP*, 03:014, 2022.

[41] Benito A. Juárez-Aubry and Jorma Louko. Quantum kicks near a Cauchy horizon. *AVS Quantum Sci.*, 4(1):013201, 2022.

[42] Diana Mendez-Avalos, Laura J. Henderson, Kensuke Gallock-Yoshimura, and Robert B. Mann. Entanglement harvesting of three Unruh-DeWitt detectors. 6 2022.

[43] Subhajit Barman, Bibhas Ranjan Majhi, and L. Sriramkumar. Radiative processes of single and entangled detectors on circular trajectories in $(2 + 1)$ dimensional Minkowski spacetime. 5 2022.

[44] Dimitris Moustos. Uniformly accelerated Brownian oscillator in (2+1)D: Temperature-dependent dissipation and frequency shift. *Phys. Lett. B*, 829:137115, 2022.

[45] Laura J. Henderson, Robie A. Hennigar, Robert B. Mann, Alexander R. H. Smith, and Jialin Zhang. Entangling detectors in anti-de Sitter space. *JHEP*, 05:178, 2019.

[46] Eduardo Martín-Martínez and Pablo Rodriguez-Lopez. Relativistic quantum optics: The relativistic invariance of the light-matter interaction models. *Phys. Rev. D*, 97(10):105026, 2018.

[47] Luis C. Barbado, Esteban Castro-Ruiz, Luca Apadula, and Časlav Brukner. Unruh effect for detectors in superposition of accelerations, 2020.

[48] Laura J. Henderson, Alessio Belenchia, Esteban Castro-Ruiz, Costantino Budroni, Magdalena Zych, Časlav Brukner, and Robert B. Mann. Quantum temporal superposition: the case of qft, 2020.

[49] Nicholas David Birrell, Nicholas David Birrell, and PCW Davies. *Quantum fields in curved space*. Cambridge university press, 1984.

[50] Joshua Foo, Robert B. Mann, and Magdalena Zych. Schrödinger's black hole cat, 2022.

[51] Eduardo Martín-Martínez, Alexander R. H. Smith, and Daniel R. Terno. Spacetime structure and vacuum entanglement. *Phys. Rev. D*, 93:044001, Feb 2016.

[52] Paul Langlois. Causal particle detectors and topology. *Annals of Physics*, 321, 2006.

[53] Richard Howl, Ali Akil, Hlér Kristjánsson, Xiaobin Zhao, and Giulio Chiribella. Quantum gravity as a communication resource, 2022.

[54] K. B. Whaley and J. C. Light. Rotating-frame transformations: A new approximation for multiphoton absorption and dissociation in laser fields. *Phys. Rev. A*, 29:1188–1207, Mar 1984.

[55] Paul Langlois. Imprints of spacetime topology in the Hawking-Unruh effect. Other thesis, 10 2005.

[56] Laura J Henderson, Robie A Hennigar, Robert B Mann, Alexander R H Smith, and Jialin Zhang. Harvesting entanglement from the black hole vacuum. *Classical and Quantum Gravity*, 35(21):21LT02, oct 2018.

[57] Gilad Lifschytz and Miguel Ortiz. Scalar field quantization on the (2+1)-dimensional black hole background. *Phys. Rev. D*, 49:1929–1943, Feb 1994.

[58] Steven Carlip. The (2+1)-Dimensional black hole. *Class. Quant. Grav.*, 12:2853–2880, 1995.

[59] Esteban Castro Ruiz, Flaminia Giacomini, and Časlav Brukner. Entanglement of quantum clocks through gravity. *Proceedings of the National Academy of Sciences*, 114(12):E2303–E2309, 2017.

[60] Joshua Foo, Cemile Senem Arabaci, Magdalena Zych, and Robert B. Mann. Quantum signatures of black hole mass superpositions. 2021.

[61] Mehdi Saravani, Siavash Aslanbeigi, and Achim Kempf. Spacetime curvature in terms of scalar field propagators. *Physical Review D*, 93(4), Feb 2016.

[62] Achim Kempf. Replacing the Notion of Spacetime Distance by the Notion of Correlation. *Front. in Phys.*, 9:247, 2021.

[63] N. D. Birrell and Paul Davies. Quantum fields in curved space. 1980.

[64] Yongjoon Kwon and Soonkeon Nam. Area spectra of the rotating BTZ black hole from quasinormal modes. *Classical and Quantum Gravity*, 27(12):125007, apr 2010.

[65] Warwick P Bowen and Gerard J Milburn. *Quantum optomechanics*. CRC press, 2015.

[66] Carlos Barceló, Luis J. Garay, and Gerardo García-Moreno. Analogue gravity simulation of superpositions of spacetimes. *Eur. Phys. J. C*, 82(8):727, 2022.

[67] Silke Weinfurtner, Edmund W. Tedford, Matthew C. J. Penrice, William G. Unruh, and Gregory A. Lawrence. Measurement of stimulated hawking emission in an analogue system. *Phys. Rev. Lett.*, 106:021302, Jan 2011.

APPENDICES

Appendix A

Transition Probability Derivation for the Superposition of (3+1)D Minkowski spacetime

In this Appendix, we present in detail the calculation for the transition probability for a detector in a superposition of Minkowski spacetimes with different periodic identifications. We begin by deriving the expression for the "local contributions" from the individual spacetime amplitudes:

$$
\begin{aligned}
P_D = & \frac{1}{\sum_n \eta^{2n}} \sum_{n,m} \int_{-\infty}^{\infty} \mathrm{d}\tau \int_{-\infty}^{\infty} \mathrm{d}\tau' e^{-\frac{\tau^2}{2\sigma^2}} e^{-\frac{\tau'^2}{2\sigma^2}} e^{-i\Omega(\tau-\tau')} \\
& \left[\frac{\mathrm{sgn}(\tau-\tau')\delta((\tau-\tau')^2 - l^2(n-m)^2)}{4\pi i} - \frac{1}{4\pi^2((\tau-\tau')^2 - l^2(n-m)^2)} \right] \\
= & \frac{1}{\sum_n \eta^{2n}} \sum_{n=m} \int_{-\infty}^{\infty} \mathrm{d}\tau \int_{-\infty}^{\infty} \mathrm{d}\tau' e^{-\frac{\tau^2}{2\sigma^2}} e^{-\frac{\tau'^2}{2\sigma^2}} e^{-i\Omega(\tau-\tau')} \\
& \left[\frac{\mathrm{sgn}(\tau-\tau')\delta((\tau-\tau')^2}{4\pi i} - \frac{1}{4\pi^2(\tau-\tau')^2} \right] \\
& + \frac{1}{\sum_n \eta^{2n}} \sum_{n\neq m} \int_{-\infty}^{\infty} \mathrm{d}\tau \int_{-\infty}^{\infty} \mathrm{d}\tau' e^{-\frac{\tau^2}{2\sigma^2}} e^{-\frac{\tau'^2}{2\sigma^2}} e^{-i\Omega(\tau-\tau')} \\
& \left[\frac{\mathrm{sgn}(\tau-\tau')\delta((\tau-\tau')^2 - l^2(n-m)^2)}{4\pi i} - \frac{1}{4\pi^2((\tau-\tau')^2 - l^2(n-m)^2)} \right]
\end{aligned}
$$

$$= \frac{1}{4\pi}\left[e^{-\sigma^2\Omega^2} - \sqrt{\pi}\sigma\Omega\mathrm{erf}(\sigma\Omega)\right] + P_I \tag{A.1}$$

where $P_I = I_1 - I_2$ is the image sum term. We have

$$\begin{aligned}
I_1 &= \frac{1}{\sum_n \eta^{2n}} \sum_{n\neq m} \int_{-\infty}^{\infty} \mathrm{d}\tau \int_{-\infty}^{\infty} \mathrm{d}\tau' e^{-\frac{\tau^2}{2\sigma^2}} e^{-\frac{\tau'^2}{2\sigma^2}} e^{-i\Omega(\tau-\tau')} \\
&\quad \frac{\mathrm{sgn}(\tau-\tau')\delta((\tau-\tau')^2 - l^2(n-m)^2)}{4\pi i} \\
&= \frac{1}{\sum_n \eta^{2n}} \sum_{n\neq m} \int_{-\infty}^{\infty} \mathrm{d}u \int_{-\infty}^{\infty} \mathrm{d}s\, e^{-\frac{u^2}{2\sigma^2}} e^{-\frac{(u-s)^2}{2\sigma^2}} e^{-i\Omega s} \frac{\mathrm{sgn}(s)\delta(s^2 - l^2(n-m)^2)}{4\pi i} \\
&= \frac{\sqrt{\pi}\sigma}{\sum_n \eta^{2n}} \sum_{n\neq m} \int_{-\infty}^{\infty} \mathrm{d}s\, e^{-\frac{s^2}{4\sigma^2}} e^{-i\Omega s} \frac{\mathrm{sgn}(s)\delta(s^2 - l^2(n-m)^2)}{4\pi i} \\
&= \frac{\sqrt{\pi}\sigma}{\sum_n \eta^{2n}} \frac{1}{4\pi i} \sum_{n\neq m} \int_{-\infty}^{\infty} \mathrm{d}s\, e^{-\frac{s^2}{4\sigma^2}} e^{-i\Omega s} \mathrm{sgn}(s) \frac{1}{2|l(n-m)|} \\
&\quad \Big[\delta(s + l(n-m)) + \delta(s - l(n-m))\Big]
\end{aligned}$$

Integrating over s:

$$I_1 = \frac{\sqrt{\pi}\sigma}{\sum_n \eta^{2n}} \frac{1}{4\pi i} \sum_{n\neq m} \frac{e^{-\frac{l^2(n-m)^2}{4\sigma^2}}}{2|l(n-m)|} \left[e^{i\Omega l(n-m)}\mathrm{sgn}(-l(n-m)) + \mathrm{sgn}(l(n-m))e^{-i\Omega l(n-m)}\right]$$

We can split this up into two contributions, $n > m$ and $n < m$:

$$\begin{aligned}
&= \frac{\sqrt{\pi}\sigma}{\sum_n \eta^{2n}} \frac{1}{4\pi i} \sum_{n>m} \frac{e^{-\frac{l^2(n-m)^2}{4\sigma^2}}}{2l|n-m|} \left[- e^{i\Omega l(n-m)}\mathrm{sgn}(l(n-m)) + \mathrm{sgn}(l(n-m))e^{-i\Omega l(n-m)}\right] \\
&\quad + \frac{\sqrt{\pi}\sigma}{\sum_n \eta^{2n}} \frac{1}{4\pi i} \sum_{m>n} \frac{e^{-\frac{l^2(n-m)^2}{4\sigma^2}}}{2l|n-m|} \left[e^{i\Omega l(n-m)}\mathrm{sgn}(l(m-n)) - e^{-i\Omega l(n-m)}\mathrm{sgn}(l(m-n))\right] \\
&= \frac{\sqrt{\pi}\sigma}{\sum_n \eta^{2n}} \frac{1}{2\pi} \sum_{n>m} \frac{e^{-\frac{l^2(n-m)^2}{4\sigma^2}}}{2l|n-m|} \mathrm{sgn}(l(n-m))\sin(\Omega l(m-n)) \\
&\quad - \frac{\sqrt{\pi}\sigma}{\sum_n \eta^{2n}} \frac{1}{2\pi} \sum_{m>n} \frac{e^{-\frac{l^2(n-m)^2}{4\sigma^2}}}{2l|n-m|} \mathrm{sgn}(l(m-n))\sin(\Omega l(m-n)) \\
&= \frac{\sqrt{\pi}\sigma}{\sum_n \eta^{2n}} \frac{1}{2\pi} \frac{1}{2l} \left[\sum_{n>m} \frac{e^{-\frac{l^2(n-m)^2}{4\sigma^2}}}{n-m} \sin(\Omega l(m-n)) - \sum_{m>n} \frac{e^{-\frac{l^2(n-m)^2}{4\sigma^2}}}{m-n} \sin(\Omega l(m-n))\right]
\end{aligned}$$

$$= \frac{\sqrt{\pi}\sigma}{\sum_n \eta^{2n}} \frac{1}{2\pi l} \sum_{n>m} \frac{e^{-\frac{l^2(n-m)^2}{4\sigma^2}}}{n-m} \sin(\Omega l(m-n)) \tag{A.2}$$

The second part of the image sum term is

$$\begin{aligned}
I_2 &= -\frac{1}{\sum_n \eta^{2n}} \sum_{n\neq m} \int_{-\infty}^{\infty} \mathrm{d}\tau \int_{-\infty}^{\infty} \mathrm{d}\tau' \frac{e^{-\frac{\tau^2}{2\sigma^2}} e^{-\frac{\tau'^2}{2\sigma^2}} e^{-i\Omega(\tau-\tau')}}{4\pi^2((\tau-\tau')^2 - l^2(n-m)^2)} \\
&= -\frac{1}{4\pi^2} \frac{1}{\sum_n \eta^{2n}} \sum_{n\neq m} \int_{-\infty}^{\infty} \mathrm{d}u \int_{-\infty}^{\infty} \mathrm{d}s \, \frac{e^{-\frac{u^2}{2\sigma^2}} e^{-\frac{(u-s)^2}{2\sigma^2}} e^{-i\Omega s}}{s^2 - l^2(n-m)^2} \\
&= -\frac{\sqrt{\pi}\sigma}{4\pi^2} \frac{1}{\sum_n \eta^{2n}} \sum_{n\neq m} \int_{-\infty}^{\infty} \mathrm{d}s \, \frac{e^{-\frac{s^2}{4\sigma^2}} e^{-i\Omega s}}{s^2 - l^2(n-m)^2} \\
&= -\frac{\sqrt{\pi}\sigma}{4\pi^2} \frac{1}{\sum_n \eta^{2n}} \sum_{n\neq m} \int_{-\infty}^{\infty} \mathrm{d}s \int_{-\infty}^{\infty} \mathrm{d}s' \delta(s-s') \frac{e^{-\frac{s'^2}{4\sigma^2}} e^{-i\Omega s'}}{s^2 - l^2(n-m)^2} \\
&= -\frac{\sqrt{\pi}\sigma}{4\pi^2} \frac{1}{\sum_n \eta^{2n}} \sum_{n\neq m} \int_{-\infty}^{\infty} \mathrm{d}s \int_{-\infty}^{\infty} \mathrm{d}s' \left(\frac{1}{2\pi} \int_{-\infty}^{\infty} \mathrm{d}z \, e^{iz(s'-s)} \right) \frac{e^{-\frac{s'^2}{4\sigma^2}} e^{-i\Omega s'}}{s^2 - l^2(n-m)^2} \\
&= -\frac{\sqrt{\pi}\sigma}{8\pi^3} \frac{1}{\sum_n \eta^{2n}} \sum_{n\neq m} \int_{-\infty}^{\infty} \mathrm{d}z \left(\int_{-\infty}^{\infty} \mathrm{d}s' e^{-(\Omega-z)s'} e^{-\frac{s'^2}{4\sigma^2}} \right) \left(\int_{-\infty}^{\infty} \mathrm{d}s \, \frac{e^{-isz}}{s^2 - l^2(n-m)^2} \right) \\
&= -\frac{\sqrt{\pi}\sigma}{8\pi^3} \frac{1}{\sum_n \eta^{2n}} \sum_{n\neq m} \int_{-\infty}^{\infty} \mathrm{d}z \left(2\sqrt{\pi}\sigma e^{-(\Omega-z)^2\sigma^2} \right) \left(-\pi \mathrm{sgn}(z) \frac{\sin(l(n-m)z)}{l(n-m)} \right)
\end{aligned} \tag{A.3}$$

yielding

$$I_2 = (\sqrt{\pi}\sigma) \sum_{n\neq m} \frac{e^{-\frac{l^2(n-m)^2}{4\sigma^2}}}{4\pi l(n-m)} \mathrm{Im}\left[e^{il(n-m)\Omega} \mathrm{erf}\left(\frac{il(n-m)}{2\sigma} + \sigma\Omega \right) \right] \tag{A.4}$$

This yields the final expression for the transition probability,

$$P_D = P_{\mathcal{M}} - \frac{\sigma}{4\sqrt{\pi} l_D \sum_n \eta^{2n}} \Big[S_1 - S_2 \Big] \tag{A.5}$$

where

$$S_1 = 2 \sum_{n>m} \frac{e^{-\frac{l_D^2(n-m)^2}{4\sigma^2}}}{n-m} \sin(\Omega l_D(n-m)) \tag{A.6}$$

$$S_2 = \sum_{n\neq m} \frac{e^{-\frac{l_D^2(n-m)^2}{4\sigma^2}}}{(n-m)} \mathrm{Im}\left[e^{il_D(n-m)\Omega}\mathrm{erf}\left(\frac{il_D(n-m)}{2\sigma}+\sigma\Omega\right)\right] \tag{A.7}$$

and

$$P_{\mathcal{M}} = \frac{1}{4\pi}\left[e^{-\sigma^2\Omega^2} - \sqrt{\pi}\sigma\Omega\mathrm{erfc}(\sigma\Omega)\right] \tag{A.8}$$

is the transition probability of a single detector in flat Minkowski spacetime with no identifications. We see that there is Minkowski contribution and an image sum contribution which accounts for the possible identifications in the M/J_0 space.

Meanwhile, the cross-correlation term, that is the superposition case, We have

$$\begin{aligned}
L_{AB} &= \frac{1}{\sum_n \eta^{2n}} \sum_{n,m} \int_{-\infty}^{\infty} \mathrm{d}\tau \int_{-\infty}^{\infty} \mathrm{d}\tau' e^{-\frac{\tau^2}{2\sigma^2}} e^{-\frac{\tau'^2}{2\sigma^2}} e^{-i\Omega(\tau-\tau')} \\
&\quad \left[\frac{\mathrm{sgn}(\tau-\tau')\delta((\tau-\tau')^2-(l_An-l_Bm)^2}{4\pi i} - \frac{1}{4\pi^2((\tau-\tau')^2-(l_An-l_Bm)^2}\right] \\
L_{AB} &= \frac{1}{\sum_n \eta^{2n}} \sum_{l_An=l_Bm} \int_{-\infty}^{\infty} \mathrm{d}\tau \int_{-\infty}^{\infty} \mathrm{d}\tau' e^{-\frac{\tau^2}{2\sigma^2}} e^{-\frac{\tau'^2}{2\sigma^2}} e^{-i\Omega(\tau-\tau')} \\
&\quad \left[\frac{\mathrm{sgn}(\tau-\tau')\delta((\tau-\tau')^2)}{4\pi i} - \frac{1}{4\pi^2(\tau-\tau')^2}\right] \\
&\quad + \frac{1}{\sum_n \eta^{2n}} \sum_{l_An\neq l_Bm} \int_{-\infty}^{\infty} \mathrm{d}\tau \int_{-\infty}^{\infty} \mathrm{d}\tau' e^{-\frac{\tau^2}{2\sigma^2}} e^{-\frac{\tau'^2}{2\sigma^2}} e^{-i\Omega(\tau-\tau')} \\
&\quad \left[\frac{\mathrm{sgn}(\tau-\tau')\delta((\tau-\tau')^2-(l_An-l_Bm)^2)}{4\pi i} - \frac{1}{4\pi^2((\tau-\tau')^2-(l_An-l_Bm)^2)}\right] \\
L_{AB} &= \frac{\sum_{l_An=l_Bm}}{\sum_n \eta^{2n}} \left[\frac{1}{4\pi}\left[e^{-\sigma^2\Omega^2} - \sqrt{\pi}\sigma\Omega\mathrm{erf}\sigma\Omega\right]\right] \\
&\quad + \frac{1}{\sum_n \eta^{2n}} \sum_{l_An\neq l_Bm} \int_{-\infty}^{\infty} \mathrm{d}\tau \int_{-\infty}^{\infty} \mathrm{d}\tau' e^{-\frac{\tau^2}{2\sigma^2}} e^{-\frac{\tau'^2}{2\sigma^2}} e^{-i\Omega(\tau-\tau')} \\
&\quad \left[\frac{\mathrm{sgn}(\tau-\tau')\delta((\tau-\tau')^2-(l_An-l_Bm)^2)}{4\pi i} - \frac{1}{4\pi^2((\tau-\tau')^2-(l_An-l_Bm)^2)}\right]
\end{aligned} \tag{A.9}$$

Let us look at the image sum integrals:

$$\begin{aligned}
I_1 &= \frac{1}{\sum_n \eta^{2n}} \sum_{l_An\neq l_Bm} \int_{-\infty}^{\infty} \mathrm{d}\tau \int_{-\infty}^{\infty} \mathrm{d}\tau' e^{-\frac{\tau^2}{2\sigma^2}} e^{-\frac{\tau'^2}{2\sigma^2}} e^{-i\Omega(\tau-\tau')} \\
&\quad \frac{\mathrm{sgn}(\tau-\tau')\delta((\tau-\tau')^2-(l_An-l_Bm)^2)}{4\pi i}
\end{aligned}$$

$$
\begin{aligned}
I_1 &= \frac{1}{\sum_n \eta^{2n}} \sum_{l_A n \neq l_B m} \int_{-\infty}^{\infty} \mathrm{d}u \int_{-\infty}^{\infty} \mathrm{d}s \, e^{-\frac{u^2}{2\sigma^2}} e^{-\frac{(u-s)^2}{2\sigma^2}} e^{-i\Omega s} \frac{\mathrm{sgn}(s)\delta(s^2 - (l_A n - l_B m)^2)}{4\pi i} \\
&= \frac{\sqrt{\pi}\sigma}{\sum_n \eta^{2n}} \sum_{l_A n \neq l_B m} \int_{-\infty}^{\infty} \mathrm{d}s \, e^{-\frac{s^2}{4\sigma^2}} e^{-i\Omega s} \frac{\mathrm{sgn}(s)\delta(s^2 - (l_A n - l_B m)^2)}{4\pi i} \\
&= \frac{\sqrt{\pi}\sigma}{\sum_n \eta^{2n}} \frac{1}{4\pi i} \sum_{l_A n \neq l_B m} \int_{-\infty}^{\infty} \mathrm{d}s \, e^{-\frac{s^2}{4\sigma^2}} e^{-i\Omega s} \mathrm{sgn}(s) \frac{1}{2|l_A n - l_B m|} \\
&\quad \Big[\delta(s + l_A n - l_B m) + \delta(s - l_A n + l_B m)\Big]
\end{aligned}
$$

Integrating over s:

$$
\begin{aligned}
I_1 = \frac{\sqrt{\pi}\sigma}{\sum_n \eta^{2n}} \frac{1}{4\pi i} \sum_{l_A n \neq l_B m} \Bigg[& \frac{e^{-\frac{(l_A n - l_B m)^2}{4\sigma^2}} e^{i\Omega(l_A n - l_B m)} \mathrm{sgn}(-l_A n + l_B m)}{2|l_A n - l_B m|} \\
& + \frac{e^{-\frac{(l_A n - l_B m)^2}{4\sigma^2}} e^{-i\Omega(l_A n - l_B m)} \mathrm{sgn}(l_A n - l_B m)}{2|l_A n - l_B m|} \Bigg]
\end{aligned}
$$

Again, we can split the sum into terms whre $l_A n > l_B m$ and $l_A n < l_B m$:

$$
\begin{aligned}
I_1 = & \frac{\sqrt{\pi}\sigma}{\sum_n \eta^{2n}} \frac{1}{4\pi i} \sum_{l_A n > l_B m} \Bigg[\frac{e^{-\frac{(l_A n - l_B m)^2}{4\sigma^2}} e^{i\Omega(l_A n - l_B m)} \mathrm{sgn}(-l_A n + l_B m)}{2|l_A n - l_B m|} \\
& + \frac{e^{-\frac{(l_A n - l_B m)^2}{4\sigma^2}} e^{-i\Omega(l_A n - l_B m)} \mathrm{sgn}(l_A n - l_B m)}{2|l_A n - l_B m|} \Bigg] \\
& + \frac{\sqrt{\pi}\sigma}{\sum_n \eta^{2n}} \frac{1}{4\pi i} \sum_{l_B m > l_A n} \Bigg[\frac{e^{-\frac{(l_A n - l_B m)^2}{4\sigma^2}} e^{i\Omega(l_A n - l_B m)} \mathrm{sgn}(-l_A n + l_B m)}{2|l_A n - l_B m|} \\
& + \frac{e^{-\frac{(l_A n - l_B m)^2}{4\sigma^2}} e^{-i\Omega(l_A n - l_B m)} \mathrm{sgn}(l_A n - l_B m)}{2|l_A n - l_B m|} \Bigg]
\end{aligned}
$$

This simplifies to

$$
\begin{aligned}
I_1 &= \frac{\sqrt{\pi}\sigma}{\sum_n \eta^{2n}} \frac{1}{4\pi i} \sum_{l_A n > l_B m} \frac{\mathrm{sgn}(l_A n - l_B m)}{2|l_A n - l_B m|} e^{-\frac{(l_A n - l_B m)^2}{4\sigma^2}} \left[e^{-i\Omega(l_A n - l_B m)} - e^{i\Omega(l_A n - l_B m)} \right] \\
&\quad + \frac{\sqrt{\pi}\sigma}{\sum_n \eta^{2n}} \frac{1}{4\pi i} \sum_{l_B m > l_A n} \frac{\mathrm{sgn}(l_B m - l_A n)}{2|l_A n - l_B m|} e^{-\frac{(l_A n - l_B m)^2}{4\sigma^2}} \left[e^{i\Omega(l_A n - l_B m)} - e^{-i\Omega(l_A n - l_B m)} \right] \\
&= \frac{\sqrt{\pi}\sigma}{\sum_n \eta^{2n}} \frac{1}{4\pi} \Bigg[\sum_{l_A n > l_B m} \frac{e^{-\frac{(l_A n - l_B m)^2}{4\sigma^2}}}{l_A n - l_B m} \sin(\Omega(l_B m - l_A n))
\end{aligned}
$$

$$
\begin{aligned}
&\quad - \sum_{l_B m > l_A n} \frac{e^{-\frac{(l_A n - l_B m)^2}{4\sigma^2}}}{l_B m - l_A n} \sin(\Omega(l_B m - l_A n))\Big] \\
&= \frac{\sqrt{\pi}\sigma}{\sum_n \eta^{2n}} \frac{1}{2\pi} \sum_{l_A n > l_B m} \frac{e^{-\frac{(l_A n - l_B m)^2}{4\sigma^2}}}{l_A n - l_B m} \sin(\Omega(l_B m - l_A n)) \qquad \text{(A.10)}
\end{aligned}
$$

Next,

$$
\begin{aligned}
I_2 &= \frac{1}{\sum_n \eta^{2n}} \sum_{l_A n \neq l_B m} \int_{-\infty}^{\infty} \mathrm{d}\tau \int_{-\infty}^{\infty} \mathrm{d}\tau' \frac{e^{-\frac{\tau^2}{2\sigma^2}} e^{-\frac{\tau'^2}{2\sigma^2}} e^{-i\Omega(\tau - \tau')}}{4\pi^2((\tau - \tau')^2 - (l_A n - l_B m)^2)} \\
&= \frac{1}{\sum_n \eta^{2n}} \sum_{l_A n \neq l_B m} \int_{-\infty}^{\infty} \mathrm{d}u \int_{-\infty}^{\infty} \mathrm{d}s \, \frac{e^{-\frac{u^2}{2\sigma^2}} e^{-\frac{(u-s)^2}{2\sigma^2}} e^{-i\Omega s}}{4\pi^2(s^2 - (l_A n - l_B m)^2)} \\
&= \frac{\sqrt{\pi}\sigma}{\sum_n \eta^{2n}} \frac{1}{4\pi^2} \sum_{l_A n \neq l_B m} \int_{-\infty}^{\infty} \mathrm{d}s \, \frac{e^{-\frac{s^2}{4\sigma^2}} e^{-i\Omega s}}{s^2 - (l_A n - l_B m)^2} \\
&= \frac{\sqrt{\pi}\sigma}{\sum_n \eta^{2n}} \frac{1}{4\pi^2} \sum_{l_A n \neq l_B m} \int_{-\infty}^{\infty} \mathrm{d}s \int_{-\infty}^{\infty} \mathrm{d}s' \delta(s - s') \frac{e^{-\frac{s'^2}{4\sigma^2}} e^{-i\Omega s'}}{s^2 - (l_A n - l_B m)^2} \\
&= \frac{\sqrt{\pi}\sigma}{\sum_n \eta^{2n}} \frac{1}{4\pi^2} \sum_{l_A n \neq l_B m} \int_{-\infty}^{\infty} \mathrm{d}s \int_{-\infty}^{\infty} \mathrm{d}s' \left(\frac{1}{2\pi} \int_{-\infty}^{\infty} \mathrm{d}z \, e^{iz(s' - s)} \right) \frac{e^{-\frac{s'^2}{4\sigma^2}} e^{-i\Omega s'}}{s^2 - (l_A n - l_B m)^2} \\
&= \frac{\sqrt{\pi}\sigma}{8\pi^3} \frac{1}{\sum_n \eta^{2n}} \sum_{l_A n \neq l_B m} \int_{-\infty}^{\infty} \mathrm{d}z \left(\int_{-\infty}^{\infty} \mathrm{d}s' e^{-(\Omega - z)^2 s'} e^{-\frac{s'^2}{4\sigma^2}} \right) \left(\int_{-\infty}^{\infty} \mathrm{d}s \, \frac{e^{-isz}}{s^2 - (l_A n - l_B m)^2} \right) \\
&= \frac{\sqrt{\pi}\sigma}{8\pi^3} \frac{1}{\sum_n \eta^{2n}} \sum_{l_A n \neq l_B m} \int_{-\infty}^{\infty} \mathrm{d}z \, \left(2\sqrt{\pi}\sigma e^{-(\Omega - z)^2 \sigma^2} \right) \left(-\pi \mathrm{sgn}(z) \frac{\sin((l_A n - l_B m)z}{l_A n - l_B m} \right) \\
&= \frac{\sigma}{4\pi} \frac{1}{\sum_n \eta^{2n}} \sum_{l_A n \neq l_B m} \frac{e^{-\frac{(l_A n - l_B m)^2}{4\sigma^2}}}{(l_A n - l_B m)} \mathrm{Im} \left[e^{i(l_A n - l_B m)\Omega} \mathrm{erf} \left(\frac{i(l_A n - l_B m)}{2\sigma} + \sigma\Omega \right) \right]
\end{aligned}
\qquad \text{(A.11)}
$$

Finally, we can express the transition probability for cross correlation Wightman function using the simplified image sum terms at eqn. A.10 and at eqn. A.11 ,

$$
L_{AB} = \frac{K_\gamma}{\sum_n \eta^{2n}} P_{\mathcal{M}} + \frac{\sigma}{4\sqrt{\pi} \sum_n \eta^{2n}} \Big[J_1 - J_2 \Big] \qquad \text{(A.12)}
$$

where

$$J_1 = \sum_{l_A n \neq l_B m} \frac{e^{-\frac{l_{nm}^2}{4\sigma^2}}}{l_{nm}} \mathrm{Im}\left[e^{i l_{nm}\Omega} \mathrm{erf}\left[\frac{i l_{nm}}{2\sigma} + \sigma\Omega \right] \right] \tag{A.13}$$

$$J_2 = 2 \sum_{l_{nm}>0} \frac{e^{-\frac{l_{nm}^2}{4\sigma^2}}}{l_{nm}} \sin(\Omega l_{nm}) \tag{A.14}$$

and $l_{nm} = l_A n - l_B m$. Likewise, we have defined

$$K_\gamma = \mathsf{coeff}\left(\sum_{n,m} f\left(n - \gamma m\right), f(0) \right) \tag{A.15}$$

as stated in the main text.

Appendix B

Conditional Transition Probability Derivation for the Mass-Superposed BTZ Black Hole

The dynamical evolution of the BTZ black hole mass superposition is given by:

$$|\psi(t_f)\rangle = e^{-i\hat{H}_{0,S}t_f}\hat{U}e^{i\hat{H}_{0,S}t_i}|\psi(t_i)\rangle \tag{B.1}$$

$$= e^{-i\hat{H}_{0,S}t_f}\left[I - i\lambda\int_{t_i}^{t_f}\mathrm{d}\tau\,\hat{H}_{\text{int.}}(\tau) - \lambda^2\int_{t_i}^{t_f}\mathrm{d}\tau\int_{t_i}^{\tau}\mathrm{d}\tau'\hat{H}_{\text{int.}}(\tau)\hat{H}_{\text{int.}}(\tau')\right]e^{i\hat{H}_{0,S}t_i}|\psi(t_i)\rangle$$

$$\begin{aligned}= e^{-i\hat{H}_{0,S}t_f}e^{i\hat{H}_{0,S}t_i}|\psi(t_i)\rangle \\ - e^{-i\hat{H}_{0,S}t_f}(i\lambda)\int_{t_i}^{t_f}\mathrm{d}\tau\,\hat{H}_{\text{int.}}(\tau)e^{i\hat{H}_{0,S}t_i}|\psi(t_i)\rangle \\ - e^{-i\hat{H}_{0,S}t_f}(\lambda^2)\int_{t_i}^{t_f}\mathrm{d}\tau\int_{t_i}^{\tau}\mathrm{d}\tau'\hat{H}_{\text{int.}}(\tau)\hat{H}_{\text{int.}}(\tau')e^{i\hat{H}_{0,S}t_i}|\psi(t_i)\rangle\end{aligned} \tag{B.2}$$

$$\begin{aligned}= e^{-i\hat{H}_{0,S}t_f}e^{i\hat{H}_{0,S}t_i}\frac{1}{\sqrt{2}}(|M_A\rangle + |M_B\rangle)|0\rangle|g\rangle \\ - e^{-i\hat{H}_{0,S}t_f}(i\lambda)\int_{t_i}^{t_f}\mathrm{d}\tau\,\hat{H}_{\text{int.}}(\tau)e^{i\hat{H}_{0,S}t_i}\frac{1}{\sqrt{2}}(|M_A\rangle + |M_B\rangle)|0\rangle|g\rangle \\ - e^{-i\hat{H}_{0,S}t_f}(\lambda^2)\int_{t_i}^{t_f}\mathrm{d}\tau\int_{t_i}^{\tau}\mathrm{d}\tau'\hat{H}_{\text{int.}}(\tau)\hat{H}_{\text{int.}}(\tau')e^{i\hat{H}_{0,S}t_i}\frac{1}{\sqrt{2}}(|M_A\rangle + |M_B\rangle)|0\rangle|g\rangle\end{aligned} \tag{B.3}$$

$$
\begin{aligned}
&= e^{-i\hat{H}_{0,S}t_f}\frac{1}{\sqrt{2}}(e^{iE_At_i}|M_A\rangle + e^{iE_Bt_i}|M_B\rangle)|0\rangle|g\rangle \\
&\quad - e^{-i\hat{H}_{0,S}t_f}(i\lambda)\int_{t_i}^{t_f}\mathrm{d}\tau\,\hat{H}_{\text{int.}}(\tau)\frac{1}{\sqrt{2}}(e^{iE_At_i}|M_A\rangle + e^{iE_Bt_i}|M_B\rangle)|0\rangle|g\rangle \\
&\quad - e^{-i\hat{H}_{0,S}t_f}(\lambda^2)\int_{t_i}^{t_f}\mathrm{d}\tau\int_{t_i}^{\tau}\mathrm{d}\tau'\hat{H}_{\text{int.}}(\tau)\hat{H}_{\text{int.}}(\tau')\frac{1}{\sqrt{2}}(e^{iE_At_i}|M_A\rangle + e^{iE_Bt_i}|M_B\rangle)|0\rangle|g\rangle
\end{aligned}
\tag{B.4}
$$

$$
\begin{aligned}
&= e^{-i\hat{H}_{0,S}t_f}\frac{1}{\sqrt{2}}e^{iE_At_i}(|M_A\rangle + e^{i(E_B-E_A)t_i}|M_B\rangle)|0\rangle|g\rangle \\
&\quad - e^{-i\hat{H}_{0,S}t_f}(i\lambda)\int_{t_i}^{t_f}\mathrm{d}\tau\,\hat{H}_{\text{int.}}(\tau)\frac{1}{\sqrt{2}}e^{iE_At_i}(|M_A\rangle + e^{i(E_B-E_A)t_i}|M_B\rangle)|0\rangle|g\rangle \\
&\quad - e^{-i\hat{H}_{0,S}t_f}(\lambda^2)\int_{t_i}^{t_f}\mathrm{d}\tau\int_{t_i}^{\tau}\mathrm{d}\tau'\hat{H}_{\text{int.}}(\tau)\hat{H}_{\text{int.}}(\tau')\frac{1}{\sqrt{2}}e^{iE_At_i}(|M_A\rangle \\
&\quad + e^{i(E_B-E_A)t_i}|M_B\rangle)|0\rangle|g\rangle \\
&= e^{-i\hat{H}_{0,S}t_f}\frac{1}{\sqrt{2}}(|M_A\rangle + e^{i\Delta Et_i}|M_B\rangle)|0\rangle|g\rangle \\
&\quad - e^{-i\hat{H}_{0,S}t_f}(i\lambda)\int_{t_i}^{t_f}\mathrm{d}\tau\,\hat{H}_{\text{int.}}(\tau)\frac{1}{\sqrt{2}}(|M_A\rangle + e^{i\Delta Et_i}|M_B\rangle)|0\rangle|g\rangle \\
&\quad - e^{-i\hat{H}_{0,S}t_f}(\lambda^2)\int_{t_i}^{t_f}\mathrm{d}\tau\int_{t_i}^{\tau}\mathrm{d}\tau'\hat{H}_{\text{int.}}(\tau)\hat{H}_{\text{int.}}(\tau')\frac{1}{\sqrt{2}}(|M_A\rangle + e^{i\Delta Et_i}|M_B\rangle)|0\rangle|g\rangle
\end{aligned}
$$

where $\Delta E = E_B - E_A$ and we neglected the global phase

$$
\begin{aligned}
|\psi(t_f)\rangle &= \frac{1}{\sqrt{2}}(e^{-iE_At_f}|M_A\rangle + e^{-iE_Bt_f}e^{i\Delta Et_i}|M_B\rangle)|0\rangle|g\rangle \\
&\quad - (i\lambda)\int_{t_i}^{t_f}\mathrm{d}\tau\,\hat{H}_{\text{int.}}(\tau)\frac{1}{\sqrt{2}}(e^{-iE_At_f}|M_A\rangle + e^{-iE_Bt_f}e^{i\Delta Et_i}|M_B\rangle)|0\rangle|g\rangle \\
&\quad - (\lambda^2)\int_{t_i}^{t_f}\mathrm{d}\tau\int_{t_i}^{\tau}\mathrm{d}\tau'\hat{H}_{\text{int.}}(\tau)\hat{H}_{\text{int.}}(\tau')\frac{1}{\sqrt{2}}(e^{-iE_At_f}|M_A\rangle + e^{-iE_Bt_f}e^{i\Delta Et_i}|M_B\rangle)|0\rangle|g\rangle \\
&= \frac{1}{\sqrt{2}}e^{-iE_At_f}(|M_A\rangle + e^{-i(E_B-E_A)t_f}e^{i\Delta Et_i}|M_B\rangle)|0\rangle|g\rangle \\
&\quad - (i\lambda)\int_{t_i}^{t_f}\mathrm{d}\tau\,\hat{H}_{\text{int.}}(\tau)\frac{1}{\sqrt{2}}e^{-iE_At_f}(|M_A\rangle + e^{-i(E_B-E_A)t_f}e^{i\Delta Et_i}|M_B\rangle)|0\rangle|g\rangle \\
&\quad - (\lambda^2)\int_{t_i}^{t_f}\mathrm{d}\tau\int_{t_i}^{\tau}\mathrm{d}\tau'\hat{H}_{\text{int.}}(\tau)\hat{H}_{\text{int.}}(\tau')\frac{1}{\sqrt{2}}e^{-iE_At_f}(|M_A\rangle
\end{aligned}
$$

$$+ e^{-i(E_B-E_A)t_f} e^{i\Delta E t_i}|M_B\rangle)|0\rangle|g\rangle$$

we again neglected the global phase which is $e^{-iE_A t_f}$

$$\begin{aligned}
|\psi(t_f)\rangle &= \frac{1}{\sqrt{2}}(|M_A\rangle + e^{-i\Delta E t_f} e^{i\Delta E t_i}|M_B\rangle)|0\rangle|g\rangle \\
&\quad - (i\lambda)\int_{t_i}^{t_f} \mathrm{d}\tau\, \hat{H}_{\text{int.}}(\tau)\frac{1}{\sqrt{2}}(|M_A\rangle + e^{-i\Delta E t_f} e^{i\Delta E t_i}|M_B\rangle)|0\rangle|g\rangle \\
&\quad - (\lambda^2)\int_{t_i}^{t_f} \mathrm{d}\tau \int_{t_i}^{\tau} \mathrm{d}\tau' \hat{H}_{\text{int.}}(\tau)\hat{H}_{\text{int.}}(\tau')\frac{1}{\sqrt{2}}(|M_A\rangle + e^{-i\Delta E t_f} e^{i\Delta E t_i}|M_B\rangle)|0\rangle|g\rangle \\
&= \frac{1}{\sqrt{2}}(|M_A\rangle + e^{-i\Delta E \Delta t}|M_B\rangle)|0\rangle|g\rangle \\
&\quad - (i\lambda)\int_{t_i}^{t_f} \mathrm{d}\tau\, \hat{H}_{\text{int.}}(\tau)\frac{1}{\sqrt{2}}(|M_A\rangle + e^{-i\Delta E \Delta t}|M_B\rangle)|0\rangle|g\rangle \\
&\quad - (\lambda^2)\int_{t_i}^{t_f} \mathrm{d}\tau \int_{t_i}^{\tau} \mathrm{d}\tau' \hat{H}_{\text{int.}}(\tau)\hat{H}_{\text{int.}}(\tau')\frac{1}{\sqrt{2}}(|M_A\rangle + e^{-i\Delta E \Delta t}|M_B\rangle)|0\rangle|g\rangle
\end{aligned} \tag{B.5}$$

where $\Delta t = t_f - t_i$. Let us look at the individual terms. We have

$$|\psi(t_f)\rangle^{(0)} = \frac{1}{\sqrt{2}}(|M_A\rangle + e^{-i\Delta E \Delta t}|M_B\rangle)|0\rangle|g\rangle \tag{B.6}$$

$$\begin{aligned}
|\psi(t_f)\rangle^{(1)} &= -\frac{i\lambda}{\sqrt{2}}\int_{t_i}^{t_f} \mathrm{d}\tau\, \eta(\tau)\sigma(\tau)\Big[\hat{\psi}(\mathsf{x}_A)|M_A\rangle\langle M_A| + \hat{\psi}(\mathsf{x}_B)|M_B\rangle\langle M_B|\Big] \\
&\qquad (|M_A\rangle + e^{-i\Delta E \Delta t}|M_B\rangle)|0\rangle|g\rangle \\
&= -\frac{i\lambda}{\sqrt{2}}\int_{t_i}^{t_f} \mathrm{d}\tau\, \eta(\tau)e^{i\Omega\tau}\Big[\hat{\psi}(\mathsf{x}_A)|M_A\rangle + \hat{\psi}(\mathsf{x}_B)e^{-i\Delta E \Delta t}|M_B\rangle\Big]|0\rangle|e\rangle
\end{aligned} \tag{B.7}$$

$$\begin{aligned}
|\psi(t_f)\rangle^{(2)} &= -\frac{\lambda^2}{\sqrt{2}}\int_{t_i}^{t_f} \mathrm{d}\tau \int_{t_i}^{\tau} \mathrm{d}\tau' \eta(\tau)\eta(\tau')e^{-i\Omega(\tau-\tau')}\Big[\hat{\psi}(\mathsf{x}_A)|M_A\rangle\langle M_A| + \hat{\psi}(\mathsf{x}_B)|M_B\rangle\langle M_A|\Big] \\
&\qquad \Big[\hat{\psi}(\mathsf{x}'_A)|M_A\rangle\langle M_A| + \hat{\psi}(\mathsf{x}'_B)|M_B\rangle\langle M_B|\Big]|(|M_A\rangle + e^{-i\Delta E \Delta t}|M_B\rangle)0\rangle|g\rangle \\
&= -\frac{\lambda^2}{\sqrt{2}}\int_{t_i}^{t_f} \mathrm{d}\tau \int_{t_i}^{\tau} \mathrm{d}\tau' \eta(\tau)\eta(\tau')e^{-i\Omega(\tau-\tau')}\Big[\hat{\psi}(\mathsf{x}_A)|M_A\rangle\langle M_A| + \hat{\psi}(\mathsf{x}_B)|M_B\rangle\langle M_B|\Big] \\
&\qquad \Big[\hat{\psi}(\mathsf{x}'_A)|M_A\rangle\langle M_A| + \hat{\psi}(\mathsf{x}'_B)|M_B\rangle\langle M_B|\Big](|M_A\rangle + e^{-i\Delta E \Delta t}|M_B\rangle)|0\rangle|g\rangle \\
&= -\frac{\lambda^2}{\sqrt{2}}\int_{t_i}^{t_f} \mathrm{d}\tau \int_{t_i}^{\tau} \mathrm{d}\tau' \eta(\tau)\eta(\tau')e^{-i\Omega(\tau-\tau')}\Big[\hat{\psi}(\mathsf{x}_A)\hat{\psi}(\mathsf{x}'_A)|M_A\rangle\langle M_A|
\end{aligned}$$

$$+\hat{\psi}(\mathsf{x}_B)\hat{\psi}(\mathsf{x}'_B)|M_B\rangle\langle M_B|\Big](|M_A\rangle + e^{-i\Delta E\Delta t}|M_B\rangle)|0\rangle|g\rangle$$
$$= -\frac{\lambda^2}{\sqrt{2}}\int_{t_i}^{t_f}\mathrm{d}\tau\int_{t_i}^{\tau}\mathrm{d}\tau'\eta(\tau)\eta(\tau')e^{-i\Omega(\tau-\tau')}\Big[\hat{\psi}(\mathsf{x}_A)\hat{\psi}(\mathsf{x}'_A)|M_A\rangle$$
$$+\hat{\psi}(\mathsf{x}_B)\hat{\psi}(\mathsf{x}'_B)e^{-i\Delta E\Delta t}|M_B\rangle\Big]|0\rangle|g\rangle \tag{B.8}$$

To repeat:

$$|\psi(t_f)\rangle^{(0)} = \frac{1}{\sqrt{2}}(|M_A\rangle + e^{-i\Delta E\Delta t}|M_B\rangle)|0\rangle|g\rangle \tag{B.9}$$
$$|\psi(t_f)\rangle^{(1)} = -\frac{i\lambda}{\sqrt{2}}\int_{t_i}^{t_f}\mathrm{d}\tau\,\eta(\tau)e^{i\Omega\tau}\Big[\hat{\psi}(\mathsf{x}_A)|M_A\rangle + \hat{\psi}(\mathsf{x}_B)e^{-i\Delta E\Delta t}|M_B\rangle\Big]|0\rangle|e\rangle \tag{B.10}$$
$$|\psi(t_f)\rangle^{(2)} = -\frac{\lambda^2}{\sqrt{2}}\int_{t_i}^{t_f}\mathrm{d}\tau\int_{t_i}^{\tau}\mathrm{d}\tau'\eta(\tau)\eta(\tau')e^{-i\Omega(\tau-\tau')}\Big[\hat{\psi}(\mathsf{x}_A)\hat{\psi}(\mathsf{x}'_A)|M_A\rangle$$
$$+\hat{\psi}(\mathsf{x}_B)\hat{\psi}(\mathsf{x}'_B)e^{-i\Delta E\Delta t}|M_B\rangle\Big]|0\rangle|g\rangle \tag{B.11}$$

B.0.1 Measurement in the $|\pm\rangle = (|M_A\rangle \pm |M_B\rangle)/\sqrt{2}$ Basis

$$\langle\pm|\psi(t_f)\rangle^{(0)} = \frac{1}{2}(1 \pm e^{-i\Delta E\Delta t})|0\rangle|g\rangle \tag{B.12}$$
$$\langle+|\psi(t_f)\rangle^{(1)} = -\frac{i\lambda}{2}\int_{t_i}^{t_f}\mathrm{d}\tau\,\eta(\tau)e^{i\Omega\tau}\Big[\hat{\psi}(\mathsf{x}_A) \pm \hat{\psi}(\mathsf{x}_B)e^{-i\Delta E\Delta t}\Big]|0\rangle|e\rangle \tag{B.13}$$
$$\langle+|\psi(t_f)\rangle^{(2)} = -\frac{\lambda^2}{2}\int_{t_i}^{t_f}\mathrm{d}\tau\int_{t_i}^{\tau}\mathrm{d}\tau'\eta(\tau)\eta(\tau')e^{-i\Omega(\tau-\tau')}\Big[\hat{\psi}(\mathsf{x}_A)\hat{\psi}(\mathsf{x}'_A)$$
$$\pm\hat{\psi}(\mathsf{x}_B)\hat{\psi}(\mathsf{x}'_B)e^{-i\Delta E\Delta t}\Big]|0\rangle|g\rangle \tag{B.14}$$

We have the terms (in the density matrix) given by

$$\mathrm{Tr}_\psi\left[\hat{U}^{(0)}\hat{\rho}_{\mathrm{FD}}\hat{U}^{(0)\dagger}\right] = \frac{1}{4}\Big[2 \pm 2\cos\Delta E\Delta t\Big]|0\rangle|g\rangle\langle g|\langle 0| \tag{B.15}$$
$$\mathrm{Tr}_\psi\left[\hat{U}^{(0)}\hat{\rho}_{\mathrm{FD}}\hat{U}^{(2)\dagger}\right] = -\frac{\lambda^2|g\rangle\langle g|}{4}\int_{t_i}^{t_f}\mathrm{d}\tau\int_{t_i}^{\tau}\mathrm{d}\tau'\eta(\tau)\eta(\tau')e^{i\Omega(\tau-\tau')}(1 \pm e^{-i\Delta E\Delta t})|0\rangle\langle 0|$$
$$\Big[\hat{\psi}(\mathsf{x}_A)\hat{\psi}(\mathsf{x}'_A) \pm \hat{\psi}(\mathsf{x}_B)\hat{\psi}(\mathsf{x}'_B)e^{i\Delta E\Delta t}\Big]$$
$$= -\frac{\lambda^2|g\rangle\langle g|}{4}\int_{t_i}^{t_f}\mathrm{d}\tau\int_{t_i}^{\tau}\mathrm{d}\tau'\eta(\tau)\eta(\tau')e^{i\Omega(\tau-\tau')}\Big[|0\rangle\langle 0|\hat{\psi}(\mathsf{x}_A)\hat{\psi}(\mathsf{x}'_A)$$

$$\pm |0\rangle\langle 0|\hat{\psi}(\mathsf{x}_B)\hat{\psi}(\mathsf{x}'_B)e^{i\Delta E\Delta t} \pm e^{-i\Delta E\Delta t}|0\rangle\langle 0|\hat{\psi}(\mathsf{x}_A)\hat{\psi}(\mathsf{x}'_A)$$
$$+ |0\rangle\langle 0|\hat{\psi}(\mathsf{x}_B)\hat{\psi}(\mathsf{x}'_B)\Big] \tag{B.16}$$

$$\mathrm{Tr}_\psi\left[\hat{U}^{(2)}\hat{\rho}_{\mathrm{FD}}\hat{U}^{(0)\dagger}\right] = -\frac{\lambda^2|g\rangle\langle g|}{4}\int_{t_i}^{t_f}\mathrm{d}\tau\int_{t_i}^{\tau}\mathrm{d}\tau'\eta(\tau)\eta(\tau')e^{-i\Omega(\tau-\tau')}\Big[\hat{\psi}(\mathsf{x}_A)\hat{\psi}(\mathsf{x}'_A)|0\rangle\langle 0|$$
$$\pm \hat{\psi}(\mathsf{x}_B)\hat{\psi}(\mathsf{x}'_B)e^{-i\Delta E\Delta t}|0\rangle\langle 0| \pm \hat{\psi}(\mathsf{x}_A)\hat{\psi}(\mathsf{x}'_A)e^{i\Delta E\Delta t}|0\rangle\langle 0|$$
$$+ \hat{\psi}(\mathsf{x}_B)\hat{\psi}(\mathsf{x}'_B)|0\rangle\langle 0|\Big] \tag{B.17}$$

$$\mathrm{Tr}_\psi\left[\hat{U}^{(1)}\hat{\rho}_{\mathrm{FD}}\hat{U}^{(1)\dagger}\right] = \frac{\lambda^2|e\rangle\langle e|}{4}\iint\mathrm{d}\tau\mathrm{d}\tau'\eta(\tau)\eta(\tau')e^{i\Omega(\tau-\tau')}\Big[\hat{\psi}(\mathsf{x}_A)|0\rangle\langle 0|\hat{\psi}(\mathsf{x}'_A)$$
$$\pm \hat{\psi}(\mathsf{x}_A)|0\rangle\langle 0|\hat{\psi}(\mathsf{x}'_B)e^{i\Delta E\Delta t} \pm \hat{\psi}(\mathsf{x}_B)|0\rangle\langle 0|\hat{\psi}(\mathsf{x}'_A)e^{-i\Delta E\Delta t}$$
$$+ \hat{\psi}(\mathsf{x}_B)|0\rangle\langle 0|\hat{\psi}(\mathsf{x}'_B)\Big] \tag{B.18}$$

Tracing out the field and simplifying,

$$\mathrm{Tr}_\psi\left[\hat{U}^{(0)}\hat{\rho}_{\mathrm{FD}}\hat{U}^{(0)\dagger}\right] = \frac{1}{4}\Big[2 \pm 2\cos\Delta E\Delta t\Big]|g\rangle\langle g| \tag{B.19}$$

$$\mathrm{Tr}_\psi\left[\hat{U}^{(0)}\hat{\rho}_{\mathrm{FD}}\hat{U}^{(2)\dagger}\right] = -\frac{\lambda^2|g\rangle\langle g|}{4}\int_{t_i}^{t_f}\mathrm{d}\tau\int_{t_i}^{\tau}\mathrm{d}\tau'\eta(\tau)\eta(\tau')e^{i\Omega(\tau-\tau')}\Big[W(\mathsf{x}_A,\mathsf{x}'_A)\Big(1 \pm e^{-i\Delta E\Delta t}\Big)$$
$$+ W(\mathsf{x}_B,\mathsf{x}'_B)\Big(1 \pm e^{i\Delta E\Delta t}\Big)\Big] \tag{B.20}$$

$$\mathrm{Tr}_\psi\left[\hat{U}^{(2)}\hat{\rho}_{\mathrm{FD}}\hat{U}^{(0)\dagger}\right] = -\frac{\lambda^2|g\rangle\langle g|}{4}\int_{t_i}^{t_f}\mathrm{d}\tau\int_{t_i}^{\tau}\mathrm{d}\tau'\eta(\tau)\eta(\tau')e^{-i\Omega(\tau-\tau')}\Big[W(\mathsf{x}_A,\mathsf{x}'_A)\Big(1 \pm e^{i\Delta E\Delta t}\Big)$$
$$+ W(\mathsf{x}_B,\mathsf{x}'_B)\Big(1 \pm e^{-i\Delta E\Delta t}\Big)\Big] \tag{B.21}$$

$$\mathrm{Tr}_\psi\left[\hat{U}^{(1)}\hat{\rho}_{\mathrm{FD}}\hat{U}^{(1)\dagger}\right] = \frac{\lambda^2|e\rangle\langle e|}{4}\int_{t_i}^{t_f}\mathrm{d}\tau\int_{t_i}^{\tau}\mathrm{d}\tau'\eta(\tau)\eta(\tau')e^{-i\Omega(\tau-\tau')}\Big[W(\mathsf{x}_A,\mathsf{x}'_A) + W(\mathsf{x}_B,\mathsf{x}'_B)$$
$$\pm W(\mathsf{x}_A,\mathsf{x}'_B)\Big(2\cos\Delta E\Delta t\Big)\Big] \tag{B.22}$$

The sum of the second order terms is

$$\mathrm{Tr}_\psi\left[\hat{U}^{(0)}\hat{\rho}_{\mathrm{FD}}\hat{U}^{(2)\dagger}\right] + \mathrm{Tr}_\psi\left[\hat{U}^{(2)}\hat{\rho}_{\mathrm{FD}}\hat{U}^{(0)\dagger}\right] \tag{B.23}$$
$$= -\frac{\lambda^2|g\rangle\langle g|}{4}\int_{t_i}^{t_f}\mathrm{d}\tau\int_{t_i}^{\tau}\mathrm{d}\tau'\eta(\tau)\eta(\tau')e^{-i\Omega(\tau-\tau')}\Big[2W(\mathsf{x}_A,\mathsf{x}'_A)\Big(1+\cos\Delta E\Delta t\Big)$$
$$+ 2W(\mathsf{x}_B,\mathsf{x}'_B)\Big(1 \pm \cos\Delta E\Delta t\Big)\Big] \tag{B.24}$$

$$= -\frac{\lambda^2|g\rangle\langle g|}{2}\int_{t_i}^{t_f}\mathrm{d}\tau\int_{t_i}^{\tau}\mathrm{d}\tau'\eta(\tau)\eta(\tau')e^{-i\Omega(\tau-\tau')}\Big(W(\mathsf{x}_A,\mathsf{x}'_A)+W(\mathsf{x}_B,\mathsf{x}'_B)\Big)\Big(1\pm\cos\Delta E\Delta t\Big) \tag{B.25}$$

Thus the ground and excited transition probabilities respectively are given by

$$P_G = \frac{1}{2}\Big(1\pm\cos\Delta E\Delta t\Big)\Big[1-\frac{\lambda^2}{2}\int_{t_i}^{t_f}\mathrm{d}\tau\int_{t_i}^{t_f}\mathrm{d}\tau'\mathrm{d}\eta(\tau)\eta(\tau')e^{-i\Omega(\tau-\tau')}\Big(W(\mathsf{x}_A,\mathsf{x}'_A)+W(\mathsf{x}_B,\mathsf{x}'_B)\Big)\Big] \tag{B.26}$$

$$P_E = \frac{\lambda^2|e\rangle\langle e|}{4}\int_{t_i}^{t_f}\mathrm{d}\tau\int_{t_i}^{t_f}\mathrm{d}\tau'\eta(\tau)\eta(\tau')e^{-i\Omega(\tau-\tau')}\Big[W(\mathsf{x}_A,\mathsf{x}'_A)+W(\mathsf{x}_B,\mathsf{x}'_B) \pm W(\mathsf{x}_A,\mathsf{x}'_B)\Big(2\cos\Delta E\Delta t\Big)\Big] \tag{B.27}$$

We can write this as

$$P_G = \frac{1}{2}\Big(1\pm\cos\Delta E\Delta t\Big)\Big[1-\frac{\lambda^2}{2}\Big(P_A+P_B\Big)\Big] \tag{B.28}$$

$$P_E = \frac{\lambda^2}{4}\Big(P_A+P_B\pm 2\cos\Delta E\Delta t L_{AB}\Big) \tag{B.29}$$

as stated in the main text.

B.0.2 Total Transition Probability for $|\pm\rangle$ Basis

We have (unnormalised)

$$P_G^+ = \frac{1}{2}\Big(1+\cos\Delta E\Delta t\Big)\Big[1-\frac{\lambda^2}{2}\Big(P_A+P_B\Big)\Big] \tag{B.30}$$

$$P_G^- = \frac{1}{2}\Big(1-\cos\Delta E\Delta t\Big)\Big[1-\frac{\lambda^2}{2}(P_A+P_B)\Big] \tag{B.31}$$

$$P_E^+ = \frac{\lambda^2}{4}\Big(P_A+P_B+2\cos\Delta E\Delta t L_{AB}\Big) \tag{B.32}$$

$$P_E^- = \frac{\lambda^2}{4}\Big(P_A+P_B-2\cos\Delta E\Delta t L_{AB}\Big) \tag{B.33}$$

Note that $P_G^+ + P_G^- + P_E^+ + P_E^- = 1$. That is,

$$\sum_{i=g,e}\sum_{j=+,-}\Big|\langle i|\langle j|\hat{U}|\psi(t_i)\rangle\Big|^2 = 1 \tag{B.34}$$

as stated in the main text.

B.0.3 Integral Expressions for P_D and L_{AB} with Gaussian Switching

Here, we calculate the simplified integral form of P_D and L_{AB} for a Gaussian detector switching, as shown in Eq. (4.58) and (4.59) in the main text. Inserting the Wightman functions into the expression for the transition probability, we obtain the following expression

$$\frac{P_D}{\sigma} = \frac{\sqrt{\pi}\gamma_D}{2}\left(\frac{1}{4\pi l\sqrt{2}}\right)\frac{1}{\sum_n \eta^{2n}}\sum_{n,m}\frac{1}{\gamma_D}\int_{-t_f}^{t_f} \mathrm{d}s\, \frac{e^{-\frac{\gamma_D^2 s^2}{4\sigma^2}} e^{-i\Omega\gamma_D s} H_0(s)}{\sqrt{\frac{R_D^2}{\gamma_D^2 l^2}\cosh(2\pi(n-m)\sqrt{M}) - \frac{1}{\gamma_D^2} - \cosh(s/l)}}, \tag{B.35}$$

where $H_0(s) = \mathrm{erf}\left[\frac{\gamma_D(s+2t_f)}{2\sigma}\right] - \mathrm{erf}\left[\frac{\gamma_D(s-2t_f)}{2\sigma}\right]$. Splitting up the summation into contributions where $n = m$ and $n \neq m$ yields

$$\begin{aligned}\frac{P_D}{\sigma} = &\frac{\sqrt{\pi}\gamma_D}{2}\left(\frac{1}{4\pi l\sqrt{2}}\right)\frac{1}{\sum_n \eta^{2n}}\sum_{n=m}\frac{1}{\gamma_D}\int_{-t_f}^{t_f} \mathrm{d}s\, \frac{e^{-\frac{\gamma_D^2 s^2}{4\sigma^2}} e^{-i\Omega\gamma_D s} H_0(s)}{\sqrt{1-\cosh(s/l)}} \\ &+ \frac{\sqrt{\pi}\gamma_D}{2}\left(\frac{1}{4\pi l\sqrt{2}}\right)\frac{1}{\sum_n \eta^{2n}}\sum_{n\neq m}\frac{1}{\gamma_D}\int_{-t_f}^{t_f} \mathrm{d}s\, \frac{e^{-\frac{\gamma_D^2 s^2}{4\sigma^2}} e^{-i\Omega\gamma_D s} H_0(s)}{\sqrt{\frac{R_D^2}{\gamma_D^2 l^2}\cosh(2\pi(n-m)\sqrt{M}) - \frac{1}{\gamma_D^2} - \cosh(s/l)}}.\end{aligned} \tag{B.36}$$

Using the identity $\sinh^2(s/2l) = \cosh(s/l) - 1$ and making simplifying substitutions of the integration variable yields

$$\begin{aligned}\frac{P_D}{\sigma} = &\frac{\sqrt{\pi}\gamma_D}{2}\left(\frac{1}{2\pi\sqrt{2}}\right)\frac{1}{\sum_n \eta^{2n}}\sum_{n=m}\frac{1}{\gamma_D}\int_{-t_f/2l}^{t_f/2l} \mathrm{d}z\, \frac{e^{-\frac{\gamma_D^2 l^2 z^2}{\sigma^2}} e^{-2i\Omega\gamma_D l z} H_0(2lz)}{i\sqrt{2}\sinh(z)} \\ &+ \frac{\sqrt{\pi}\gamma_D}{2}\left(\frac{1}{4\pi\sqrt{2}}\right)\frac{1}{\sum_n \eta^{2n}}\sum_{n\neq m}\frac{1}{\gamma_D}\int_{-t_f/l}^{t_f/l} \mathrm{d}z\, \frac{e^{-\frac{\gamma_D^2 l^2 z^2}{4\sigma^2}} e^{-i\Omega\gamma_D l z} H_0(lz)}{\sqrt{\frac{R_D^2}{\gamma_D^2 l^2}\cosh(2\pi(n-m)\sqrt{M}) - \frac{1}{\gamma_D^2} - \cosh(z)}}.\end{aligned} \tag{B.37}$$

To deal with the poles in the first integral, it is convenient to utilise the Sokhotski formula,

$$\frac{1}{\sinh(z - i\epsilon)} = i\pi\delta(z) + \mathrm{PV}\frac{1}{\sinh(z)} \tag{B.38}$$

which allows for the simplification:

$$\frac{P_D}{\sigma} = \frac{\sqrt{\pi}H_0(0)}{8} - \frac{i}{8\sqrt{\pi}}\mathrm{PV}\int_{-t_f/2l}^{t_f/2l} \mathrm{d}z\, \frac{X_0(2lz)H_0(2lz)}{\sinh(z)} \tag{B.39}$$

$$+ \frac{1}{4\sqrt{2\pi}}\frac{1}{\sum_n \eta^{2n}} \sum_{n\neq m} \mathrm{Re}\int_0^{t_f/l} \mathrm{d}z\, \frac{X_0(lz)H_0(lz)}{\sqrt{\beta_{nm} - \cosh(z)}}, \tag{B.40}$$

having defined

$$X_0(s) = e^{-\frac{\gamma_D^2 s^2}{4\sigma^2}} e^{-i\Omega\gamma_D s}, \tag{B.41}$$

$$\beta_{nm} = \frac{R_D^2}{\gamma_D^2 l^2}\cosh(2\pi(n-m)\sqrt{M}) - \frac{1}{\gamma_D^2}. \tag{B.42}$$

This is the result stated in Eq. (4.58) in the main text. In the infinite interaction-time limit, this reduces to Eq.(17) derived in [37]. Likewise, substituting the Wightman function for the cross-term into Eq. (4.56), we obtain

$$\frac{L_{AB}}{\sigma} = \frac{Y_0}{\sum_n \eta^{2n}} \sum_{n,m} \int_0^{t_f/l} \frac{\mathrm{d}z\, Z_0(lz)Q_0(lz)}{\sqrt{\alpha_{nm} - \cosh(z)}} \tag{B.43}$$

where $Q_0(s)$ is given in (4.57) and we have defined

$$Y_0 = \frac{\sqrt{\gamma_A\gamma_B}\sqrt{\pi}}{4\pi\sqrt{\gamma_A^2+\gamma_B^2}} e^{-\frac{(\gamma_A-\gamma_B)^2\sigma^2\Omega^2}{2(\gamma_A^2+\gamma_B^2)}}, \tag{B.44}$$

$$Z_0(lz) = e^{-\frac{\gamma_A^2\gamma_B^2 l^2 z^2}{2(\gamma_A^2+\gamma_B^2)\sigma^2}} e^{-\frac{i\Omega l z\gamma_A\gamma_B(\gamma_A+\gamma_B)}{\gamma_A^2+\gamma_B^2}}, \tag{B.45}$$

$$\alpha_{nm} = \frac{1}{\gamma_A\gamma_B}\left[\frac{R_D^2\cosh(2\pi(m\sqrt{M_A} - n\sqrt{M_B}))}{\sqrt{M_A M_B}l^2} - 1\right]. \tag{B.46}$$

This is Eq. (4.59) as shown in the main text.